

# NEURAL MECHANISMS OF AVERSIVE PREDICTION ERRORS

RACHEL A. WALKER

A dissertation  
submitted to the Faculty of  
the department of  
Psychology and Neuroscience  
in partial fulfillment  
of the requirements for the degree of  
Doctor of Philosophy

Boston College  
Morrissey College of Arts and Sciences  
Graduate School

December 2020



## **Title: Neural Mechanisms of Aversive Prediction Errors**

**By:** Rachel A. Walker

**Advisor:** Michael A. McDannald, PhD

**Abstract:** Uncertainty is a pervasive facet of life, and responding appropriately and proportionally to uncertain threats is critical for adaptive behavior. Aversive prediction errors are signals that allow for appropriate fear responses, especially in the face of uncertainty, and provide a critical updating mechanism to adapt to change. Positive prediction errors (+PE) are generated when an actual outcome of an event is worse than the predicted outcome and *increase* fear upon future encounters with the related predictive cue. Negative prediction errors (-PE) are generated when the predicted outcome is worse than the actual outcome and *decrease* fear upon future encounters with the related predictive cue. While some regions have been offered as the neural source of positive and negative prediction errors, no causal evidence has been able to identify their sources of generation. The objective of this dissertation was to causally identify the neural basis of aversive prediction error signaling. Using precise neural manipulations paired with a robust behavioral fear discrimination task, I present causal evidence for vIPAG generation of +PEs and for a ventrolateral periaqueductal grey (vIPAG) to medial central amygdala (CeM) pathway to carry out +PE fear updating. Further, I demonstrate that while dorsal raphe serotonergic neurons are not the source of -

PE generation, they appear to receive and utilize this signal. Understanding the neural network responsible for aversive prediction error signaling will not only inform understanding of the neurological basis of fear but also may provide insights into disorders, such as PTSD and anxiety disorders, that are characterized by excessive/inappropriate fear responses.

## TABLE OF CONTENTS

<b>Table of Contents .....</b>	<b>i</b>
<b>List of figures .....</b>	<b>iv</b>
<b>List of abbreviations.....</b>	<b>Error! Bookmark not defined.</b>
<b>Acknowledgements .....</b>	<b>ix</b>
<b>CHAPTER 1: Introduction to Prediction Errors and the Underlying Fear</b>	
<b>Network.....</b>	<b>1</b>
<b>1.1 Prediction Errors.....</b>	<b>2</b>
<b>1.2 Behavioral and Neural Evidence of Aversive Prediction Errors.....</b>	<b>5</b>
1.2.1 Positive Prediction Errors.....	5
1.2.2 Negative Prediction Errors.....	8
<b>1.3 Composition and Function of Anatomical Substrates.....</b>	<b>9</b>
1.3.1 vIPAG.....	10
1.3.2 CeM.....	12
1.3.3 DRN.....	14
<b>1.4 Dissertations Aims and Synopsis.....</b>	<b>16</b>
<b>CHAPTER 2: The Ventrolateral Periaqueductal Gray Updates Fear via Positive Prediction Error.....</b>	
<b>2.1 Introduction.....</b>	<b>21</b>
<b>2.2 Materials and Methods.....</b>	<b>23</b>
2.2.1 Experimental Subjects.....	23
2.2.2 Apparatus.....	24
2.2.3 Nose Poke Acquisition.....	25
2.2.4 Pre-Exposure.....	25
2.2.5 Fear Discrimination.....	26
2.2.6 +PE Optogenetic Manipulation .....	27
2.2.7 Histology .....	27
2.2.8 Quantification and Statistical Analysis .....	28
2.2.8.1 Baseline Nose Poke Analyses.....	28
2.2.8.2 Calculating and Analyzing Suppression Ratios.....	28
2.2.8.3 Session-by-Session Analyses.....	29
2.2.8.4 Trial-by-Trial Analyses.....	29
<b>2.3 Summary of Experiments and Results.....</b>	<b>29</b>

2.3.1 Baseline Nose Poke Rates.....	29
2.3.2 vIPAG Inhibition During Foot Shock Selectively Reduces Subsequent Fear to Uncertainty.....	30
2.3.3 vIPAG Inhibition during Foot Shock Blocks Fear Updating to Uncertainty.....	36
<b>2.4 Discussion.....</b>	<b>38</b>

<b>CHAPTER 3: A Ventrolateral Periaqueductal Gray to Central Amygdala Circuit for Fear Updating via Positive Prediction Error.....</b>	<b>40</b>
<b>3.1 Introduction.....</b>	<b>41</b>
<b>3.2 Materials and Methods.....</b>	<b>42</b>
3.2.1 Experimental Subjects.....	42
3.2.1.1 Experiment 1.....	43
3.2.1.2 Experiment 2.....	44
3.2.2 Apparatus.....	44
3.2.3 Nose Poke Acquisition.....	45
3.2.4 Pre-Exposure.....	46
3.2.5 Fear Discrimination.....	47
3.2.6 Single Unit Data Acquisition.....	48
3.2.7 DREADD Procedure.....	48
3.2.8 Optogenetic Manipulations.....	49
3.2.8.1 +PE Optogenetic Manipulation.....	49
3.2.8.2 Cue Optogenetic Manipulation.....	50
3.2.8.3 ITI Optogenetic Manipulation.....	50
3.2.9 Histology .....	51
3.2.10 Quantification and Statistical Analysis .....	51
3.2.10.1 Baseline Nose Poke Analyses.....	51
3.2.10.2 Calculating and Analyzing Suppression Ratios.....	52
3.2.10.3 Normalization of Firing.....	52
3.2.10.4 Identifying Danger Excited and Inhibited Neurons....	53
3.2.10.5 Population and Single-Unit Firing Analyses.....	53
3.2.10.6 Analysis of Baseline Firing Rates.....	54
3.2.10.7 Session-by-Session Analyses.....	54
3.2.10.8 Trial-by-Trial Analyses.....	54
<b>3.3 Summary of Experiments and Results.....</b>	<b>55</b>
3.3.1 Experiment 1.....	55
3.3.1.1 Baseline Nose Poke Rates.....	55
3.3.1.2 vIPAG Inactivation Decreases Fear to Uncertainty.....	56
3.3.1.3 vIPAG Inactivation Reduces Discriminative Firing in Danger Inhibited Units.....	58
3.3.2 Experiment 2.....	63
3.3.2.1 Baseline Nose Poke Rates.....	63
3.3.2.2 vIPAG-CeM Inhibition during Foot Shock Selectively Reduces Fear to Uncertainty.....	64
3.3.2.3 vIPAG-CeM Inhibition during Cue or ITI Does Not Alter Cued Fear or Fear Expression.....	69

3.4 Discussion.....	72
<b>CHAPTER 4: Dorsal Raphe Serotonin Regulation of Fear Updating .....</b>	<b>76</b>
4.1 Introduction.....	77
4.2 Materials and Methods.....	78
4.2.1 Experimental Subjects.....	78
4.2.1.1 Experiment 1.....	78
4.2.1.2 Experiment 2.....	79
4.2.2 Apparatus.....	79
4.2.3 Nose Poke Acquisition.....	80
4.2.4 Pre-Exposure.....	81
4.2.5 Fear Discrimination.....	81
4.2.6 Selective Extinction .....	82
4.2.7 Optogenetic Manipulations .....	83
4.2.7.1 +PE Optogenetic Manipulation.....	83
4.2.7.2 -PE Optogenetic Manipulation.....	84
4.2.8 Histology .....	84
4.2.9 Quantification and Statistical Analysis .....	84
4.2.8.1 Baseline Nose Poke Analyses.....	84
4.2.8.2 Calculating and Analyzing Suppression Ratios.....	85
4.2.8.3 Session-by-Session Analyses.....	85
4.2.8.4 Trial-by-Trial Analyses.....	86
<b>4.3 Summary of Experiments and Results.....</b>	<b>86</b>
4.3.1 Experiment 1.....	86
4.3.1.1 Baseline Nose Poke Rates.....	86
4.3.1.2 Deletion of DRN 5-HT Does Not Impact Fear Discrimination.....	87
4.3.1.3 Deletion of DRN 5-HT Impairs Extinction of Uncertainty.....	89
4.3.2 Experiment 2.....	90
4.3.2.1 Baseline Nose Poke Rates.....	90
4.3.2.2 Inhibition of DRN 5-HT during +PE Does Not Impact Fear Discrimination.....	91
4.3.2.3 Inhibition of DRN 5-HT during –PE Alters Extinction of Uncertainty.....	93
<b>4.4 Discussion.....</b>	<b>95</b>
<b>CHAPTER 5: Discussion.....</b>	<b>99</b>
5.1 Summary of Findings.....	100
5.2 Additional Experimental Findings .....	104
5.3 Consideration of Biological Sex in Prediction Error Signaling.....	108
5.4 Relevance to Clinical Research .....	110
5.5 Revision of Initial Hypotheses .....	112
5.6 Conclusion.....	115
<b>References.....</b>	<b>116</b>

## LIST OF FIGURES

### CHAPTER 1

**Figure 1.1:** Prediction error behavioral design

**Figure 1.2:** Schematic of hypothesized sources of aversive prediction error

### CHAPTER 2

**Figure 2.1:** YFP vs. eNpHR baseline nose poke rates

**Figure 2.2:** vIPAG optogenetic inhibition during foot shock decreases fear to uncertainty

**Figure 2.3** Sex impacts on optogenetic fear discrimination

**Figure 2.4** vIPAG +PE updates within-session fear behavior

### CHAPTER 3

**Figure 3.1:** Saline vs. J60 session baseline nose poke rates

**Figure 3.2:** DREADD expression and electrode placements

**Figure 3.3:** J60 decreases fear to uncertainty

**Figure 3.4:** J60 does not impact discriminative firing in danger excited units

**Figure 3.5:** J60 decreases discriminative firing in danger inhibited units

**Figure 3.6:** Baseline firing does not differ for danger excited and inhibited populations

**Figure 3.7:** YFP vs. eNpHR baseline nose poke rates

**Figure 3.8:** YFP and eNpHR optical ferrule placements

**Figure 3.9:** vIPAG-CeM optogenetic inhibition during foot shock decreases fear to uncertainty

**Figure 3.10:** vIPAG-CeM optogenetic inhibition during cue or ITI does not alter fear

#### CHAPTER 4

**Figure 4.1:** YFP vs. Caspase baseline nose poke rates

**Figure 4.2:** DRN 5-HT deletion does not impact discrimination but impairs extinction of uncertainty

**Figure 4.3:** YFP vs. eNpHR baseline nose poke rates

**Figure 4.4:** Inhibition of DRN 5-HT does not impact +PE-mediated fear discrimination

**Figure 4.5:** Inhibition of DRN 5-HT during –PE alters extinction of uncertainty

#### CHAPTER 5

**Figure 5.1:** Revised schematic of sources of aversive prediction error

## LIST OF ABBREVIATIONS

<b>AHN</b>	Anterior Hypothalamic Nucleus
<b>BLA</b>	Basolateral Amygdala
<b>BNST</b>	Bed Nucleus of the Stria Terminalis
<b>CeA</b>	Central Amygdala
<b>CeC</b>	Central Amygdala, Capsular division
<b>CeL</b>	Central Amygdala, Lateral division
<b>CeM</b>	Central Amygdala, Medial division
<b>CR</b>	Conditioned Response
<b>CRF</b>	Corticotropin-Releasing Factor
<b>CS</b>	Conditioned Stimulus
<b>DA</b>	Dopamine
<b>DMH</b>	Dorsomedial Hypothalamus
<b>DRD</b>	Dorsal Raphe Nucleus, dorsal
<b>DREADD</b>	Designer Receptors Exclusively Activated by Designer Drugs
<b>DRL</b>	Dorsal Raphe Nucleus, lateral
<b>DRN</b>	Dorsal Raphe Nucleus
<b>DRV</b>	Dorsal Raphe Nucleus, ventral
<b>eNpHR</b>	Enhanced Natronomonas Halorhodopsin
<b>FR-1</b>	Fixed Ratio-1
<b>GABA</b>	Gamma-Aminobutyric Acid
<b>GP</b>	Globus Pallidus
<b>ITI</b>	Inter-trial Interval

<b>J60</b>	JHU37160 Dihydrochloride
<b>LA</b>	Lateral Amygdala
<b>IPAG</b>	Lateral Periaqueductal Grey
<b>MIT</b>	Midline Intralaminar Thalamus
<b>MOR</b>	$\mu$ -Opioid Receptor
<b>mPFC</b>	Medial Prefrontal Cortex
<b>PAG</b>	Periaqueductal Grey
<b>PDR</b>	Posterodorsal Raphe Nucleus
<b>+PE</b>	Positive Prediction Error
<b>-PE</b>	Negative Prediction Error
<b>PE</b>	Prediction Error
<b>PTSD</b>	Post-Traumatic Stress Disorder
<b>PVT</b>	Paraventricular Nucleus of the Thalamus
<b>TH+</b>	Tyrosine Hydroxylase Positive
<b>TPH-2</b>	Tryptophan Hydroxylase 2
<b>Unc-S</b>	Uncertainty-Shock
<b>Unc-O</b>	Uncertainty-Omission
<b>US</b>	Unconditioned Stimulus
<b>vGlut2</b>	Vesicular Glutamate Transporter 2
<b>VI-30</b>	Variable Interval, 30 s
<b>VI-60</b>	Variable Interval, 60 s
<b>vIPAG</b>	Ventrolateral Periaqueductal Grey
<b>VTA</b>	Ventral Tegmental Area

<b>YFP</b>	Yellow Fluorescent Protein
<b>5-HT</b>	5-Hydroxytryptamine (Serotonin)

## **ACKNOWLEDGEMENTS**

My deepest thanks go to my mom, dad, sister and brother, who have all supported, encouraged, and loved me through everything that it took to get me to this point. Thank you for allowing me follow whichever path I chose and giving me every opportunity you could. Mom, I would not be here today if it weren't for you knowing me better than I knew myself, suggesting I might not be happy giving up academics for art school. To my husband, Joe – thank you for your unwavering love and support for these many years. I'll always be grateful for your encouragement to follow my own dreams even when that meant being far apart. To the rest of my family and friends – thank you for your love and support. I am truly fortunate to have each one of you in my life.

I would like to thank my advisor, Dr. Mike McDannald, for believing in me and focusing a large amount of time and effort on my training. I truly could not have asked for a better advisor, or human being, to had to have worked with these five and a half years. It was an honor to work and grow with the lab from its beginnings, and I know there are great things in store for its future because of your efforts and kind heart. Thank you to the other members of the McDannald lab, Kristina, Maddie, Mahsa, Jasmin, and Amanda, who helped with training or supporting me along the way. I am grateful for the assistance of numerous dedicated undergraduate research assistants, including So-Hyeon, Scott, Taylor, Rebecca, Nora, Caitlin, Kevin, Andrew, Alexa, and Jillian, whose efforts made this work possible.

To my dissertation committee members, Drs. Gorica Petrovich, Maureen Ritchey, and Travis Todd: thank you for the time and effort you contributed by acting on my

committee. Your insights and feedback have not only improved this research, but also contributed to my personal development as a scientist.

Thank you to Bret Judson and the Boston College Imaging Core for infrastructure and support. Thank you to the Boston College Animal Care Facility and its staff for infrastructure and support. Research reported in this publication was supported by the National Institute of Mental Health of the National Institutes of Health under Award Numbers R01MH117791 (MAM), R00DA034010 (MAM), and F31MH118801 (RAW). The content is solely the responsibility of the authors and does not necessarily represent the official views of the National Institutes of Health.

## **Chapter 1: Introduction to Prediction Errors and the Underlying Fear Network**

## 1.1 Prediction Errors

Life is innately filled with uncertainty. Humans and non-human animals alike face novel situations daily. In order to respond adaptively in the face of novelty, animals draw on past experiences to form an expectation of a situation's outcome. These expectations are not always correct, but a surprising outcome can subsequently be used to more accurately predict future situational outcomes. In learning theory such an occurrence is referred to as a 'prediction error' (PE; (Behrens et al., 2007; Bush & Mosteller, 1951; Rescorla & Wagner, 1972; Schultz, 1997; Terao et al., 2015). Prediction errors occur when a predicted outcome differs from the actual outcome and can occur in both aversive (Belova et al., 2007; Wright et al., 2015) and reward (Diederer et al., 2016; Montague et al., 1996; Schultz, 1997; Takahashi et al., 2011; Tobler et al., 2006) settings, can be small or large (Matsumoto et al., 2007), and can be directionally positive or negative (McHugh et al., 2014).

The concept of prediction errors is rooted in learning theory. In the early 20<sup>th</sup> century when Ivan Pavlov discovered that repeated pairings of an unconditioned stimulus (US) with a conditioned stimulus (CS) eventually produces a conditioned response (CR) to the conditioned stimulus alone (Pavlov et al., 1928), he sparked an entirely new field of associative learning. Robert Rescorla and Allan Wagner, two prominent American psychologists, proposed in 1972 a theory that is known as the Rescorla-Wagner model of Pavlovian conditioning. In a now classic piece of literature, they put forth the formula:

$$\Delta V = \alpha\beta(\lambda - V_{\text{total}})$$

to describe change in associative strength between a Pavlovian CS and the US (Rescorla & Wagner, 1972). In the formula,  $\alpha$  represents the salience of a given CS,  $\beta$  represents

the associative learning rate of the US,  $\lambda$  represents the maximum learning available supported by the US employed, and  $V_{total}$  is the total current associative strength of all present CSs. Although Rescorla and Wagner used aversive USs, the theory can be applied in both aversive and reward settings.

This formula provides a mathematical basis for prediction errors, as the section:  $(\lambda - V_{total})$  can be thought of as the difference between the possible outcome of a predictor (usually 0 or 1) and the current associative strength. The association begins at zero prior to conditioning and changes based on experience. This representation of prediction errors allows for signed prediction errors, that is, the calculation of this value may result in a positive or negative value, or outcome, representing the directionality of associative changes (increasing or decreasing strength). The magnitude of a prediction error is determined by the absolute value of the calculated error, usually bounded by 0 and 1, with values closer to 1 representing higher magnitudes, or stronger errors. Prediction errors are the key to altering associations based on the Rescorla-Wagner model, as no learning can occur if the error term amounts to zero. Thus, the element of surprise provided by prediction errors drives changes in associative strength.

While Rescorla and Wagner were not the first to propose the presence of prediction errors – Robert Bush and Frederick Mosteller suggested this phenomenon occurs during basic associative learning (Bush & Mosteller, 1951) – they were the first to propose that the prediction itself is comprised of the sum of the associative strengths of all present cues (Rescorla & Wagner, 1972). Rescorla and Wagner's model was also influenced by the work of Leon Kamin, whose blocking and unblocking experiments demonstrated the significance of surprise in conditioning (L. J. Kamin, 1969; Leon J.

Kamin, 1967). Their theory has been tested by a slew of experiments since its introduction and, despite a number of shortcomings (Miller et al., 1995), it has helped to promote research on prediction errors.

Substantive focus has been given to reward prediction errors and the dopamine system, yet aversive prediction errors remain relatively understudied. In evidence, a PubMed search (2 Dec 2020) for “prediction error” and “reward” yielded 1331 results, while a search for “prediction error” and “aversion” yielded only 227 results. Findings have implicated a number of brain regions in aversive prediction error signaling (Berg et al., 2014; Johansen et al., 2010; S. S. Y. Li & McNally, 2015; McHugh et al., 2014; McNally & Cole, 2006; A. Sengupta & McNally, 2014), but the neural circuitry responsible for generating aversive prediction errors is still uncertain. Questions such as: How are aversive prediction errors generated in the brain? What neural systems carry out the results of aversive prediction errors? Does biological sex influence prediction error signaling? and Where are updated expectations formed from aversive prediction errors saved for future use? await rigorous scientific testing.

## 1.2 Behavioral and Neural Evidence of Aversive Prediction Errors

Based on anatomical connections and experimental evidence, a number of brain regions have been suggested to be involved in aversive prediction error signaling. These include the periaqueductal grey (Assareh et al., 2017; Cole & McNally, 2009; Groessl et al., 2018; Johansen et al., 2010; McNally & Cole, 2006; Ozawa et al., 2017; Roy et al., 2014), dorsal raphe nucleus (Berg et al., 2014), amygdala (Johansen et al., 2010), nucleus accumbens core (S. S. Y. Li & McNally, 2015), and midline/intralaminar thalamus (MIT) (A. Sengupta & McNally, 2014). Below, the experiments providing evidence for the regions involved in positive and negative PE *generation* are detailed.

### 1.2.1 Positive Prediction Errors

Several studies have provided evidence for the existence of prediction errors on both behavioral and neural levels since the foundational works of Pavlov, Rescorla, Wagner, and others. Signed aversive prediction errors are of particular interest due to their ability to update behavior related to a critical survival mechanism – fear. As noted above, signed prediction errors can be positive or negative. A positive prediction error (+PE) occurs when the actual outcome is worse than predicted (e.g. not expecting a foot shock, but receiving one). This signal acts to strengthen the cue-outcome association (Rescorla, 1970), increasing fear to the predictive cue upon future encounters. Critically, +PE occurs at the time of foot shock, but updates and strengthens the cue-shock association for future use (Rescorla & Wagner, 1972).

Past findings have implicated the ventrolateral sub-region of the periaqueductal grey (vlPAG) in the creation of positive aversive prediction errors. Single unit recordings

in the rat PAG demonstrated weaker excitatory US responding when the US was expected (Johansen et al., 2010). Further, vIPAG inactivation via muscimol prevented fear learning signals being sent to the amygdala during conditioning (Johansen et al., 2010). In an associative blocking paradigm, vIPAG  $\mu$ -opioid receptor (MOR) antagonism via naloxone putatively blocked +PEs during Pavlovian fear conditioning by preventing blocking effects (McNally & Cole, 2006) and modulating vIPAG MOR activity alters predictive learning driven by +PE (Assareh et al., 2017; Cole & McNally, 2009; McNally & Cole, 2006; Ozawa et al., 2017). Others have offered dopaminergic neurons spanning the vIPAG and dorsal raphe nucleus (DRN) as the possible source of +PE. Using a combination fear conditioning and associative blocking design, chemogenetic and optogenetic inhibition of vIPAG/DRN dopamine (DA) neurons led to decreased acquisition of conditioned freezing responses to an auditory CS (Groessl et al., 2018). Optogenetic illumination occurred during the cue period and chemogenetic inhibition lasted for the entire session, however, so the effects found by Groessl and colleagues (2018) are not tied to +PEs. While the results are not specific to the vIPAG nor +PE periods, these findings suggest prediction error signals could be carried to the rest of the brain by dopaminergic projections

Outside of rodent evidence, there is also human evidence of PAG +PE signaling. PAG activation via fMRI has been shown during +PE in an instrumental pain avoidance task. PAG activation was higher when pain was unexpected compared to when it was expected (Roy et al., 2014), and this difference supports the idea that the PAG is not simply responding to pain or salience alone. While fMRI lacks the spatial sensitivity to

differentiate between activity in different PAG sub-regions, this study nonetheless provides further evidence of possible vIPAG generation of +PE.

Although the literature points strongly to vIPAG generation of aversive +PEs, no previous study has tied precise manipulation of vIPAG activity to the +PE period to show future fear updating. One experiment did use optogenetics to inhibit at the time of shock presentation, however, inhibition was not specific to vIPAG, as IPAG was also included (Assareh et al., 2017). Further, inhibition occurred during acquisition of conditioning to a fully reinforced cue that co-terminated with shock, and inhibition led to greater fear expression on subsequent test trials. If +PE signals were prevented due to inhibition, fear should be lower in the inhibition group. These results could be accounted for by the inclusion of IPAG in inhibition area or due to the timing of the inhibition itself. Illumination occurred only during the 0.5 s shock, which co-terminated with the CS. Illumination during this period confounds activity to the cue with possible PE activity, so the +PE period needs to be isolated for more targeted manipulations.

Particularly lacking in the current literature is evidence that vIPAG +PE activity updates within-session fear to a predictive cue. This is despite the fact that such updating would be an expected consequence of strengthening the cue-shock association. Because the vIPAG is involved in threat expectancy, fear expression, and pain responses (Bertoglio & Zangrossi, 2005; Faull et al., 2016; Graeff, 2004; Mendes-Gomes et al., 2011; Tovote et al., 2016), it is a prime candidate to act on multiple aspects of prediction error signaling. Using approaches such as lesions, pharmacological inactivation, or DREADDs, however, cannot distinguish between the vIPAG's role in fear expression and prediction error signaling, as these methods inhibit the vIPAG during both. It is therefore

crucial to manipulate the vIPAG only at the time of +PE to determine whether activity there is necessary for +PE signaling.

### *1.2.2 Negative Prediction Errors*

In direct opposition to +PEs, a negative prediction error (-PE) occurs when the predicted outcome is worse than the actual outcome (e.g. expecting a foot shock, but receiving none). This signal acts to weaken the cue-outcome association (Rescorla, 1970), decreasing fear to the predictive cue upon future encounters. Much less evidence has been put forth to suggest a locus of aversive negative, compared to positive, PEs, but one region has been suggested: the dorsal raphe nucleus (DRN).

One review hypothesized that DRN 5-HT may be the locus of an aversive PE based on known function and anatomical substrates (Daw et al., 2002), but only one study has experimentally tested DRN involvement in PE. During fear conditioning, neurotoxic lesions of the DRN were shown to prevent decreases in fear to an uncertain cue (Berg et al., 2014). Further, DRN lesions resulted in reduced fear extinction of a deterministic cue compared to controls. Because of the impaired ability to decrease fear, these findings suggested disrupted -PE signaling as the source of these effects. Little other evidence has been put forth to suggest a locus of -PEs in aversive settings (S. S. Li & McNally, 2014), although other findings have shown -PEs in reward settings. As with the evidence of vIPAG +PEs, the evidence suggesting DRN-generation of -PEs is not tied to the error period, warranting further investigating with temporally precise manipulations targeting -PE.

### **1.3 Composition and Function of Anatomical Substrates**

When mapping out a neural circuit for prediction errors, it is important to consider how these regions would receive inputs carrying prediction and actual outcome information necessary to compute an error. Further, the region should be poised to update associative strength through its projections. The neural basis of Pavlovian fear conditioning has been the subject of much research, and it is known that the lateral amygdala (LA) receives inputs with CS information (Collins & Pare, 2000; Mascagni et al., 1993; McDonald, 1998; Romanski & LeDoux, 1993), which may carry prediction information, and with US information (Shi & Davis, 1999). These inputs include sensory information from the thalamus and cortex (Boatman & Kim, 2006; Bukalo et al., 2015; LeDoux, Cicchetti, et al., 1990; LeDoux et al., 1985; LeDoux, Farb, et al., 1990; Mascagni et al., 1993; Shi & Davis, 1999). LA sends outputs to the basolateral amygdala (BLA), which in turn sends information to the central nucleus of the amygdala (CeA) (Pare et al., 1995; Smith & Pare, 1994). There are also direct LA-CeA projections (Smith & Pare, 1994). The CeA projects to the vIPAG to mediate freezing behavior, and CeA projections to the lateral hypothalamus (LH) mediate conditioned increases in blood pressure (LeDoux et al., 1988). Given the interconnections of regions involved in fear responses and expression, it is not surprising that the neural pathway for aversive prediction errors has yet to be identified. Looking at the composition, anatomy, and function of proposed regions can provide clues as to their likelihood of PE generation and how they may fit into a broader PE network. While not exhaustive, the regions of interest for this work are considered below based on these features.

### 1.3.1 vIPAG

The vIPAG is probably most widely known for its role in conditioned freezing behavior. It is one subregion of the PAG, which is organized in four distinct anatomical and functional columns (Bandler & Shipley, 1994; Carrive, 1993). This midbrain structure is mainly comprised of dopaminergic, glutamatergic, and GABAergic neurons (Behbehani & Fields, 1979; Samineni et al., 2017; Suckow et al., 2013; Tovote et al., 2016), and corelease of DA and glutamate has been found (C. Li et al., 2016). vIPAG neurons also notably express  $\mu$ -opioid receptors, which are involved in proported +PE regulation of fear (McNally & Cole, 2006).

While the vIPAG is distinct from the other three PAG columns, all of the columns are highly interconnected (Beitz, 1982). Outside of PAG connectivity, the vIPAG receives inputs from the brainstem and spinal cord, including the ventral medulla, the dorsal horn, and medial nucleus of the solitary tract (Carrive, 1993). Dense prefrontal inputs target the vIPAG, including those from dorsomedial prefrontal cortex (Rozeske et al., 2018), prelimbic cortex (Beitz, 1982), medial/ventral/dorsolateral divisions of orbital cortex, and dorsal/posterior divisions of agranular insular cortex (Floyd et al., 2000). Each of these prefrontal regions play essential and unique roles in fear learning and/or expression (Ray et al., 2018; Rozeske et al., 2018; Sarlitto et al., 2018; Vidal-Gonzalez et al., 2006; Yau & McNally, 2015) and are likely to provide overlapping and distinct predictions about impending aversive outcomes to the vIPAG. Other inputs include the anterior hypothalamic nucleus (AHN), medial preoptic area, paraventricular nucleus of the thalamus (PVT), bed nucleus of the stria terminalis (BNST), medial central amygdala (CeM), and DRN (Carrive, 1993; Jansen et al., 1998; Semenenko & Lumb, 1992).

The vIPAG in turn projects to a host of brain regions implicated in prediction and prediction error, including the major dopamine containing regions (A8 retrorubral field, A9 substantia nigra, and A10 ventral tegmental area) (Watabe-Uchida, Zhu, Ogawa, Vamanrao, & Uchida, 2012), dorsomedial hypothalamus (DMH) (Vianna & Brandão, 2003), the diagonal band, and the lateral BNST (Beitz, 1982). vIPAG projections to the midline/intralaminar thalamus (MIT) (Krout & Loewy, 2000) and reciprocal connections to the CeM (Vianna & Brandão, 2003) may provide probable circuitry for prediction error broadcasting (A. Sengupta & McNally, 2014). The vIPAG is also the only column sending projections to the ventral horn (Mouton & Holstege, 1994). These anatomical connections demonstrate the vIPAG is situated to send and receive information from regions involved in prediction, prediction error, shock, and behavioral responding.

The PAG is involved in many functions, especially related to defensive behaviors, and the vIPAG specifically is best known for its role in freezing and analgesic responses (McNally et al., 2011). Seminal work by LeDoux and colleagues demonstrated that CeM-vIPAG projections mediate conditioned freezing behavior (LeDoux et al., 1988). Further, the CeM-vIPAG pathway sets learning strength, giving predictive information needed for PE calculation (Ozawa et al., 2017). Optical stimulation of the vIPAG cell bodies can elicit freezing behavior, which is distinguished from defense responses generated by other PAG subregions (Assareh et al., 2016). Excitatory inputs from the dorsal medial prefrontal cortex (dmPFC) to the vIPAG regulate pain responses, as optical stimulation of this pathway generates analgesic effects as well as producing antianxiety behaviors in open field and elevated plus maze tests (Yin et al., 2020).

vIPAG regulation of analgesia appears to act on the endogenous opioid system (Loyd et al., 2008) through DA neurons (Taylor et al., 2019). Dopaminergic vIPAG neurons are also involved in fear learning (Groessl et al., 2018). vIPAG/DRN neurons that co-release DA and glutamate regulate nociceptive behavior (C. Li et al., 2016) and are responsive to numerous 'salient' stimuli such as foot shock, conspecifics, and reward (Cho et al., 2017). These DA neurons project strongly to the medial division of the CeL and lead to EPSPs in both SST+ and PKC $\delta$  + neurons via release of DA and glutamate (Groessl et al., 2018). This projection pattern, however, suggests these effects may stem more from DRN neurons rather than vIPAG, as DRN and vIPAG outputs mainly target CeL and CeM, respectively (Halberstadt & Balaban, 2008; Vertes, 1991; Vianna & Brandão, 2003). The cellular, anatomical, and functional features relayed here along with the +PE related behavioral evidence related above showcase vIPAG as a highly likely candidate for +PE generation.

### 1.3.2 *CeM*

The region proposed here to receive direct vIPAG +PE signals is the medial subdivision of the central amygdala (CeM) due to its well-established role in fear learning and plasticity in addition to dense anatomical connectivity. The central nucleus of the amygdala contains capsular, lateral, and medial subdivisions. The medial division is best known as the major output region of the amygdala (Hopkins & Holstege, 1978; Rizvi et al., 1991; Vianna & Brandão, 2003). CeM neurons tend to be densely packed and are immunoreactive for nitric oxide, substance P, somatostatin, corticotropin-releasing factor (CRF), and galanin (Cassell & Gray, 1989; Olucha-Bordonau et al., 2015). The CeA is

known for its GABAergic composition, and while GABAergic neurons are present in the CeM, it contains lower levels than other CeA divisions (N. Sun & Cassell, 1993).

Lateral central amygdala (CeL) GABAergic neurons provide a major input to CeM, especially CeM neurons that in turn provide input to the brainstem (N. Sun & Cassell, 1993; Ning Sun et al., 1994). Complex amygdala microcircuitry has often made it difficult to determine the exact function of intra-amygdalar connections, but there is evidence of tonic CeM inhibition from CeL (Ciocchi et al., 2010). Units have been identified in the CeL that display fear 'on' (CS+ excitation) and 'off' (CS+ inhibition) patterns after fear conditioning, and both of these populations synapse onto and regulate activity of CeM units (Ciocchi et al., 2010). These data indicate CeL neurons mediate fear acquisition while CeM neurons are responsible for response output. Although reciprocal connections with the vIPAG target the CeM specifically (Vianna & Brandão, 2003), these findings suggest a possible wider role for CeA neurons in the prediction error network. Interestingly, the DRN also projects to CeA, and while its projections target the CeL (Halberstadt & Balaban, 2008; Vertes, 1991), it is possible this activity modulates CeL-CeM activity. Outside of the vIPAG, main targets of CeM projections are the parabrachial nucleus, the dorsal vagal complex, and LH (Gray & Magnuson, 1987; LeDoux et al., 1988; Veening et al., 1984).

As noted above, CeM projections to LH and vIPAG have been classified by their ability to mediate conditioned increases in blood pressure and freezing behavior, respectively (LeDoux et al., 1988). The CeM is also known to be active during Pavlovian conditioning (Duvarci et al., 2011), and previous findings have demonstrated a role for the central amygdala in reward prediction errors (Holland & Gallagher, 2006; Lee et al.,

2010). Neural plasticity related to fear learning also occurs in the CeM (Samson & Pare, 2005), and lesions of the CeA block fear-potentiated startle and conditioned freezing (Campeau & Davis, 1995; Goosens & Maren, 2001). Despite the known function of CeM-vIPAG projections, knowledge of vIPAG-CeM function is lacking but leaves open the possibility that these projections carry +PE signals.

### 1.3.3 DRN

The DRN is known as the largest source of serotonergic (5-HT) neurons in the central nervous system with these neurons projecting widely throughout the brain (Steinbusch, 1981). This midbrain structure bordering the vIPAG contains cells using many other transmitters, however, including GABA, glutamate, dopamine, galanin, CRF, and substance P (Michelsen et al., 2007). 5-HT neurons commonly co-express glutamate, substance P, CRF, or galanin (Michelsen et al., 2007), with a large overlap in 5-HT and substance P expression, particularly in the rostral DRN (Baker et al., 1991). Serotonergic neurons are found across all subregions of the DRN, however, and make up almost 70% of DRN's neuronal population (Baker et al., 1991). Widespread projections along with co-expression of other transmitters suggests many actions for DRN serotonin.

In terms of connectivity, DRN receives widespread forebrain input, including the cingulate, infralimbic, orbital, and insular cortices; ventral pallidum; claustrum; preoptic areas; lateral habenula; hypothalamus; BNST; and amygdala (C Peyron et al., 1997). Inputs from particular regions have been shown to target certain DRN populations in some cases, for example, glutamatergic input from mPFC preferentially targets DRN 5-HT and GABAergic neurons (Geddes et al., 2016). Retrograde tracing has also

demonstrated extensive brainstem input to the DRN, including the substantia nigra, ventral tegmental area (VTA), supramammillary nucleus, and PAG (Christelle Peyron et al., 2018). Interestingly, the vIPAG is the only PAG subregion that projects to DRN (Kalén et al., 1985), and the central nucleus is responsible for amygdalar inputs to the DRN (C Peyron et al., 1997).

DRN projections are organized in three main ascending and four descending pathways. Ascending projections are widely distributed throughout the brain but target the striatum, substantia nigra, amygdala, cortex, hippocampus, thalamus, hypothalamus, septum, and habenula most heavily (Michelsen et al., 2007). Descending DRN projections target the spinal cord, lower brainstem, and cerebellum (Michelsen et al., 2007). DRN projections to the amygdala target central, basolateral, and lateral nuclei (Halberstadt & Balaban, 2008; Vertes, 1991), but serotonergic DRN neurons most densely innervate the BLA (Steinbusch, 1981). Notably for the present experiments, DRN densely innervates the vIPAG and these areas are reciprocally connected (Kalén et al., 1985; Vertes, 1991; Vianna & Brandão, 2003). DRN-vIPAG projections are also partly serotonergic (Steinbusch, 1981).

In terms of function, serotonin is widely known as a neuromodulator involved in regulating anxiety, mood, and arousal. DRN serotonin specifically has been shown to be functionally involved in active coping responses and these neurons respond to reward and foot shock (Grahn et al., 1999; Y. Li et al., 2016; M. Luo et al., n.d.; Ren et al., 2018; Schweimer & Ungless, 2010). DRN 5-HT BLA inputs have been shown to regulate fear conditioning and extinction in a simple auditory fear conditioning paradigm (Ayesha Sengupta & Holmes, 2019), suggesting a pathway for possible DRN 5-HT –PE fear

updating. Projections to the central amygdala are involved in anxiety-promoting behaviors, as demonstrated in open field and elevated plus maze tests, in addition to showing excitatory responses to reward and foot shock (Ren et al., 2018). Outside of 5-HT, DRN GABAergic neurons have been shown to be involved in avoidance behavior in a social defeat paradigm (Challis et al., 2013), and DA neurons show activity related to social isolation in mice (Matthews et al., 2016). Further, DRN DA neurons are activated by a host of salient stimuli, including social interaction, food, predator odor, foot shocks, and air puffs in addition to physical restraint and motivational responding during tail suspension in mice (Cho et al., 2017).

Given that the DRN, and its serotonergic neurons in particular, is anatomically positioned to both receive and send information related to Pavlovian fear and demonstrates activation to related stimuli, there is strong support for a possible role in – PEs. The significant and reciprocal connectivity between the vIPAG, CeA, and DRN (Jansen et al., 1998; Kalén et al., 1985; C Peyron et al., 1997; Vianna & Brandão, 2003) could additionally allow for signaling between regions implicated in different types of aversive prediction errors. The subsequently described aims will provide empirical tests of suggested vIPAG, CeM, and DRN involvement in aversive PEs.

#### **1.4 Dissertation Aims and Synopsis**

The overarching goal of this dissertation was to determine the neural sites of positive and negative aversive PE generation. To test questions related to PE signaling, I employed a behavioral paradigm specifically designed to require the use of both positive and negative PEs (Fig. 1.1A). Rats were trained to discriminate three auditory cues

associated with a different probability of foot shock: danger ( $p = 1.00$ ), uncertainty ( $p = 0.25 - 0.375$ ), and safety ( $p = 0.00$ ). The uncertainty cue was of particular interest, as fear to this cue should be maintained by +PEs generated by shock trials and -PEs generated on omission trials even after extensive training. The exact probability of foot shock for the uncertainty cue was altered based on directional change in fear expected due to planned manipulations. For example, if a manipulation was expected to decrease fear, then a higher probability of shock was used to avoid potential floor effects in fear behavior. Danger and safety cues acted as measuring sticks for fear behavior related to deterministic cues and as control periods for manipulations to compare non-PE mediated effects. Further, I designed a selective extinction paradigm used to follow fear discrimination training in chapter 4 (Fig. 1.1B). This paradigm was designed to maximize -PE signaling to the uncertainty cue, as it was no longer paired with foot shock and -PEs are necessary to decrease fear. Danger and safety cues were reinforced as in discrimination to provide comparisons of fear behavior. The behavioral measure used to indicate fear in this task, nose poke suppression, permitted objective and temporally precise measurement of fear to uncertainty, which was critical to test my hypotheses. This behavioral paradigm was paired with temporally specific optogenetic manipulations and *in vivo* electrophysiology, among other manipulations, to target precise prediction error and control periods.

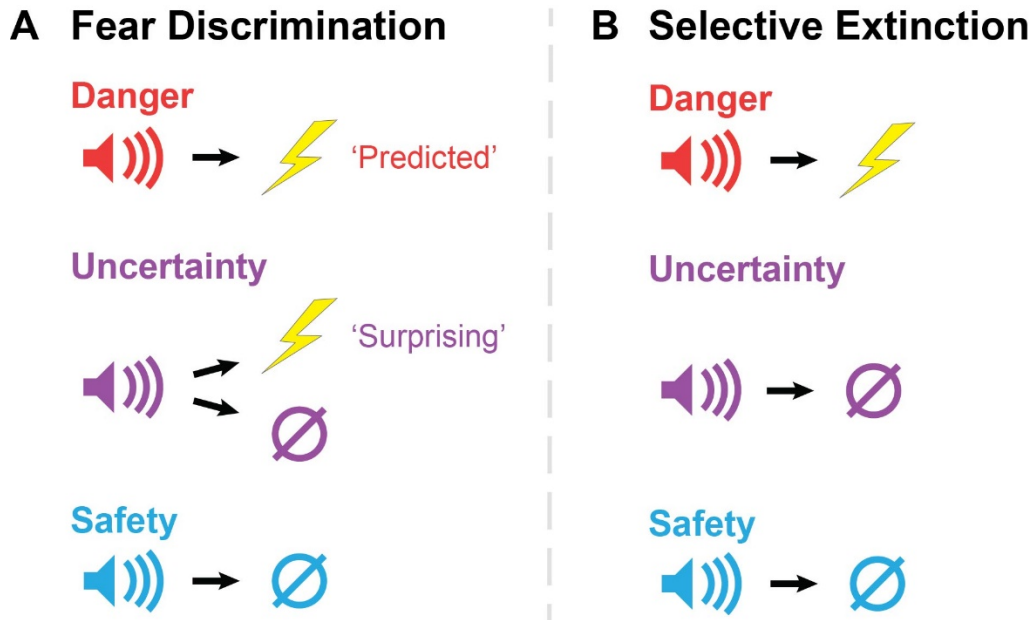


**Figure 1.1 Prediction error behavioral design.** (A) Fear discrimination behavioral paradigm as used throughout the five experiments included in this work. A danger cue (red) is paired with foot shock on 100% of trials, an uncertainty cue (purple) is paired with foot shock on 25-37.5% of trials, and a safety cue (blue) is never paired with foot shock. +PEs are generated on uncertainty-shock trials, and -PEs are generated on uncertainty-omission trials. (B) Selective extinction behavioral paradigm as used in chapter 4. Probability of foot shock receipt remains the same for danger and safety cues, but the uncertainty cue is no longer associated with foot shock. Only -PEs are generated on uncertainty trials in this phase.

Throughout these chapters, I aimed to explicitly test the hypotheses that 1) the vIPAG generates aversive +PEs and 2) sends these signals to the CeM to update future fear while 3) serotonergic neurons in the DRN generate aversive -PEs (Fig. 1.2). Chapter 2 first demonstrated that vIPAG activity at the time of surprising foot shock is necessary to generate +PE signals. Using optogenetics, vIPAG activity was inhibited during +PE on uncertainty-shock trials, and subsequent decreases in fear to uncertainty were observed (Walker et al., 2019). Inhibition during fully predicted foot shock did not change future fear to the danger cue, demonstrating this effect occurs through +PE signaling. These findings

established that vIPAG activity is necessary for +PE fear updating and showed optogenetics as an efficacious method for targeted PE manipulations.

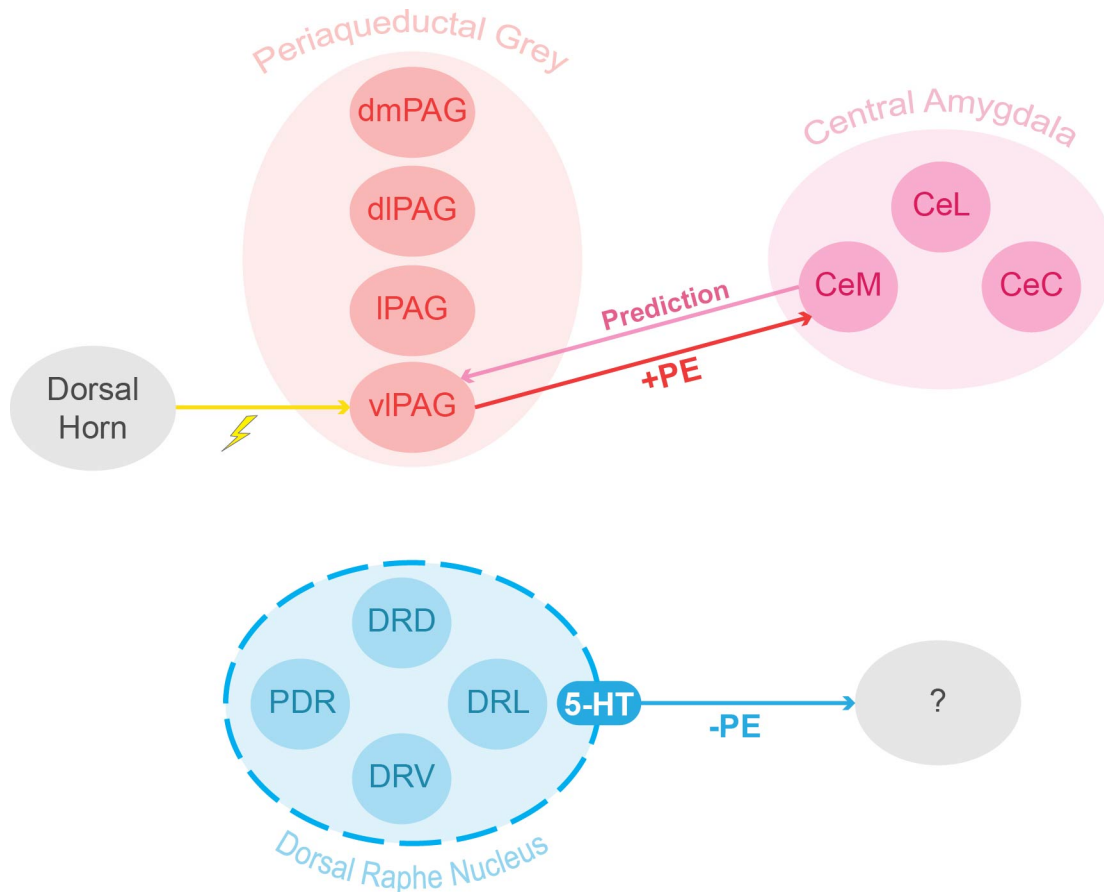


**Figure 1.2 Schematic of hypothesized sources of aversive prediction error.** It is hypothesized that vIPAG neurons use shock information from the dorsal horn and prediction information from the CeM to generate +PEs and send this information directly to CeM. It is also hypothesized that 5-HT neurons throughout the dorsal raphe nucleus generate –PEs, but it is unknown where these errors are sent. Abbreviations: **dmPAG**: dorsomedial periaqueductal grey; **dIPAG**: dorsolateral periaqueductal grey; **IPAG**: lateral periaqueductal grey; **vIPAG**: ventrolateral periaqueductal grey; **CeC**: central amygdala, capsular; **CeL**: central amygdala, lateral; **CeM**: central amygdala, medial; **DRD**: dorsal raphe nucleus, dorsal; **DRL**: dorsal raphe nucleus, lateral; **DRV**: dorsal raphe nucleus, ventral; **PDR**: posterodorsal raphe nucleus; **+PE**: positive prediction error; **-PE**: negative prediction error; **5-HT**: serotonin.

Chapter 3 built upon the main finding established in chapter 2 by testing if vIPAG +PEs are sent to CeM. *In vivo* recordings during fear discrimination when the vIPAG was active and when it was chemogenetically silenced demonstrated that CeM processes fear cues and this activity was dependent on vIPAG input. In a separate experiment, vIPAG terminals in the CeM were optogenetically inhibited during +PE as in chapter 2, revealing a similar but more transient effect on fear to uncertainty. These two experiments demonstrated that vIPAG projections to CeM play a critical role in fear and carry +PE signals.

Chapter 4 demonstrated that DRN 5-HT is not the source of –PE, but rather uses this signal to carry out fear updating. Experiment 1 showed that deletion of DRN 5-HT resulted in reduced extinction of an uncertain cue. With the optogenetic design adapted to target –PEs, activity of DRN 5-HT neurons was inhibited during shock omission to uncertainty during selective extinction. Experiment 2 demonstrated that immediate fear to uncertainty was not impacted by inhibition, but extinction was facilitated in post-illumination sessions. These findings established that DRN 5-HT does not generate –PE signals, rather, this population likely receives the –PE signal to carry out fear updating effects. Taken together, these chapters lend strong support to the hypothesis vIPAG is necessary to generate +PE signals and sends this information to the CeM while also demonstrating that DRN 5-HT is necessary for –PE fear updating but not generation.

## **Chapter 2: The ventrolateral periaqueductal grey updates fear via positive prediction error**

*The work presented in this chapter has been published in the following research article:*

Walker, R. A., Wright, K. M., Jhou, T. C., & McDannald, M. A. (2019). The ventrolateral periaqueductal grey updates fear via positive prediction error. *European Journal of Neuroscience*, 51(3), 866-880. doi:10.1111/ejn.14536

## 2.1 Introduction

Neural activity consistent with +PE has been observed in the ventrolateral periaqueductal grey (vlPAG) (Johansen et al., 2010; Roy et al., 2014), and modulating vlPAG activity alters predictive learning driven by +PE (Assareh et al., 2017; Cole & McNally, 2009; McNally & Cole, 2006; Ozawa et al., 2017). vlPAG/dorsal raphe dopamine/glutamate neurons regulate nociceptive behavior (C. Li et al., 2016) and have been offered as a possible source of the +PE (Groessl et al., 2018). However, this population is responsive to a wide variety of 'salient' biologically significant events such as foot shock, conspecifics, and reward (Cho et al., 2017). Biological salience is here operationally defined as in Cho and colleagues (2017), referring to stimuli producing an unconditioned response. Still, lacking in the current literature is evidence that vlPAG +PE activity updates within-session fear to a predictive cue. This is despite the fact that such updating would be an expected consequence of strengthening the cue-shock association.

In this chapter, I sought to uncover a relationship between vlPAG +PE activity and fear updating. To do so, I employed a fear discrimination procedure in which a danger cue predicted shock deterministically and an uncertainty cue predicted shock probabilistically (Berg et al., 2014; Walker et al., 2018; Wright et al., 2015). I selectively inhibited vlPAG activity around the time of predicted and surprising foot shock delivery. Analyses focused on subsequent changes in fear to the danger and uncertainty cues and the temporal emergence of these changes. This experiment allowed me to determine if vlPAG activity is necessary to update and increase future fear via +PE.

## 2.2 Materials and Methods

### 2.2.1 Experimental Subjects

Final subjects were 7 female and 6 male adult Long-Evans rats (Charles River Laboratories, Raleigh, NC). All rats underwent stereotaxic surgery with isofluorane (Henry Schein, Melville, NY) anesthesia. Rats received 0.3  $\mu$ l bilateral infusions of halorhodopsin (eNpHR; AAV5-hSyn-eNpHR3.0-EYFP; n = 6; 3 females) or YFP (AAV5-hSyn-EYFP; n = 7; 4 females) in the vIPAG (-7.80 AP,  $\pm$ 1.77 ML, -5.89 DV from skull at  $\pm$ 10° angle). Ten minutes elapsed before the syringe was withdrawn to allow for viral diffusion. Fiber optic ferrules were bilaterally implanted just above the infusion sites (-5.69 DV from skull at  $\pm$ 10° angle) to permit 532 nm light illumination. Implants were secured to the skull using dental cement (Henry Schein) and surrounded by a 50 mL centrifuge tube cut to create an enclosure around the electrode implant to prevent possible damage. Post-surgery, rats received 2 weeks of undisturbed recovery with prophylactic antibiotic treatment (cephalexin; Henry Schein) before beginning fear discrimination. In order to be considered for analysis, rats had to maintain a nose poke rate higher than 5 poke/min (low rates make suppression ratios unreliable) and had to show a suppression ratio to uncertainty above 0.25 (in order to have room to observe decreases in fear). Six rats were excluded from analyses, three based on nose poke criteria and three based on suppression ratio criteria.

All rats were maintained on a 12-hour light-dark cycle (lights on 0600 – 1800). Rats were single housed and food restricted to 85% of their free-feeding body weight during Pavlovian fear conditioning with standard laboratory chow (18% Protein Rodent Diet #2018, Harlan Teklad Global Diets, Madison, WI). Water was available *ad libitum* in the

home cage but was not available during behavioral testing, at which time only Dustless Precision Test Pellets (Bio-Serv: Cat #F0021) were present. All protocols were approved by the Boston College Animal Care and Use Committee, and all experiments were carried out in accordance with the NIH guidelines regarding the care and use of rats for experimental procedures.

### 2.2.2 *Apparatus*

The apparatus for Pavlovian fear discrimination consisted of six, individual sound-attenuated enclosures that each housed a behavior chamber with aluminum front and back walls, clear acrylic sides and top, and a metal grid floor. Each grid floor bar was electrically connected to an aversive shock generator (Med Associates, St. Albans, VT). A single food cup and a central nose poke opening, equipped with infrared photocells, were present on one wall. Auditory stimuli were presented through two speakers mounted on the ceiling of each sound-attenuated enclosure. Behavior chambers were modified to allow for free movement of the optical cables during behavior; plastic funnels were epoxied to the top of the behavior chambers with the larger end facing down, and the tops of the chambers were cut to the opening of the funnel. Green (532 nm, 500 mW) lasers (Shanghai Laser & Optics Century Co., Ltd.; Shanghai, China) were used to illuminate the vIPAG. Optical cables were connected to the lasers via 1X2 fiber optic rotatory joints (Doric; Quebec, Canada). Rats were bilaterally connected to the optical cables by a ceramic sleeve placed over the implanted ferrule and ceramic ferrule end of the cable. Black shrink-wrap was also placed on the ends of the cables to block light emission into

the behavioral chamber. A PM160 light meter (Thorlabs; Newton, NJ) was used to measure light output.

### *2.2.3 Nose Poke Acquisition*

Before behavioral testing began, all rats were given 2 days of pre-exposure in the home cage to the pellets used for rewarded nose poking. Rats were then shaped to nose poke for these pellets in the experimental chamber. During the first session, rats were issued one pellet every 60 seconds with the nose poke port removed for 30 minutes. Rats were then issued pellets on a fixed ratio schedule in which one nose poke yielded one pellet until they reached at least 50 nose pokes (FR1) in a session. Over the next 5 days, rats were reinforced for nose pokes on a variable interval schedule first on average every 30 seconds (VI-30), for one session, then on average every 60 seconds (VI-60), for four sessions. All subsequent conditioning sessions were run with a background VI-60 reinforcement schedule that was completely independent of auditory cue or foot shock presentation on conditioning trials. Rats were trained through four VI-60 sessions then underwent surgery and recovery before receiving two reminder VI-60 sessions and beginning pre-exposure.

### *2.2.4 Pre-Exposure*

In two separate sessions, each rat was pre-exposed to the three 10 s auditory cues to be used in Pavlovian fear discrimination. These 42 min sessions consisted of four presentations of each cue (12 total presentations) with a mean inter-trial interval (ITI) of 3.5 min. The order of trial type presentation was randomly determined by the behavioral

program and differed for each rat during each session. Auditory cues consisted of repeating motifs of: broadband click, phaser, or trumpet and can be found here: <http://mcdannaldlab.org/resources/ardbark>. Extensive testing has found these cues to be equally salient, yet discriminable (Walker et al., 2018; Wright et al., 2015).

### 2.2.5 *Fear Discrimination*

Each rat received 16, 67-minute sessions of fear discrimination before plug in sessions. Auditory cues were 10 s in duration and consisted of repeating motifs of a broadband click, phaser, or trumpet. Every session began with a 5-minute habituation period, and ITIs were 3.5 minutes on average. Each cue was associated with a unique probability of foot shock (0.5 mA, 0.5 s): danger,  $p = 1.00$ ; uncertainty,  $p = 0.375$ ; and safety,  $p = 0.00$ . Cue identity was counterbalanced within groups. Foot shock was administered 2 s following the termination of the auditory cue on danger and uncertainty-shock trials. There were 18 total trials per session consisting of 6 danger trials, 5 uncertainty-omission trials, 3 uncertainty-shock trials, and 4 safety trials. Rats received an additional 3 sessions of fear discrimination during which the rats were connected to cables like those used during the optogenetic manipulation, but that did not deliver light, to habituate them to the cables. Thus, rats received a total of 19 fear discrimination sessions before the optogenetic manipulation. The order of trial type presentation was randomly determined by the behavioral program, and differed for each rat, each session for both experiments.

### 2.2.6 +PE Optogenetic Manipulation

Rats underwent 3 sessions of vIPAG illumination via optical cables followed by 3 sessions without illumination or cables. The vIPAG was illuminated during the foot shock on uncertainty-shock and danger trials. Illumination on both uncertainty and danger trials occurred for 4 seconds, beginning immediately after auditory cue offset (2 s), continuing during foot shock (0.5 s), and ending 1.5 s after foot shock offset. Optical inhibition was achieved via delivery of 25 mW of 532 nm 'green' light on each side. Light was produced by a DPSS laser connected to an optical commutator attached to a custom made behavioral cable (Multimode Fiber, 0.22 NA, High-OH, Ø200 µm Core), which connected to the implanted optical ferrule (2.5mm OD, 230 µm Bore Multimode Ceramic Zirconia). Light output of 25 mW was chosen based on calculations the optical fibers will produce ~5 mW/mm<sup>2</sup> of light at distance of 1.2 mm from fiber tip.

### 2.2.7 Histology

Rats were deeply anesthetized using isoflurane and perfused with 0.9% biological saline and 4% paraformaldehyde in a 0.2 M Potassium Phosphate Buffered Solution. Brains were extracted and post-fixed in a 10% neutral-buffered formalin solution for 24 hrs, stored in 10% sucrose/formalin, frozen at -80°C and sectioned via a sliding microtome. Brains with optical implants were processed for fluorescent microscopy. Sections were mounted on glass microscope slides, coverslipped using VECTASHIELD HardSet Antifade Mounting Medium with DAPI (Vector Laboratories, Burlingame, CA), and viral transfection and optical implant sites were confirmed (Paxinos & Watson, 2007). A subset of tissue was processed with fluorescent anti-tryptophan hydroxylase

immunohistochemistry and NeuroTrace™ (ThermoFisher Scientific, Waltham, MA) in order to ensure viral transfections did not diffuse into the dorsal raphe nucleus. This tissue was mounted on glass slides with VECTASHIELD HardSet Antifade Mounting Medium.

## *2.2.8 Quantification and Statistical Analysis*

### *2.2.8.1 Baseline Nose Poke Analyses*

The time stamp for every nose poke and event onset (cues and shocks) during each session was recorded automatically. Raw data were processed in MATLAB to extract nose poke rates during three periods: the baseline, which was 20 seconds prior to cue onset; the 10-s cue; and the post-cue period, which was 4 seconds following cue offset. Baseline nose pokes are reported in pokes/min and analyzed with ANOVA.

### *2.2.8.2 Calculating and Analyzing Suppression Ratios*

Suppression of rewarded nose poking was used as the behavioral indicator of fear. Nose poke rates were calculated for two temporal windows. A suppression ratio for total cued fear was calculated from nose poke rates during a 20 s baseline period just prior to cue onset and the 10 s cue period:  $(\text{baseline} - \text{cue} / \text{baseline} + \text{cue})$ . Complete nose poke suppression was signified by a suppression ratio of '1.00' during the cue relative to baseline, indicating a high level of fear. No nose poke suppression was signified by a suppression ratio of '0.00,' indicating no fear. Intermediate values indicated graded levels of fear.

#### 2.2.8.3 Session-by-Session Analyses

ANOVA for suppression ratios with between factors of group (eNpHR vs. YFP) and sex (female vs male), plus within factors of session (2 pre-exposure, 16 discrimination, and 3 tethered) and cue (danger vs. uncertainty vs. safety) were used compare pre-illumination behavior. An identical ANOVA but for 6 sessions during and following illumination (3 illumination and 3 tethered) were performed to determine the effects of optogenetic inhibition.

#### 2.2.8.4 Trial-by-Trial Analyses

For the second illumination session, the first uncertainty-shock and danger trials (n) were identified for each subject. For each uncertainty 'n' trial the next three uncertainty trials were identified, irrespective of shock contingency (n+1, n+2 and n+3) and the same was done for danger. Suppression ratios for uncertainty were calculated for each trial (n, n+1, n+2 and n+3). ANOVA with between subjects factors of group (YFP vs. eNpHR) and sex (female vs. male), plus within subjects factors of trial (n+1, n+2 and n+3) and cue (danger vs. uncertainty) was used to determine trial-by-trial changes in fear to each cue. Between subjects t-test for difference score was used to compare changes in YFP and eNpHR rats.

### **2.3 Summary of Experiments and Results**

#### *2.3.1 Baseline Nose Poke Rates*

YFP and eNpHR rats did not differ in baseline nose poke behavior, which was supported by ANOVA demonstrating no main effect of, or interaction with, group during

discrimination (Fig. 2.1A; all  $F < 1.3$ , all  $p > 0.28$ ) or the optogenetic manipulation (Fig. 2.1B; all  $F < 1.40$ , all  $p > 0.27$ ). However, a significant effect of sex was found during discrimination ( $F_{1,9} = 6.20$ ,  $p = 0.034$ ), with males poking at higher rates than females. A similar trend toward significance was found during the optogenetic manipulation ( $F_{1,9} = 4.88$ ,  $p = 0.055$ ).

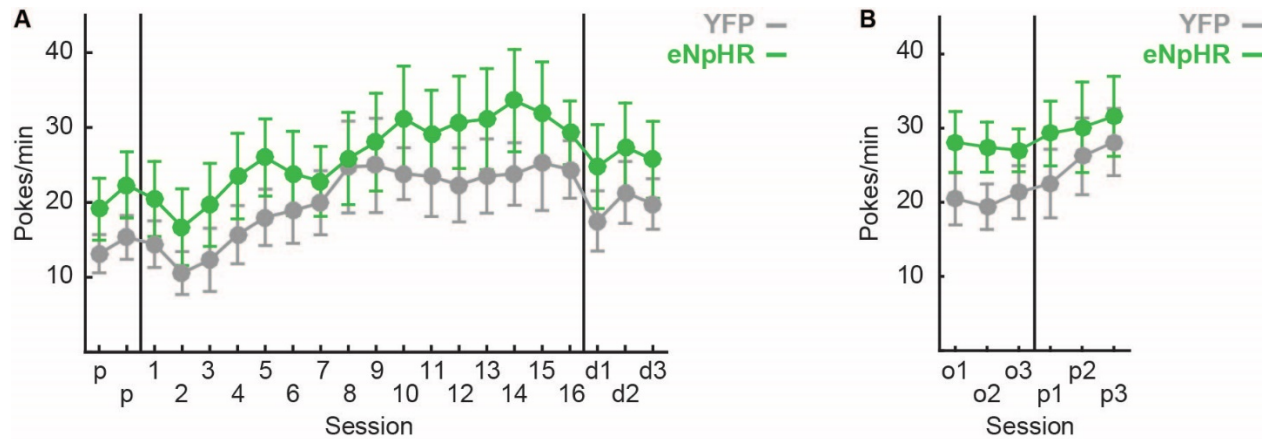


**Figure 2.1 YFP vs. eNpHR baseline nose poke rates. (A)** Mean  $\pm$  SEM baseline nose poke rates for YFP (gray) and eNpHR rats (green) are plotted for the two pre-exposure (p), 16 discrimination (1-16), and 3 ‘dummy’ tethered-only sessions (d1-d3). YFP and eNpHR rats did not differ in baseline nose pokes during these sessions, but males poked at higher rates than females ( $F_{1,9} = 6.20$ ,  $p < 0.05$ ). **(B)** Mean  $\pm$  SEM baseline nose poke rates are plotted for the three illumination (o1-o3) and 3 post-illumination untethered sessions (p1-p3) for YFP (gray) and eNpHR (green) rats. Again, no group differences in baseline nose poke rates were found, but there was a trend toward significance for higher rates in males compared to females ( $F_{1,9} = 4.88$ ,  $p = 0.055$ ).

### 2.3.2 *vIPAG* Inhibition during Foot Shock Selectively Reduces Subsequent Fear to Uncertainty

If shock-responsive *vIPAG* neurons signal +PE, then inhibition of neural activity at the time of surprising foot shock should reduce fear to uncertainty, but inhibition during predicted foot shock would have no effect on fear to danger. By contrast, if the *vIPAG*

activity reflects biological salience, then inhibiting foot shock activity should non-selectively reduce fear to uncertainty and danger.

Rats received bilateral vIPAG transfection with halorhodopsin (eNpHR, AAV5-hSyn-eNpHR3.0-EYFP; n = 6; 3 females) or a control fluorophore (YFP, AAV5-hSyn-EYFP; n = 7; 4 females) and bilateral implantation of optical ferrules over the vIPAG (Fig. 2.2A, B). Rats were trained on the fear discrimination procedure before undergoing the +PE optogenetic manipulation. The optogenetic manipulation (Fig. 2.2C) was hypothesized to decrease fear to the uncertainty cue, so higher fear to uncertainty was needed to ensure detection of decreased fear. All rats showed bilateral transfection in the lateral and ventrolateral PAG with ferrules tips just inside the vIPAG boundary (Fig. 2.2A, B). Expression was relatively uniform across individuals and there were no relationships observed between transfection area and fear behavior.

YFP (Fig. 2.2D) and eNpHR (Fig. 2.2E) rats acquired high fear to danger and uncertainty but low fear to safety over discrimination. Females demonstrated overall higher fear compared to males (main effect of sex  $F_{1,9} = 8.34$ ,  $p < 0.05$ ,  $\eta^2p = 0.48$ , power = 0.73), and YFP rats demonstrated overall higher fear compared to eNpHR rats (YFP group had higher proportion of females). Importantly, eNpHR and YFP rats showed equivalent discrimination (Fig. 2.2D, E). These findings were supported by a main effect of group ( $F_{1,9} = 6.31$ ,  $p < 0.05$ ,  $\eta^2p = 0.41$ , power = 0.61), cue ( $F_{2,18} = 30.87$ ,  $p < 0.001$ ,  $\eta^2p = 0.77$ , power = 1.00), session ( $F_{18,162} = 12.95$ ,  $p < 0.001$ ,  $\eta^2p = 0.59$ , power = 1.00), and a cue x session interaction ( $F_{36,324} = 6.20$ ,  $p < 0.001$ ,  $\eta^2p = 0.41$ , power = 1.00). There were no interactions between group and cue (all  $F < 2.15$ ,  $p > 0.05$ ). Thus, at the start of

the optogenetic manipulation, eNpHR and YFP rats showed equivalent fear discrimination.

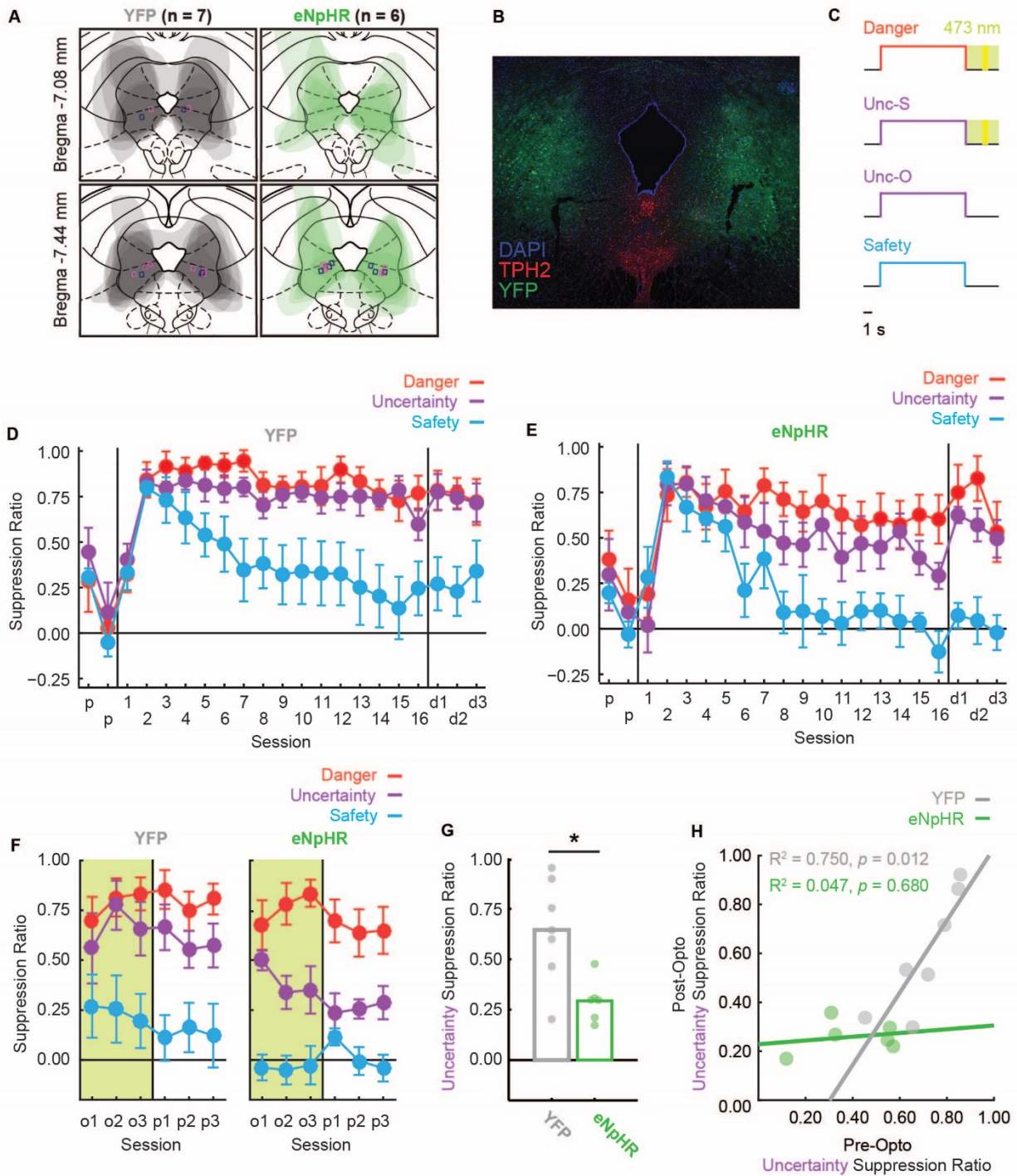


**Figure 2.2 vPAG optogenetic inhibition during foot shock decreases fear to uncertainty. (A)** Viral transfection extent was mapped for all YFP (grey) and eNpHR

(green) rats, and average transfection extent can be seen in their overlaid tracings. Rectangular markers indicate fiber optic ferrule placements (magenta = females; navy = males) were all within or on the border of vIPAG bounds. **(B)** Representative viral transfection is shown with YFP (green), TPH2 (red), and DAPI (blue). Fiber optic ferrule placement can be seen in the vIPAG in both the left and right hemispheres. Note ferrule placement shows exaggerated damage due to immunohistochemistry processing. **(C)** During optogenetic sessions, green-light illumination began at cue offset, continued during the 0.5-s shock (yellow period), and lasted 1.5 s after shock for a total of 4 s. Note illumination never occurred during cue periods. **(D)** Mean  $\pm$  SEM suppression ratios for YFP rats to danger (red), uncertainty (purple), and safety (blue) are shown for the 2 pre-exposure sessions (p), 16 discrimination sessions (1-16), and 3 dummy cable discrimination sessions (d1-d3). **(E)** eNpHR suppression ratio data shown as in C. **(F)** Mean  $\pm$  SEM suppression ratios for YFP rats (left) and eNpHR rats (right) to danger (red), uncertainty (purple), and safety (blue) over the 3 sessions of optogenetic manipulation (o1-o3) and 3 post-manipulation sessions (p1-p3). **(G)** Mean suppression ratios to uncertainty during the last two sessions of optogenetic manipulation and the three post-manipulation sessions (5 sessions total) is shown for YFP (gray bar) and eNpHR rats (green bar). Circles show average suppression ratios for individual rats. Asterisk indicates significance of a between subject's t-test ( $p < 0.05$ ). **(H)** Mean uncertainty suppression ratio for the final three discrimination sessions (pre-opto) is plotted against mean uncertainty suppression ratio for the three sessions following illumination (post-opto). Data shown for each YFP (gray) and eNpHR individual (green) along with  $R^2$  and p-value.

Over the three illumination sessions, green light (532 nm, 25 mW) was delivered for the 4-second period following cue offset on danger and uncertainty-shock trials (2-second delay, 0.5-second shock and 1.5-second post shock; Fig. 2.2C). Illumination parameters were identical for YFP and eNpHR groups, but only in the eNpHR group would vIPAG activity be inhibited. Notably, no illumination occurred during the 10-s cue period, during which fear was measured. While YFP and eNpHR rats showed equivalent levels of fear to all cues in the first illumination session, discrimination diverged thereafter (Fig. 2.2F). ENpHR rats markedly reduced fear to uncertainty, but not danger; YFP rats showed no changes in fear to either cue. This pattern continued through the 3 no-illumination untethered sessions, and results were confirmed by ANOVA, which found a cue x session x group interaction ( $F_{10,90} = 2.59$ ,  $p = 0.0084$ ,  $\eta^2_p = 0.22$ , power = 0.94).

This interaction was driven by decreased fear to uncertainty in eNpHR rats (Fig. 2.2G). This pattern was apparent in both sexes, with subtle sex effects and interactions observed for uncertainty and safety (Fig. 2.3). These results are inconsistent with a role for vIPAG shock activity in biological salience, which would have predicted reduced fear to danger and uncertainty, but support a specific and causal role for vIPAG in +PE.

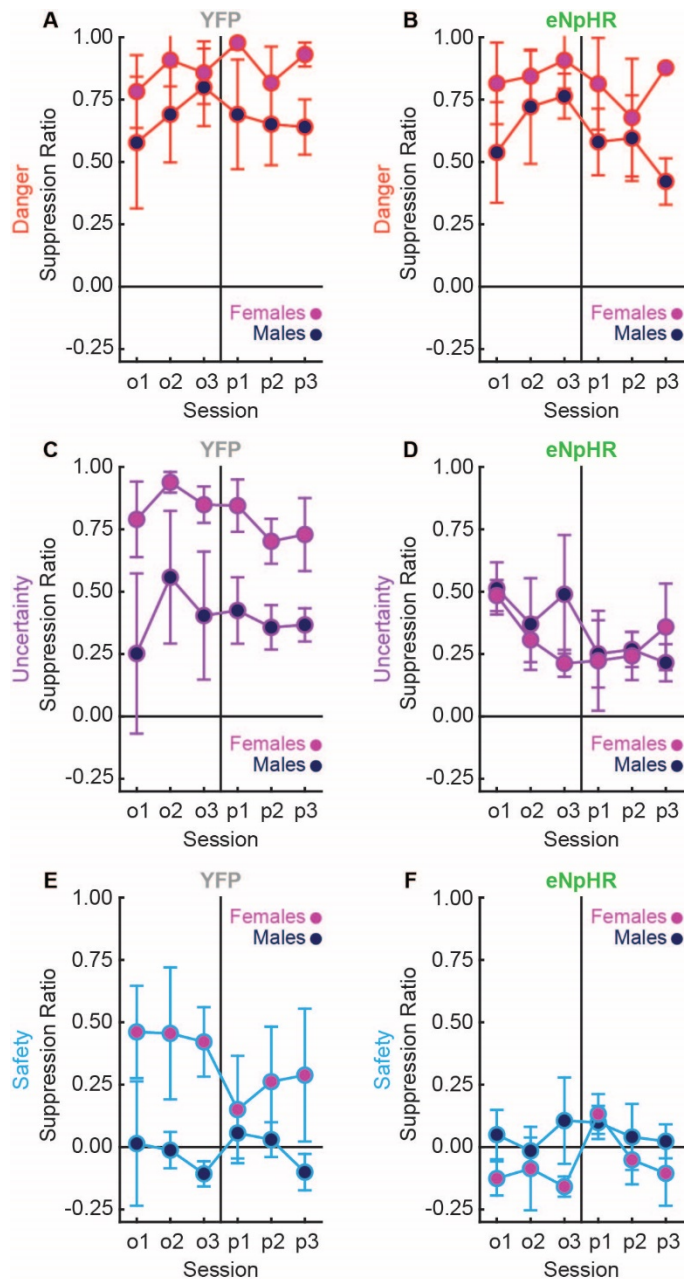


**Figure 2.3 Sex impacts on optogenetic fear discrimination.** Mean  $\pm$  SEM suppression ratio to the danger cue for YFP **(A)** and eNpHR **(B)** female (pink) and male (dark blue) rats are plotted for the 3 sessions of optogenetic manipulation (o1-o3) and 3 post-manipulation sessions (p1-p3). For the danger cue, there was no main effect of or interactions with group (all  $F < 0.628$ ,  $p > 0.05$ ). Mean  $\pm$  SEM suppression ratio to the uncertainty cue for YFP **(C)** and eNpHR **(D)** female (pink) and male (dark blue) rats are plotted for the 3 sessions of optogenetic manipulation (o1-o3) and 3 post-manipulation sessions (p1-p3). For the uncertainty cue, a main effect of group ( $F_{1,9} = 9.68$ ,  $p < 0.05$ ,  $\eta^2p = 0.52$ , power = 0.79) and group x sex interaction reached significance ( $F_{1,9} = 6.90$ ,  $p < 0.05$ ,  $\eta^2p = 0.43$ , power = 0.65), but there were no other interactions with group (all  $F < 2.19$ ,  $p > 0.05$ ). Mean  $\pm$  SEM suppression ratio to the safety cue for YFP **(E)** and eNpHR **(F)** female (pink) and male (dark blue) rats are plotted for the 3 sessions of optogenetic manipulation (o1-o3) and 3 post-manipulation sessions (p1-p3). For the safety cue, a session x group x sex interaction reached significance ( $F_{5,45} = 2.59$ ,  $p < 0.05$ ,  $\eta^2p = 0.22$ , power = 0.75), but there was no main effect of or other interactions with group (all  $F < 3.75$ ,  $p > 0.05$ ).

Finally, while ANOVA found no cue x group interaction for pre-opto discrimination, it visually appeared as though eNpHR rats achieved better discrimination. It is then possible that the low uncertainty fear observed prior to illumination sessions was explained by low uncertainty fear at the end of discrimination. To examine this possibility, we plotted individual fear to uncertainty during the final three discrimination sessions (mean) versus fear to uncertainty during the three post-illumination sessions (Fig. 2.2H). Consistent with no effect of light illumination on YFP individuals, there was a positive correlation between fear to uncertainty at the end of discrimination and following illumination ( $R^2 = 0.75$ ,  $p = 0.012$ ). In eNpHR individuals, there was no relationship ( $R^2 = 0.047$ ,  $p = 0.68$ ). All eNpHR individuals showed low fear to uncertainty following light illumination regardless of the level shown in discrimination. Light illumination thus actively reduced fear to uncertainty only in eNpHR rats.

### 2.3.3 *vIPAG Inhibition during Foot Shock Blocks Fear Updating to Uncertainty*

Because prediction error updating should occur at the trial level, I sought to determine the temporal emergence of the illumination effects. Since behavioral changes were apparent from the second optogenetic session, the first uncertainty shock trial (n) from this session was identified, as well as the next three uncertainty trials (n+1, n+2 and n+3) regardless of shock delivery or omission, for each individual (YFP and eNpHR). The same was done for the four danger trials (n, n+1, n+2 and n+3). Suppression ratios were calculated for each cue/trial. ANOVA for suppression ratios [factors: trial (4), group (YFP vs eNpHR), cue (danger vs. uncertainty) and sex (female vs. male)] revealed a group x trial x cue interaction ( $F_{3,27} = 3.32$ ,  $p = 0.035$ ,  $\eta^2p = 0.27$ ,  $op = 0.69$ ). This interaction was the result of eNpHR and YFP rats showing equivalent fear to uncertainty in the first two trials but eNpHR rats selectively reducing to uncertainty in the remaining two trials (Fig. 2.4A). T-test for change in fear falls just short of significance (Fig. 2.4B, YFP vs eNpHR,  $t_{11} = 2.14$ ,  $p = 0.056$ ), indicating the optogenetic manipulation led to decreases in fear over trials. This pattern did not emerge for danger, with YFP and eNpHR rats showing equivalent fear levels throughout the session (Fig. 2.4C) and no change over the session (Fig. 2.4D).

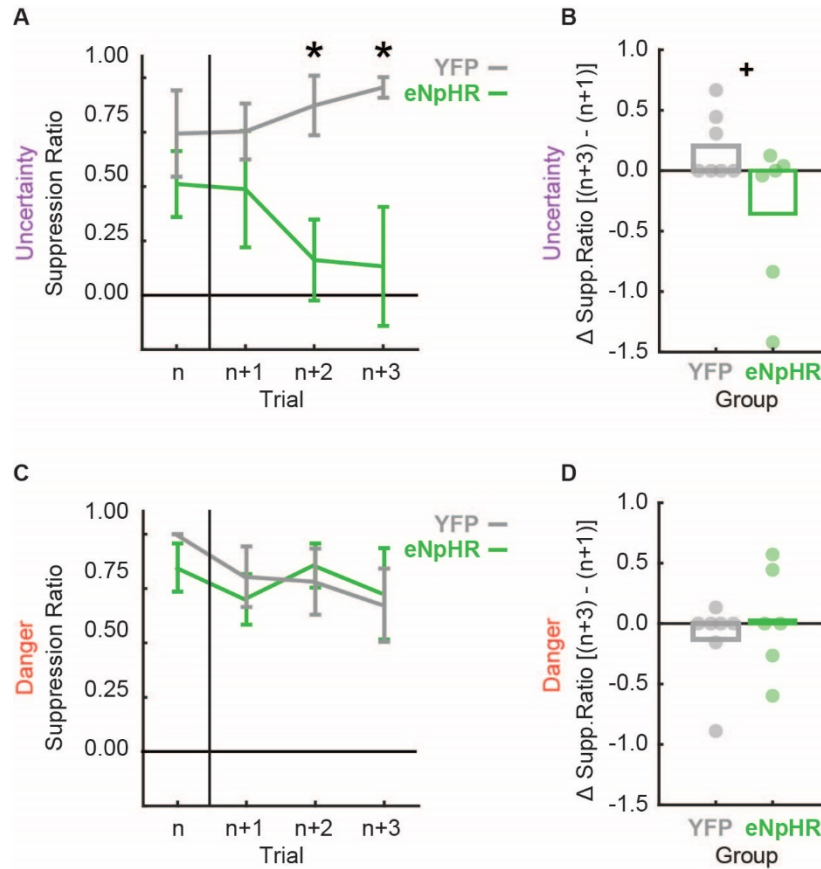


**Figure 2.4 VIPAG +PE updates within-session fear behavior. (A)** Mean  $\pm$  SEM suppression ratio is shown for the first uncertainty-shock trial (n) and the next three uncertainty trials irrespective of shock or omission (n+1, n+2 and n+3) for illumination session 2 (YFP, gray and eNpHR, green). Asterisks indicate significance of between subject's t-test ( $p < 0.05$ ). **(B)** Mean change in suppression ratio [(n+3) - (n+1)] is shown for YFP (gray) and eNpHR (green) rats. Data as in A. Circles show differences for individual rats. + indicates trend toward significance from a between subject's t-test ( $p = 0.056$ ). **(C)** Suppression ratios to the danger cue were plotted for trial n (here the first danger trial on optogenetic session 2) and the subsequent 3 danger trials in order to assess trial-by-trial changes in fear. YFP (grey line) and eNpHR (green line) rats showed equivalent levels of fear and no significant changes in fear to danger across trials. **(D)** Average change in fear to the danger cue three trials after trial n compared to the first trial after n is graphed for YFP (grey bar) and eNpHR (green bar) rats. Circles show differences for individual rats. No significant change in fear to the danger cue occurred for either group.

## 2.4 Discussion

Here I have demonstrated that vIPAG activity precisely at the time of +PE is necessary to update future fear. These results are consistent with the theoretical framework of the behavioral task requiring the use of prediction errors; by preventing +PEs on uncertainty-shock trials but leaving intact negative prediction errors on uncertainty-omission trials, eNpHR rats should only effectively receive neural signals to decrease fear to uncertainty, which matches the resultant behavioral reduction in fear. Further, I demonstrated that +PE fear updating can be seen at the trial level. These findings complement and extend previous studies demonstrating +PE correlates in the vIPAG (Groessl et al., 2018; Johansen et al., 2010; Roy et al., 2014) and critical roles for the vIPAG in predictive learning (Cole & McNally, 2009; McNally & Cole, 2006). Results are also consistent with a neural circuit framework positing that the critical comparison of expected and actual foot shock takes place in the vIPAG (McNally et al., 2011).

In considering the implications of these findings, some caveats should be noted. Firstly, there were a number of significant effects related to biological sex. Sex differences in baseline behavior (i.e. nose poke rate and absolute fear levels) in the optogenetics results are consistent with previous findings in the same behavioral task (Walker et al., 2018). While the effect of optogenetic inhibition to decrease fear to uncertainty was observed across sexes, subtle interactions with sex and the pattern of fear to uncertainty and safety were observed. Given the relatively low number of subjects used here, future experiments of aversive prediction error signaling should continue to consider biological sex as a factor to expand on possible differences.

Another interesting feature of the data concerns post-optogenetics fear behavior. Reduced fear to uncertainty emerged during optogenetic inhibition in eNpHR rats and continued in the following no-illumination sessions. On first impression this is quite odd, as +PE should be fully intact in the no-illumination sessions. However, other findings in this task (Walker et al., 2019) have demonstrated that with sufficient experience, rats readily discriminate uncertainty ( $p = 0.375$ ) from danger ( $p = 1.00$ ). The most parsimonious explanation is that YFP and eNpHR would have eventually achieved discrimination, and optogenetic inhibition served to facilitate reduction of fear to uncertainty in eNpHR rats by reducing +PE.

Concerning anatomy, the vIPAG is well-positioned to receive information about actual shock outcomes, as it receives direct and indirect nociceptive inputs from the dorsal horn (Todd, 2010). The vIPAG is positioned at an intersection of signals for predicted and actual shocks, a requirement for computing a prediction error. In this experiment, optogenetic inhibition primarily targeted vIPAG but also included portions of lateral PAG (lPAG). Although the observed correlates and behavioral effects are more consistent with those reported in vIPAG (Assareh et al., 2017), some contribution of the lPAG cannot be ruled out entirely. The current results, however, present a compelling case for vIPAG as the neural locus of +PE to causally strengthen cue-shock association and update fear.

Further questions remain within the vIPAG, namely, what neuron types compute +PE and to where is this signal broadcast. This chapter identified the vIPAG as the source of +PE generation. Chapter 3 will focus on determining where vIPAG +PE signals are sent to carry out fear updating.

**Chapter 3: A Ventrolateral Periaqueductal Gray to Central Amygdala Circuit for  
Fear Updating via Positive Prediction Error**

### 3.1 Introduction

In chapter 2, I demonstrated that activity in the vIPAG is necessary for aversive +PE fear updating. The results indicate the vIPAG is the site of +PE generation, but vIPAG outputs broadcasting the signal remain unknown. In order to fully understand aversive +PE signaling, it is critical to determine the neural pathway carrying out the effects of the signal.

The vIPAG has reciprocal connections with the medial subdivision of the central amygdala (CeM), which is a major output region of the amygdala (Rizvi et al., 1991; Vianna & Brandão, 2003). CeM-vIPAG projections are known to mediate fear expression, particularly freezing behavior (LeDoux et al., 1988), but the function of vIPAG-CeM projections are not well understood. The CeM is known to be active during Pavlovian conditioning (Duvarci et al., 2011), and previous findings have demonstrated a role for the CeA in reward prediction errors (Holland & Gallagher, 2006; Lee et al., 2010). Further, the CeM is a known site for neural plasticity related to fear learning (Samson & Pare, 2005). Given these findings, here it is proposed that the vIPAG sends +PE signals to the CeM to update future fear.

In this chapter, I sought to uncover a relationship between vIPAG-CeM activity and +PE fear updating. To do so, I employed a fear discrimination procedure in which a danger cue predicted shock deterministically and an uncertainty cue predicted shock probabilistically (Berg et al., 2014; Walker et al., 2018, 2019; Wright et al., 2015). Fear to the uncertainty cue was of particular interest, as this behavior would be reliant on +PE updating. In Experiment 1, I recorded from CeM neurons while the vIPAG was chemogenetically inactivated or functioning regularly. This allowed me to determine

whether +PE related signaling is seen in the CeM and how CeM activity changes without input from vIPAG. Specifically, changes in CeM activity during the cue period may reflect updated expectancies. In Experiment 2, I selectively inhibited vIPAG terminals in the CeM around the time of predicted and surprising foot shock delivery. Analyses focused on subsequent changes in fear to the danger and uncertainty cues and the temporal emergence of these changes. The design and analysis of Experiment 2 was modelled off that in chapter 2, which was shown to be effective in capturing +PE fear updating (Walker et al., 2019). These experiments allowed me to determine if vIPAG-CeM activity is necessary to carry out fear updating via vIPAG generated +PE.

## **3.2 Materials and Methods**

### *3.2.1 Experimental Subjects*

All rats were maintained on a 12-hour light-dark cycle (lights on 0600 – 1800). Rats were single housed and food restricted to 85% of their free-feeding body weight during Pavlovian fear conditioning with standard laboratory chow (18% Protein Rodent Diet #2018, Harlan Teklad Global Diets, Madison, WI). Water was available *ad libitum* in the home cage but was not available during behavioral testing, at which time only Dustless Precision Test Pellets (Bio-Serv: Cat #F0021) were present. All protocols were approved by the Boston College Animal Care and Use Committee, and all experiments were carried out in accordance with the NIH guidelines regarding the care and use of rats for experimental procedures.

### 3.2.1.1 Experiment 1

For experiment 1, final subjects were 5 female adult Long-Evans rats (Charles River Laboratories, Raleigh, NC). All rats underwent stereotaxic surgery under isofluorane (Henry Schein, Melville, NY) anesthesia. Rats received 0.3  $\mu$ l bilateral infusions of an inhibitory DREADD [AAV-hSyn-hM4D(Gi)-mCherry] in the vIPAG (-7.80 AP,  $\pm$ 1.77 ML, -5.89 DV from skull at  $\pm$ 10° angle). Ten minutes elapsed before the syringe was withdrawn to allow for viral diffusion. All rats were implanted with drivable microelectrode bundles in the CeM (-2.30 AP, +3.50 ML, -6.35 DV from dura). Sixteen individual recording wires were bundled and soldered to individual channels of an Omnetics connector. The bundle was integrated into a microdrive permitting advancement in  $\sim$ 0.042 mm increments. The microdrive was cemented on top of the skull and the Omnetics connector was affixed to the head cap. Before implantation, electrodes were coated with Vybrant™ Dil cell-labeling solution (ThermoFisher Scientific, Waltham, MA) to assist with locating electrode placements in brain sections. Implants were secured to the skull using dental cement (Henry Schein) and surrounded by a 50 mL centrifuge tube cut to create an enclosure around the electrode implant to prevent possible damage. Post-surgery, rats received 2 weeks of undisturbed recovery with prophylactic antibiotic treatment (cephalexin; Henry Schein). Five additional rats were excluded from analyses, one due to lack of units detected and four due to recording sites outside of CeM during recording sessions.

### 3.2.1.2 Experiment 2

For experiment 2, final subjects were 7 female and 8 male adult Long-Evans rats (Charles River Laboratories, Raleigh, NC). All rats underwent stereotaxic surgery under isofluorane (Henry Schein, Melville, NY) anesthesia. Rats received 0.3  $\mu$ l bilateral infusions of halorhodopsin (eNpHR; AAV5-hSyn-eNpHR3.0-EYFP; n = 7; 3 females) or YFP (AAV5-hSyn-EYFP; n = 8; 4 females) in the vIPAG (-7.80 AP,  $\pm$ 1.77 ML, -5.89 DV from skull at  $\pm$ 10° angle). Ten minutes elapsed before the syringe was withdrawn to allow for viral diffusion. Fiber optic ferrules were bilaterally implanted in the CeM (-2.30 AP,  $\pm$ 3.50 ML, -7.45 DV from bregma) to permit 532 nm light illumination. Implants were secured to the skull using dental cement (Henry Schein) and surrounded by a 50 mL centrifuge tube cut to create an enclosure around the implants to prevent possible damage. Post-surgery, rats received 2 weeks of undisturbed recovery with prophylactic antibiotic treatment (cephalexin; Henry Schein) before beginning fear discrimination. In order to be considered for analysis, rats had to maintain a nose poke rate higher than 5 poke/min (low rates make suppression ratios unreliable) and had to show a suppression ratio to uncertainty above 0.25 (in order to have room to observe decreases in fear). One rat was excluded based on nose poke criteria.

### 3.2.2 Apparatus

The apparatus for Pavlovian fear discrimination consisted of ten, individual sound-attenuated enclosures that each housed a behavior chamber with aluminum front and back walls, clear acrylic sides and top, and a metal grid floor. Two of the chambers were equipped for single unit recordings (Experiment 1) and the other eight were equipped with

lasers for optogenetic inhibition (Experiment 2). Each grid floor bar was electrically connected to an aversive shock generator (Med Associates, St. Albans, VT). A single food cup and a central nose poke opening, equipped with infrared photocells, were present on one wall. Auditory stimuli were presented through two speakers mounted on the ceiling of each sound-attenuated enclosure. Behavior chambers were modified to allow for free movement of the electrophysiology and optical cables during behavior; plastic funnels were epoxied to the top of the behavior chambers with the larger end facing down, and the tops of the chambers were cut to the opening of the funnel.

For Experiment 2, green (532 nm, 500 mW) lasers (Shanghai Laser & Optics Century Co., Ltd.; Shanghai, China) were used to illuminate the vIPAG. Optical cables were connected to the lasers via 1X2 fiber optic rotatory joints (Doric; Quebec, Canada). Rats were bilaterally connected to the optical cables by a ceramic sleeve placed over the implanted ferrule and ceramic ferrule end of the cable. Black shrink-wrap was also placed on the ends of the cables to block light emission into the behavioral chamber. A PM160 light meter (Thorlabs; Newton, NJ) was used to measure light output.

### *3.2.3 Nose Poke Acquisition*

Before behavioral testing began, all rats were given 2 days of pre-exposure in the home cage to the pellets used for rewarded nose poking. Rats were then shaped to nose poke for these pellets in the experimental chamber. During the first session, rats were issued one pellet every 60 seconds with the nose poke port removed for 30 minutes. Rats were then issued pellets on a fixed ratio schedule in which one nose poke yielded one pellet until they reached at least 50 nose pokes (FR1) in a session. Over the next 5 days,

rats were reinforced for nose pokes on a variable interval schedule first on average every 30 seconds (VI-30), for one session, then on average every 60 seconds (VI-60), for four sessions. All subsequent conditioning sessions were run with a background VI-60 reinforcement schedule that was completely independent of auditory cue or foot shock presentation on conditioning trials. For Experiment 1, rats were trained through five VI-60 sessions then fear discrimination training before undergoing surgery and recovery. Post-recovery, rats received one reminder VI-60 session before single-unit recording sessions began. For Experiment 2, rats were trained through four VI-60 sessions then underwent surgery and recovery before receiving one reminder VI-60 session and beginning pre-exposure.

#### *3.2.4 Pre-Exposure*

In two separate sessions, each rat in Experiment 2 was pre-exposed to the three 10 s auditory cues to be used in Pavlovian fear discrimination. These 42 min sessions consisted of four presentations of each cue (12 total presentations) with a mean inter-trial interval (ITI) of 3.5 min. The order of trial type presentation was randomly determined by the behavioral program and differed for each rat during each session. Auditory cues consisted of repeating motifs of: broadband click, phaser, or trumpet and can be found here: <http://mcdannaldlab.org/resources/ardbark>. Extensive testing has found these cues to be equally salient, yet discriminable (Walker et al., 2018, 2019; Wright et al., 2015).

### 3.2.5 *Fear Discrimination*

Rats in both experiments were trained to discriminate between three auditory cues before undergoing DREADD or optogenetic manipulation. Auditory cues were 10 s in duration and consisted of repeating motifs of a broadband click, phaser, or trumpet. Every session began with a 5-minute habituation period, and ITIs were 3.5 minutes on average. Each cue was associated with a unique probability of foot shock (0.5 mA, 0.5 s): danger,  $p = 1.00$ ; uncertainty,  $p = 0.33$ ; and safety,  $p = 0.00$ . Cue identity was counterbalanced within groups. Foot shock was administered 2 s following the termination of the auditory cue on danger and uncertainty-shock trials. There were 20 total trials per session consisting of 4 danger trials, 4 uncertainty-shock trials, 8 uncertainty-omission trials, and 4 safety trials. The order of trial type presentation was randomly determined by the behavioral program, and differed for each rat, each session for both experiments.

For Experiment 1, each rat received 8, ~70 minute sessions of fear discrimination training before surgery. After recovery and one reminder VI60 session, rats underwent 3 or 5 sessions of fear discrimination during which single-units were recorded. The DREADD recording procedure followed these fear discrimination sessions, and during this procedure, rats were tested under same behavioral program only with a DREADD agonist or saline injection prior to behavior.

For Experiment 2, each rat received 10, ~70 minute sessions of fear discrimination before plug-in days. Rats received an additional 2 sessions of fear discrimination during which the rats were connected to cables like those used during the optogenetic manipulation, but that did not deliver light, to habituate them to the cables. Thus, rats received a total of 12 fear discrimination sessions before the +PE optogenetic

manipulation. After the +PE optogenetic manipulation, rats received an additional 4 untethered fear discrimination sessions before the control cue and ITI manipulations.

### 3.2.6 *Single-Unit Data Acquisition*

During recording sessions for Experiment 1, a 1x amplifying head stage connected the Omnetics connector to the commutator via a shielding recording cable. Analog neural activity was digitized and high-pass filtered via amplifier to remove low-frequency artifacts, and sent to the Ominplex D acquisition system (Plexon Inc., Dallas TX). Behavioral events (cues, shocks, nose pokes) were controlled and recorded by a computer running Med Associates software. Time-stamped events from Med Associates were sent to Ominplex D acquisition system via a dedicated interface module (DIG-716B). The result was a single file (.pl2) containing all time stamps for recording and behavior. Single-units were sorted offline with a template-based spike-sorting algorithm (Offline Sorter V3, Plexon Inc., Dallas TX). Time-stamped spikes and events (cues, shocks, nose pokes) were extracted (Neuroexplorer), and analyzed with statistical routines in MATLAB (Natick, MA).

### 3.2.7 *DREADD Procedure*

For the DREADD procedure, all rats in Experiment 1 received 0.3mg/kg IP injection of a DREADD agonist, JHU37160 dihydrochloride (J60; Hello Bio, Princeton, NJ), or saline across 4 or 8 recording days, half of which were J60 and the other half saline. J60 and saline injections were alternated daily with the order counterbalanced amongst subjects. This design allowed for each rat to act as its own within-subject control, as saline

injections will not activate DREADD receptors but control for handling/injection taking place before test sessions. Injections were given 30 minutes before recording sessions in order to allow sufficient time for receptor activation, then CeM single-units were isolated and held for the entirety of the recording session. Preliminary data found no effect of J60 injection on fear discrimination in rats without DREADD expression (data not shown).

### *3.2.8 Optogenetic Manipulations*

Rats in Experiment 2 underwent three different optogenetic manipulations after fear discrimination training. Four sessions of +PE optogenetic manipulation were followed by 4 fear discrimination, 1 cue optogenetics, and 1 ITI optogenetics sessions. For all manipulations optical inhibition was achieved via delivery of 25 mW of 532 nm 'green' light on each side. Light was produced by a DPSS laser connected to an optical commutator attached to a custom made behavioral cable (Multimode Fiber, 0.22 NA, High-OH, Ø200 µm Core), which connected to the implanted optical ferrule (2.5mm OD, 230 µm Bore Multimode Ceramic Zirconia). Light output of 25 mW was chosen based on calculations the optical fibers will produce ~5 mW/mm<sup>2</sup> of light at distance of 1.2 mm from fiber tip.

#### 3.2.8.1 +PE Optogenetic Manipulation

During the +PE optogenetic manipulation, rats in underwent 4 sessions of CeM illumination via optical cables followed by 4 sessions without illumination or cables. The behavioral programs were exactly the same as during fear discrimination except the CeM was illuminated during the foot shock on uncertainty-shock and danger trials. Illumination

on both uncertainty and danger trials occurred for 4 seconds, beginning immediately after auditory cue offset (2 s), continuing during foot shock (0.5 s), and ending 1.5 s after foot shock offset.

#### 3.2.8.2 Cue Optogenetic Manipulation

Rats were given one session of cue optogenetic manipulation during which they received exposure to the three 10-s auditory cues, but none of the cues were associated with foot shock during this session. Each cue was presented 4 times for a total of 12 trials. The order of trial type presentation was randomly determined by the behavioral program and differed for each rat. The CeM was illuminated during all cue periods, beginning 500 ms before cue onset and ending 500 ms after cue offset for a total of 11s of illumination occurring 12 times. Session order was counterbalanced across rats with the cue and ITI optogenetic manipulations such that half of the rats in each group received the cue manipulation first and the other half received the ITI manipulation first.

#### 3.2.8.3 ITI Optogenetic Manipulation

Rats were given one session of ITI optogenetic manipulation during which they received exposure to the three 10-s auditory cues, but none of the cues were associated with foot shock during this session. Each cue was presented 4 times for a total of 12 trials. The order of trial type presentation was randomly determined by the behavioral program and differed for each rat. The CeM was illuminated during 12 randomized 11-s periods between trials to assess the vIPAG-CeM pathway's role in immediate fear expression.

### 3.2.9 *Histology*

All rats were deeply anesthetized using isoflurane and perfused with 0.9% biological saline and 4% paraformaldehyde in a 0.2 M Potassium Phosphate Buffered Solution. Brains were extracted and post-fixed in a 10% neutral-buffered formalin solution for 24 hrs, stored in 10% sucrose/formalin, frozen at -80°C and sectioned via a sliding microtome. CeM sections from brains with electrodes were processed for light microscopy using Nissl staining. Sections were mounted on glass microscope slides, imaged using a light microscope, and electrode placement confirmed (Paxinos & Watson, 2007). Other CeM sections and vIPAG sections were processed for fluorescent microscopy to confirm DREADD expression. Sections were processed with NeuroTrace™ (ThermoFisher Scientific, Waltham, MA), mounted on glass microscope slides, and coverslipped using VECTASHIELD HardSet Antifade Mounting Medium (Vector Laboratories, Burlingame, CA). DREADD expression was confirmed against a rat brain atlas (Paxinos & Watson, 2007).

Brains with optical implants were processed for fluorescent microscopy. Sections were processed with NeuroTrace™ (ThermoFisher Scientific, Waltham, MA), mounted on glass microscope slides, and coverslipped using VECTASHIELD HardSet Antifade Mounting Medium (Vector Laboratories, Burlingame, CA). Viral transfection and optical implant sites were confirmed against a rat brain atlas (Paxinos & Watson, 2007).

### 3.2.10 *Quantification and Statistical Analysis*

#### 3.2.10.1 *Baseline Nose Poke Analyses*

The time stamp for every nose poke and event onset (cues and shocks) during each session was recorded automatically. Raw data were processed in MATLAB to extract nose poke rates during three periods: the baseline, which was 20 seconds prior to cue onset; the 10-s cue; and the post-cue period, which was 4 seconds following cue offset. Baseline nose pokes are reported in pokes/min and analyzed with ANOVA.

### 3.2.10.2 Calculating and Analyzing Suppression Ratios

Suppression of rewarded nose poking was used as the behavioral indicator of fear. Nose poke rates were calculated for two temporal windows. A suppression ratio for total cued fear was calculated from nose poke rates during a 20 s baseline period just prior to cue onset and the 10 s cue period:  $(\text{baseline} - \text{cue} / \text{baseline} + \text{cue})$ . Complete nose poke suppression was signified by a suppression ratio of '1.00' during the cue relative to baseline, indicating a high level of fear. No nose poke suppression was signified by a suppression ratio of '0.00,' indicating no fear. Intermediate values indicated graded levels of fear. For Experiment 1, units were isolated for saline and J60 sessions, and average cue suppression ratios were calculated for those sessions with repeats removed for multiple units coming from the same session. Independent samples t-tests for suppression ratio were conducted to compare fear to danger, uncertainty, and safety in saline vs. J60 sessions.

### 3.2.10.3 Normalization of Firing

For each neuron, and for each trial type, firing rate (spikes/s) was calculated in 100 ms bins from 20 s prior to cue onset to 20 s following cue offset. Differential firing was

calculated for each bin by subtracting mean baseline firing rate (2 s prior to cue onset), specific to that trial type. Mean differential firing was Z-score normalized across all trial types within a single neuron, such that mean firing = 0, and standard deviation in firing = 1. Z-score normalization was applied to firing across the entirety of the recording epoch, as opposed to only the baseline period, in case neurons showed little/no baseline activity. Z-score normalized firing was analyzed with ANOVA using bin and trial-type as factors. F and p values are reported, as well as partial eta squared and observed power.

#### 3.2.10.4 Identifying Danger Excited and Inhibited Neurons

All neurons were screened for firing during the 10-s cue period. Average normalized firing during the danger cue was calculated, and units were sorted in groups based on whether they were excited or inhibited during the danger cue. Units were considered 'danger excited' if the average firing rate was a non-negative number, whereas units were considered 'danger inhibited' if the average firing rate was negative. These divisions were used in subsequent population analyses.

#### 3.2.10.5 Population and Single-Unit Firing Analyses

Firing for the danger excited and danger inhibited populations was analyzed by ANOVA with cue (danger, uncertainty, and safety) and 250 ms time bins as within subjects factors and drug (saline vs. J60) as between subjects factors. Time spanned from 2s pre-cue to 2s post-cue (14 s total = 56 bins). Paired t-tests with bootstrap confidence intervals were used for post hoc comparisons of cue onset (first 1 s) and late cue (last 5 s) firing.

#### 3.2.10.6 Analysis of Baseline Firing Rates

The first 10 seconds of recording on each trial was averaged for each unit and session to calculate baseline firing rate. ANOVA for baseline firing rate with between subjects factors of population (danger excited vs. danger inhibited) and drug (saline vs. J60) was used to determine whether the two populations of interest differed in unit characteristics and if J60 impacted baseline firing rates.

#### 3.2.10.7 Session-by-Session Analyses

Repeated measures ANOVA for suppression ratios with between factors of group (eNpHR vs. YFP), sex (female vs. male) and transfection (bilateral vs. unilateral), plus within factors of session (2 pre-exposure, 10 discrimination, and 2 tethered) and cue (danger vs. uncertainty vs. safety) were used compare pre-illumination behavior. An identical ANOVA but for 4 +PE illumination sessions was performed to determine the effects of optogenetic inhibition. T-tests with bootstrap confidence intervals were used to examine follow up effects.

#### 3.2.10.8 Trial-by-Trial Analyses

For both the cue and ITI optogenetic manipulations, repeated measures ANOVA for suppression ratios with within factors of cue (danger vs. uncertainty vs. safety) and trial (4) and between factors of group (eNpHR vs. YFP), sex (female vs. male) and transfection (bilateral vs. unilateral) were performed to determine the effects of optogenetic inhibition on cued fear expression. Finally, repeated measures ANOVA for suppression ratios over the ITI laser period with within factors of trial (4) and between

factors of group (eNpHR vs. YFP), sex (female vs. male) and transfection (bilateral vs. unilateral) was performed to determine the effects of optogenetic inhibition on immediate fear expression.

### 3.3 Summary of Experiments and Results

#### 3.3.1 Experiment 1

##### 3.3.1.1 Baseline Nose Poke Rates

Single-units were isolated during saline and J60 sessions, and nose poke rates were calculated for those sessions with repeats removed for multiple units coming from the same session. Independent samples t-test for nose poke rate did not reach significance ( $t_{16} = 1.50$ ,  $p = 0.15$ ), demonstrating there were no significant differences in nose poke rate between saline and J60 sessions (Fig. 3.1).

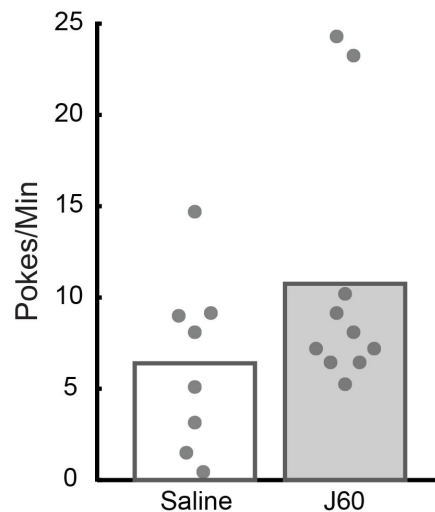


**Figure 3.1 Saline vs. J60 session baseline nose poke rates.** Mean baseline nose poke rates for saline (open bar) and J60 (filled bar) sessions are plotted. Circles show individual session rates for sessions from which CeM units were recorded with repeat sessions removed.

### 3.3.1.2 vIPAG Inactivation Decreases Fear to Uncertainty

Chapter 2 demonstrated that vIPAG activity at the time of foot shock is necessary for +PE signaling (Walker et al., 2019), so inactivation of this region during fear discrimination should interfere with typical fear behavior. Further, it is hypothesized that vIPAG projections to the CeM carry out +PE fear updating, so vIPAG inactivation during fear discrimination would also be expected to impact CeM activity. All rats received vIPAG bilateral transfection with an inhibitory DREADD and electrode implantation in the CeM. DREADD transfection was most prominent in the vIPAG but spread into other regions of the PAG, with transfection of the IPAG next most prominent (Fig. 3.2A, B). Recordings used for analyses were verified for electrode placement within CeM at the time of recording (Fig. 3.2C, D).

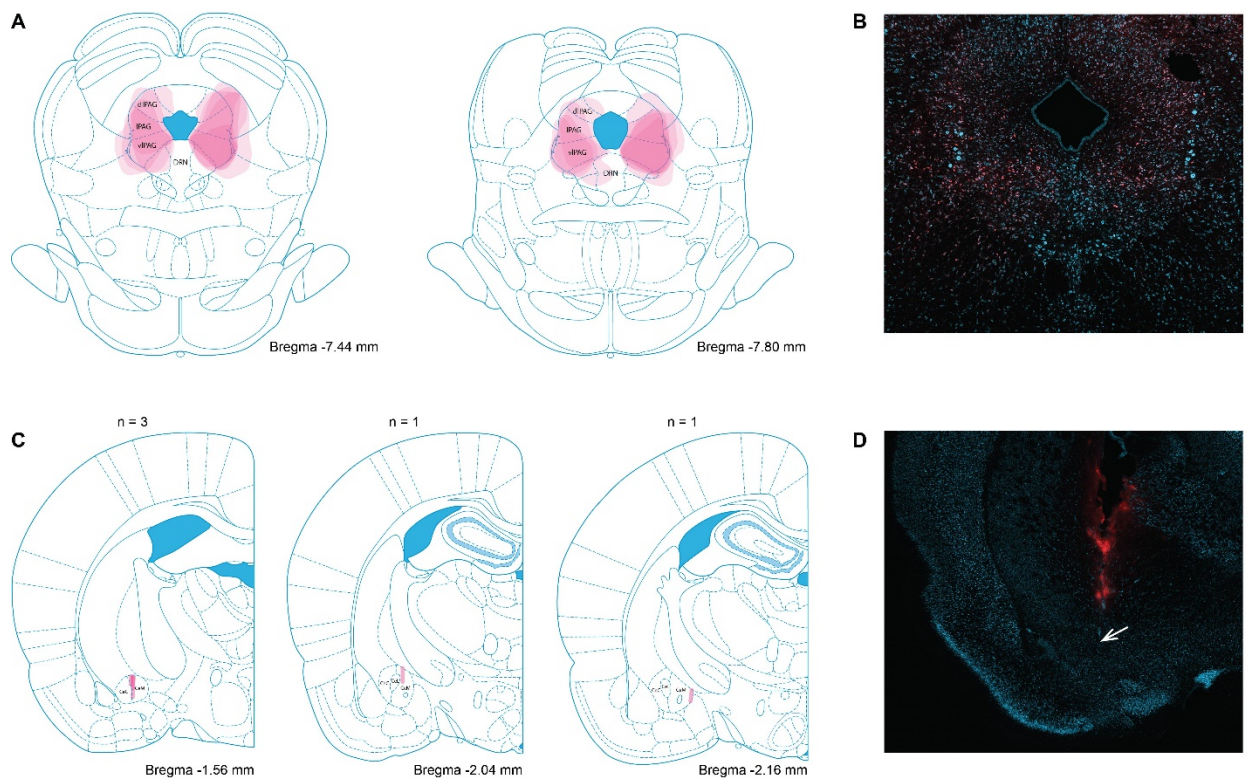


**Figure 3.2 DREADD expression and electrode placements.** (A) vIPAG DREADD transfection extent was mapped for all rats, and average transfection extent can be seen in their overlaid tracings. (B) Representative DREADD transfection (red) is shown with fluorescent Nissl staining (NeuroTrace™, blue). (C) CeM electrode placements were confirmed, and markers show placements during recording sessions used for data analysis. (D) Representative electrode placement in CeM is shown with fluorescent Nissl staining (NeuroTrace™, blue). The white arrow shows final electrode depth, and the red stain shows the electrode path (Vybrant™ Dil dye coated on electrode).

After learning the fear discrimination task, rats went through the DREADD procedure consisting of either 4 or 8 sessions of injections of saline or J60 given 30 mins before fear discrimination testing paired with single-unit recording (Fig. 3.3A). DREADD expression in the vIPAG allowed for chemogenetic inactivation. The drug originally designed to activate these receptors, CNO, has not been a reliable ligand. Newer drugs, such as JHU37160 dihydrochloride (J60), have been designed to cross the blood brain barrier and bind to these designer receptors with high affinity/selectivity.

Single-units were isolated during saline and J60 sessions, and cue suppression ratios were calculated for those sessions with repeats removed for multiple units coming from the same session. Independent samples t-tests for suppression ratio reached significance for the uncertainty cue ( $t_{16} = 2.19$ ,  $p = 0.043$ ), demonstrating that vIPAG inactivation via J60 led to decreased fear to uncertainty (Fig. 3.3B). There was also a trend toward significance for the danger cue ( $t_{16} = 1.85$ ,  $p = 0.084$ ), with lower fear during J60 sessions. Fear to the safety cue did not differ on J60 sessions compared to saline ( $t_{16} = 0.16$ ,  $p = 0.87$ ).

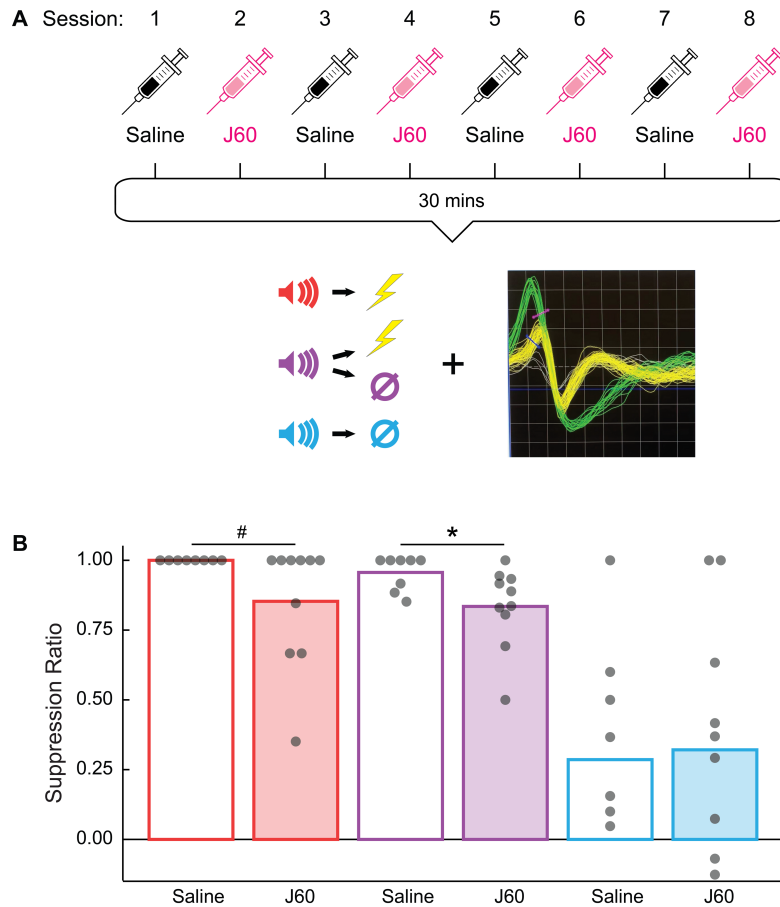


**Figure 3.3 J60 decreases fear to uncertainty. (A)** Diagram depicts DREADD recording procedure. Rats received IP injections of either saline or J60 30 mins before fear discrimination recording sessions. Drug was altered every other day and counterbalanced across rats for up to 8 sessions of recording. **(B)** Mean suppression ratios to danger (red), uncertainty (purple), and safety (blue) for saline (open bars) and J60 (filled bars) sessions are plotted. Circles show individual session suppression ratios for sessions from which CeM units were recorded with repeat sessions removed. \*  $p < 0.05$ , #  $p < 0.10$  between condition difference.

### 3.3.1.3 vIPAG Inactivation Reduces Discriminative Firing in Danger Inhibited Units

Firing across all recording epochs for CeM units was first inspected to determine defining patterns. CeM units were mostly defined by their response to danger, thus, units were grouped into two populations based on these responses. Units were considered ‘danger excited’ if average firing to the danger cue exceeded baseline firing rate, and units were considered ‘danger inhibited’ if danger cue firing was lower than baseline.

Danger excited and danger inhibited units from saline and J60 sessions were separated and analyzed to determine if activity of these populations was impacted by vIPAG inactivation.

First, danger excited units were analyzed to determine whether vIPAG inactivation impacted firing. Repeated measures ANOVA for z normalized firing in 250ms time bins (within factors: cue and time; between factors: drug) across 2 s of baseline, the 10-s cue, and 2-s post-cue period demonstrated no effect or interactions with drug (all  $F < 0.84$ , all  $p > 0.05$ ). There were, however, main effects of cue ( $F_{2,32} = 10.94$ ,  $p < 0.001$ ,  $\eta^2p = 0.41$ , power = 0.99) and time ( $F_{55,880} = 5.41$ ,  $p < 0.001$ ,  $\eta^2p = 0.25$ , power = 1.00) as well as a cue x time interaction ( $F_{110,1760} = 1.48$ ,  $p = 0.001$ ,  $\eta^2p = 0.085$ , power = 1.00). These results indicate that danger excited neurons show differential firing to the three cues across the cue period and this pattern does not differ between saline (Fig. 3.4A - C) and J60 (Fig. 3.4D - F) sessions.

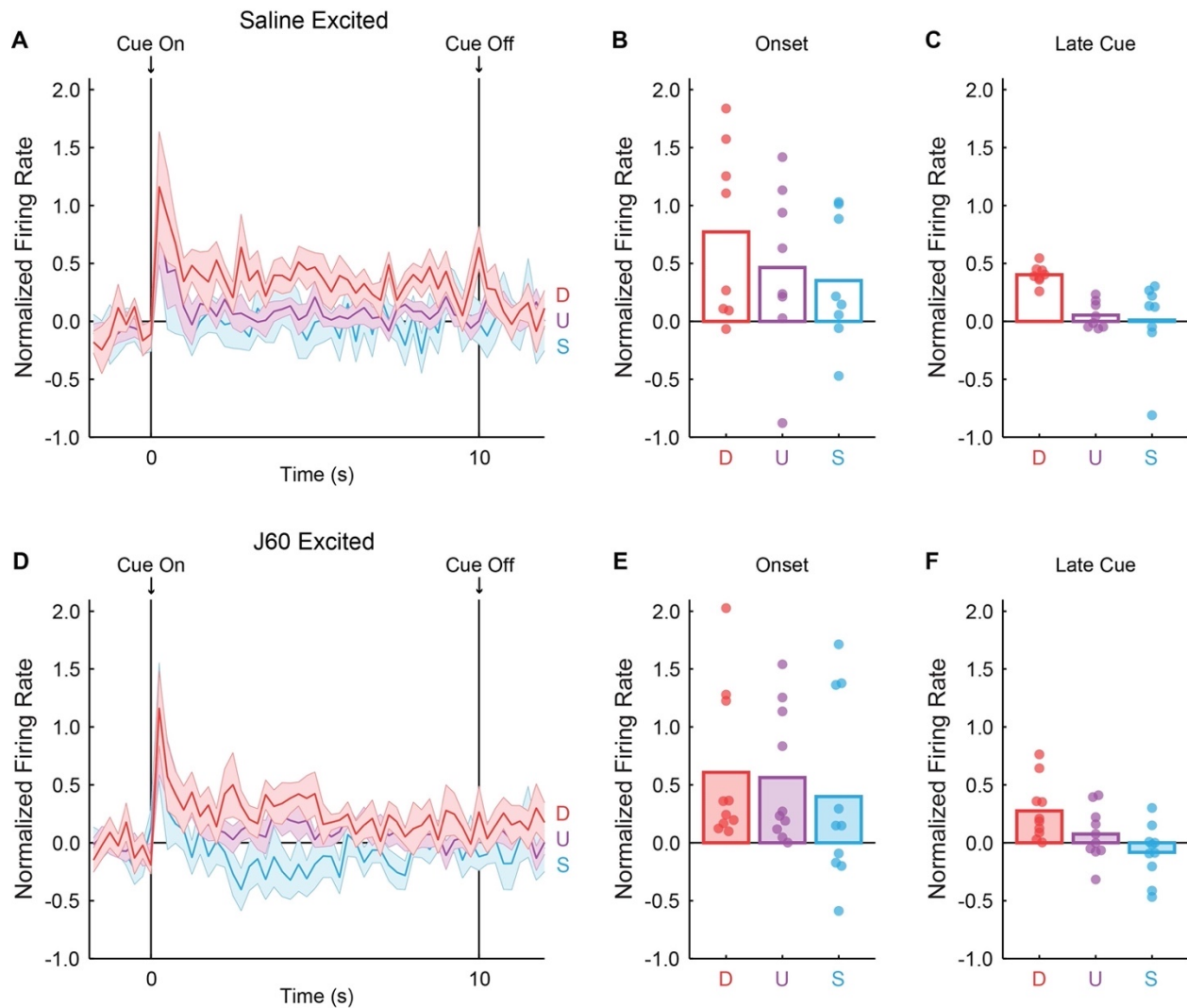


**Figure 3.4 J60 does not impact discriminative firing in danger excited units.** (A) Z-score normalized firing to danger (red), uncertainty (purple), and safety (blue) is shown for danger excited units during saline sessions. (B) Mean cue onset firing (first 1s) to danger (red), uncertainty (purple), and safety (blue) for saline sessions are plotted for danger excited units. Circles show individual session firing rates from which CeM units were recorded. (C) Mean late cue firing (last 5s) to danger (red), uncertainty (purple), and safety (blue) for saline sessions are plotted for danger excited units. Circles show individual session firing rates from which CeM units were recorded. (D) Z-score normalized firing is shown for danger excited units during J60 sessions as in A. (E) Mean cue onset firing for danger excited units during J60 sessions are plotted as in B. (F) Mean late cue firing for danger excited units during J60 sessions are plotted as in C.

Next, danger inhibited units were analyzed to determine whether vIPAG inactivation impacted firing. Repeated measures ANOVA for z normalized firing in 250ms

time bins (within factors: cue and time; between factors: drug) across 2 s of baseline, the 10-s cue, and 2-s post-cue period demonstrated main effects of cue ( $F_{2,38} = 12.49$ ,  $p < 0.001$ ,  $\eta^2p = 0.40$ , power = 0.99) and time ( $F_{55,1045} = 2.30$ ,  $p < 0.001$ ,  $\eta^2p = 0.11$ , power = 1.00) as well as a cue x time interaction ( $F_{110,2090} = 1.61$ ,  $p < 0.001$ ,  $\eta^2p = 0.078$ , power = 1.00). A trend toward significance for a cue x time x drug interaction was also present ( $F_{110,2090} = 1.19$ ,  $p = 0.097$ ,  $\eta^2p = 0.059$ , power = 1.00) and suggested that J60 may have impacted differential firing to the cues (Fig. 3.5A, D). To follow up on this, average firing was isolated for cue onset (first 1s; Fig. 3.5B, E) and late cue (last 5s; Fig. 3.5C, F) periods. Paired t-tests with bootstrap confidence intervals revealed fully discriminative late cue firing in saline units (Fig. 3.5C; all  $t > 3.00$ , all  $p < 0.05$ ), but only danger vs. safety discrimination in J60 units (Fig. 3.5F;  $t_{13} = 2.24$ ,  $p = 0.043$ ). These results indicate that danger inhibited neurons show differential firing to the three cues across the cue period and discriminative firing is impacted by vIPAG inactivation.

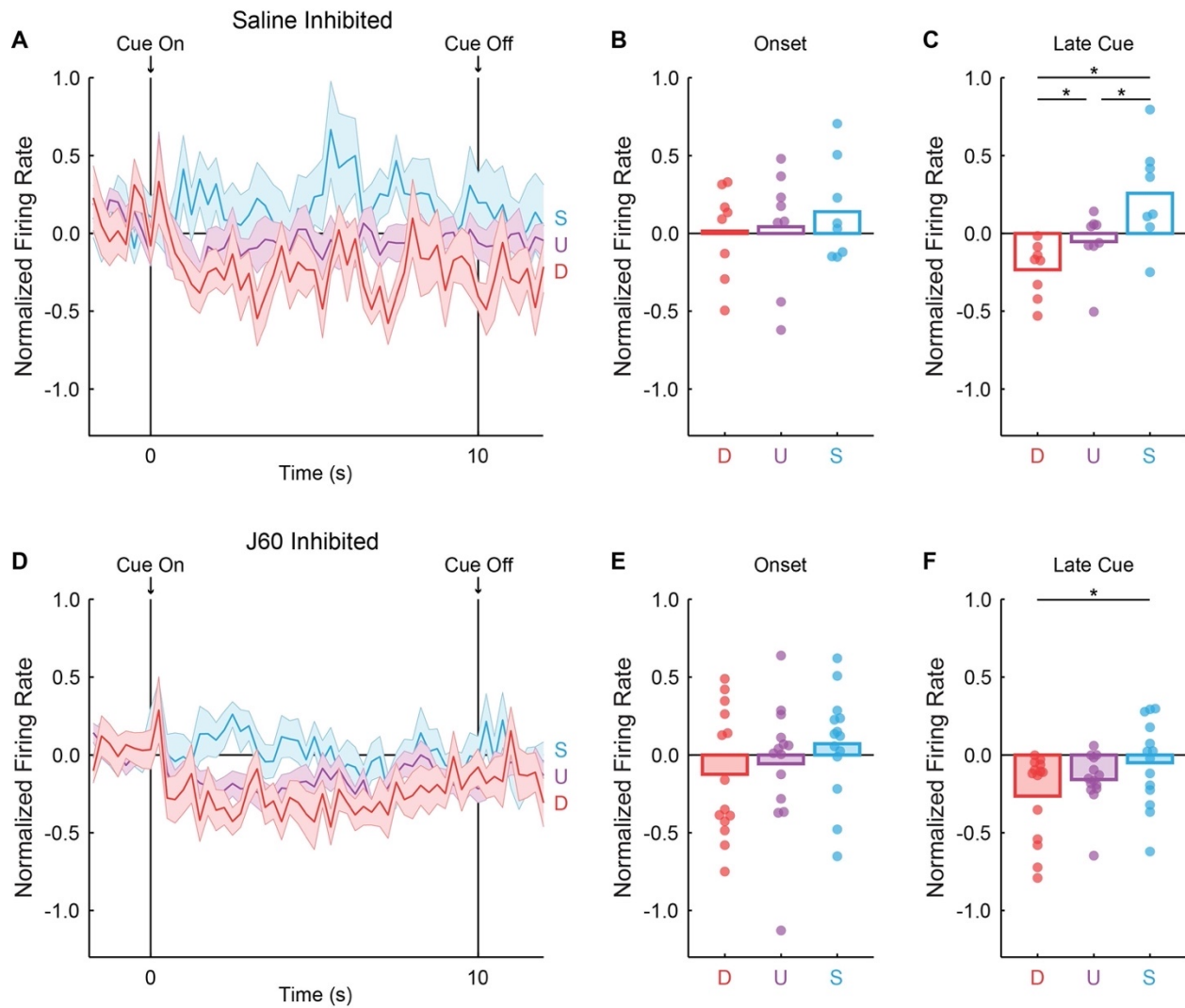


**Figure 3.5 J60 decreases discriminative firing in danger inhibited units.** (A) Z-score normalized firing to danger (red), uncertainty (purple), and safety (blue) is shown for danger inhibited units during saline sessions. (B) Mean cue onset firing (first 1s) to danger (red), uncertainty (purple), and safety (blue) for saline sessions are plotted for danger inhibited units. Circles show individual session firing rates from which CeM units were recorded. (C) Mean late cue firing (last 5s) to danger (red), uncertainty (purple), and safety (blue) for saline sessions are plotted for danger inhibited units. Circles show individual session firing rates from which CeM units were recorded. (D) Z-score normalized firing is shown for danger inhibited units during J60 sessions as in A. (E) Mean cue onset firing for danger inhibited units during J60 sessions are plotted as in B. (F) Mean late cue firing for danger inhibited units during J60 sessions are plotted as in C. \*  $p < 0.05$

To determine whether danger excited and danger inhibited units have different population characteristics, baseline firing rates were compared between the two groups.

The first 10 seconds of baseline firing was averaged for each unit across all trials for danger excited and danger inhibited populations during saline and J60 sessions. ANOVA for baseline firing rate (between factors: population and drug) showed no effect or interaction of population (all  $F < 4.5$ , all  $p > 0.05$ ), indicating that danger excited and danger inhibited populations did not differ in baseline firing (Fig. 3.6).

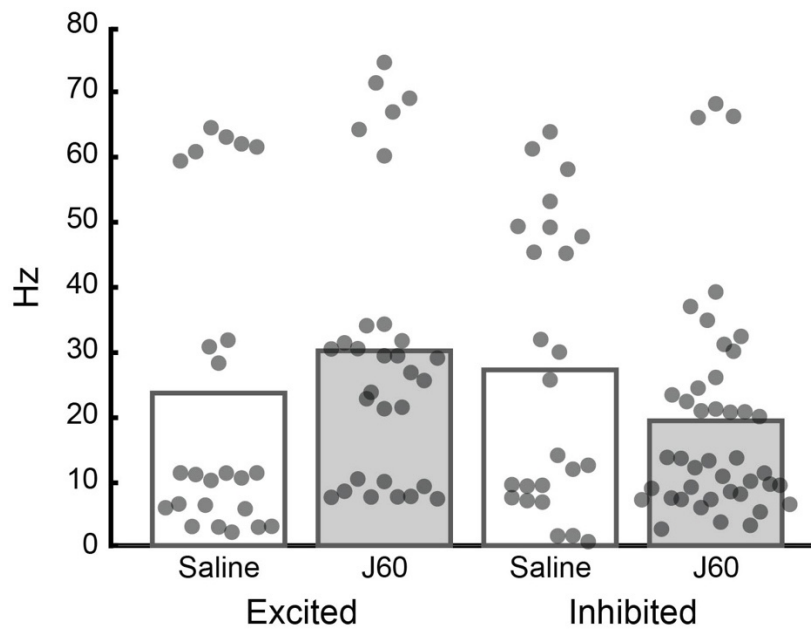


**Figure 3.6 Baseline firing does not differ for danger excited and inhibited populations.** Mean baseline firing rate for saline (open bars) and J60 (filled bars) sessions are plotted for danger excited (left two bars) and danger inhibited (right two bars) units. Circles show individual session firing rates for sessions from which CeM units used in analyses were recorded.

### 3.3.2 Experiment 2

#### 3.3.2.1 Baseline Nose Poke Rates

Repeated measures ANOVA for baseline nose poke rate (within factor: session; between factors: sex, transfection, and group) revealed main effects of session ( $F_{23,162} = 15.69$ ,  $p < 0.001$ ,  $\eta^2_p = 0.69$ , power = 1.00) and sex ( $F_{1,7} = 24.52$ ,  $p = 0.002$ ,  $\eta^2_p = 0.78$ ,

power = 0.99) in baseline nose poke behavior. Interactions of session x sex ( $F_{23,162} = 4.02$ ,  $p < 0.001$ ,  $\eta^2p = 0.37$ , power = 1.00) and session x transfection x sex ( $F_{23,162} = 2.24$ ,  $p = 0.002$ ,  $\eta^2p = 0.24$ , power = 1.00) also reached significance. Sex effects were driven by higher poke rates in males (mean = 34.97) compared to females (mean = 14.24), an effect consistent with previous behavioral findings in this task (Walker et al., 2018, 2019). Importantly, there were no significant effects or interactions with group (all  $F < 4.10$ , all  $p > 0.05$ ), indicating YFP and eNpHR rats did not differ in baseline poke rate (Fig. 3.7).

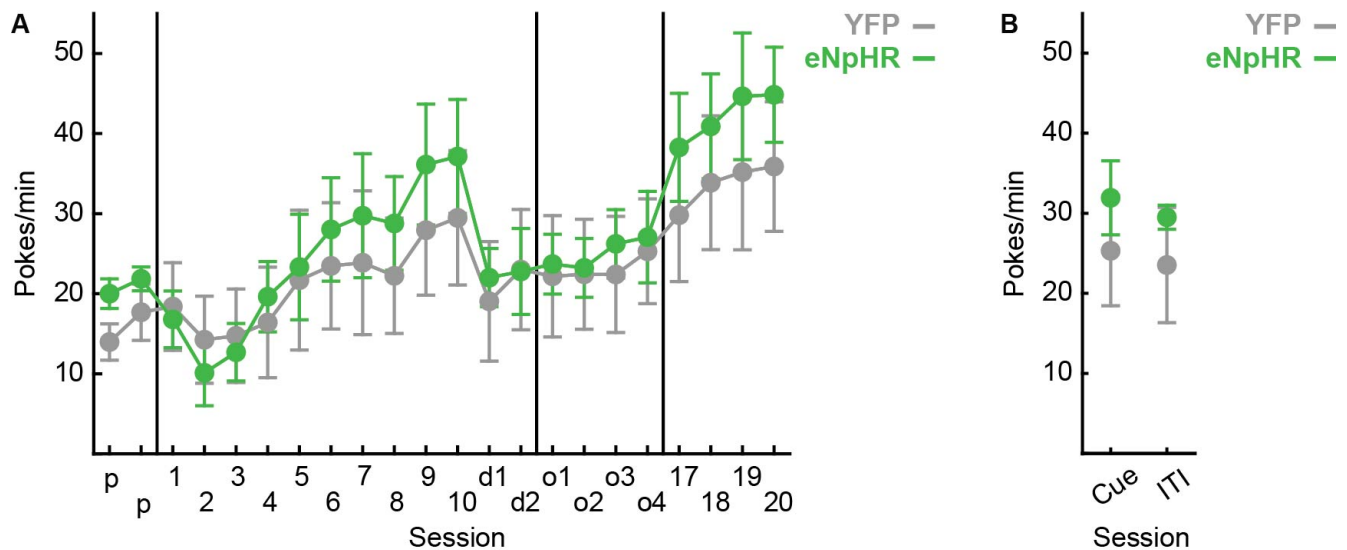


**Figure 3.7 YFP vs. eNpHR baseline nose poke rates. (A)** Mean  $\pm$  SEM baseline nose poke rates for YFP (gray) and eNpHR rats (green) are plotted for the two pre-exposure (p), 12 discrimination (1-10; 17-20), 2 ‘dummy’ tethered-only (d1-d2), and 4 +PE optogenetic manipulation sessions (o1-o4). **(B)** Mean  $\pm$  SEM baseline nose poke rates for YFP (gray) and eNpHR rats (green) are plotted for the Cue and ITI optogenetic manipulation sessions.

### 3.3.2.2 vIPAG-CeM Inhibition during Foot Shock Selectively Reduces Fear to Uncertainty

If vIPAG projections to CeM carry the +PE signal, then inhibition of neural activity in terminals at the time of surprising foot shock should reduce fear to uncertainty, but inhibition during predicted foot shock would have no effect on fear to danger. If these

projections are not involved in the +PE signal, but rather some other aspect of fear, then inhibition may impact immediate fear expression to cues or general fear behavior. The optogenetic design of this experiment was designed to test these possible alternatives.

Rats received bilateral vIPAG transfection with halorhodopsin (eNpHR; AAV5-hSyn-eNpHR3.0-EYFP; n = 7; 3 females) or a control fluorophore (AAV5-hSyn-EYFP; n = 8; 4 females) and bilateral implantation of optical ferrules over the CeM (Fig. 3.8). All rats showed transfection in the vIPAG with ferrules tips just above or inside the CeM boundary (Fig. 3.9A-C). Six rats (3 YFP, 3 eNpHR) showed only unilateral viral expression in the vIPAG. In rats with unilateral vIPAG expression, terminal expression was still seen in the contralateral CeM, albeit to a lesser extent than ipsilateral CeM. Transfection (bilateral vs. unilateral) was therefore included as a factor in analyses to determine whether transfection extent impacted behavioral effects. Rats were trained on the fear discrimination procedure before undergoing the +PE (Fig. 3.9D), Cue (Fig. 3.9E), and ITI (Fig. 3.9F) optogenetic manipulations. The +PE optogenetic manipulation was hypothesized to decrease fear to the uncertainty cue, so higher fear to uncertainty was needed to ensure detection of decreased fear.

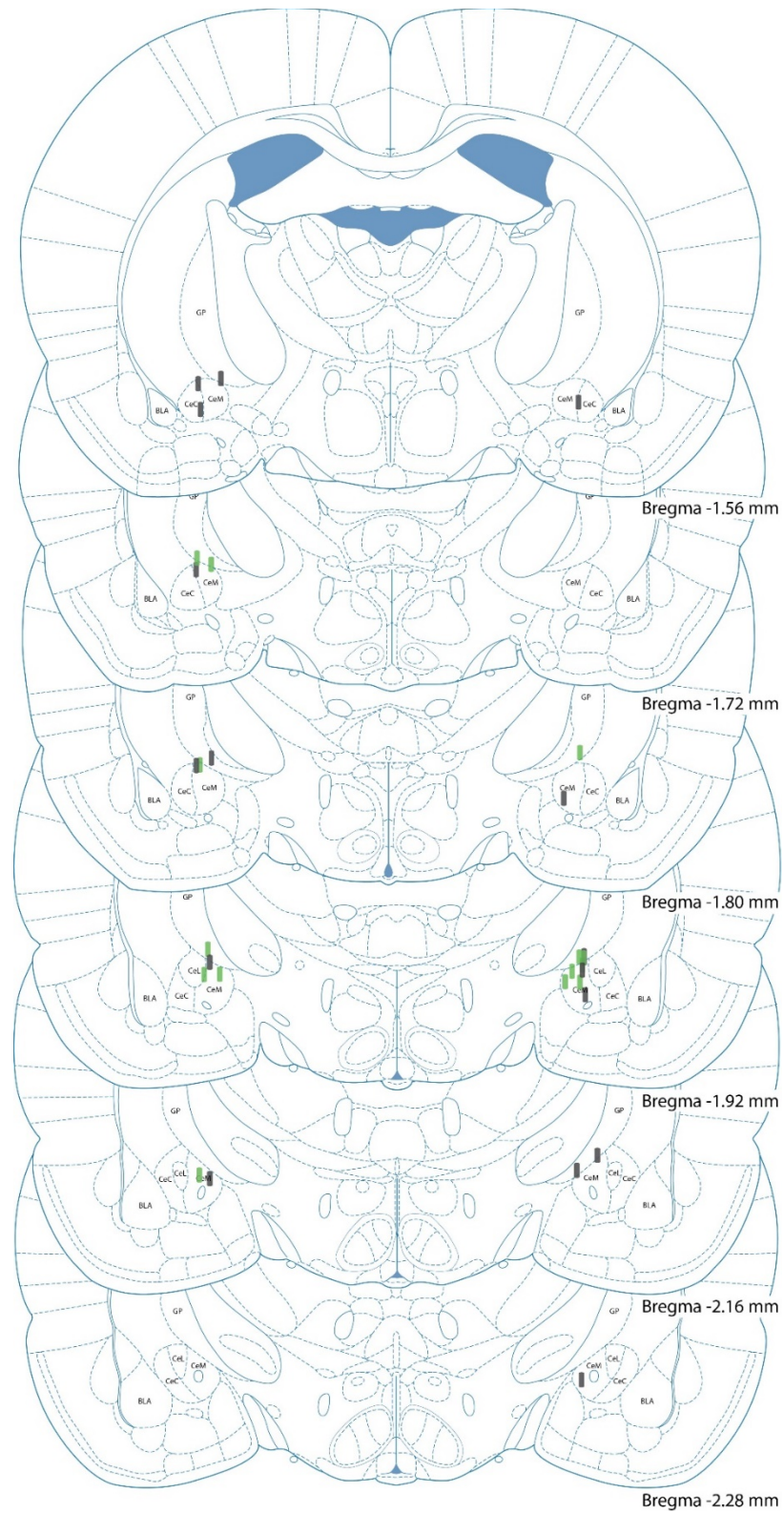


**Figure 3.8 YFP and eNpHR optical ferrule placements.** Placements are shown for bilaterally implanted fiber optic ferrules in YFP (grey) and eNpHR (green) rats. Lowest implant depth is shown by the lower tip of the implant markers.

YFP (Fig. 3.9G) and eNpHR (Fig. 3.9H) rats acquired high fear to danger and uncertainty but low fear to safety over discrimination. These findings were supported by a main effect of cue ( $F_{2,14} = 19.75$ ,  $p < 0.001$ ,  $\eta^2p = 0.74$ , power = 1.00), session ( $F_{11,77} = 9.16$ ,  $p < 0.001$ ,  $\eta^2p = 0.57$ , power = 1.00), and a cue x session interaction ( $F_{22,154} = 3.24$ ,  $p < 0.001$ ,  $\eta^2p = 0.32$ , power = 1.00). Session x sex ( $F_{11,77} = 2.43$ ,  $p = 0.012$ ,  $\eta^2p = 0.26$ , power = 0.93) and cue x session x transfection x group ( $F_{22,154} = 1.73$ ,  $p = 0.029$ ,  $\eta^2p = 0.20$ , power = 0.97) interactions were also present. When considering only the session before optogenetic manipulation (d2), there were no effects of or interactions with group (all  $F < 2.59$ ,  $p > 0.05$ ) or transfection (all  $F < 2.59$ ,  $p > 0.05$ ). Thus, at the start of the optogenetic manipulation, eNpHR and YFP rats showed equivalent fear discrimination.

Across the 4 sessions of +PE optogenetic manipulation, repeated measures ANOVA for danger and uncertainty suppression ratios (within factors: session, trial, and cue; between factors: sex, transfection, and group) revealed a main effect of cue ( $F_{1,7} = 34.37$ ,  $p = 0.001$ ,  $\eta^2p = 0.83$ , power = 1.00) and, critically, a cue x trial x group interaction ( $F_{15,105} = 2.19$ ,  $p = 0.011$ ,  $\eta^2p = 0.24$ , power = 0.96). This interaction was driven by decreased fear to uncertainty in eNpHR rats, which was most apparent between the first and second sessions of the optogenetic manipulation (Fig. 3.9I, J). Interactions of trial x sex ( $F_{15,105} = 2.65$ ,  $p = 0.002$ ,  $\eta^2p = 0.27$ , power = 0.99), trial x transfection x group ( $F_{15,105} = 1.82$ ,  $p = 0.041$ ,  $\eta^2p = 0.21$ , power = 0.91), trial x transfection x sex ( $F_{15,105} = 2.98$ ,  $p = 0.001$ ,  $\eta^2p = 0.30$ , power = 0.99), and cue x trial x sex ( $F_{15,105} = 1.81$ ,  $p = 0.042$ ,  $\eta^2p = 0.21$ , power = 0.52) were also present.

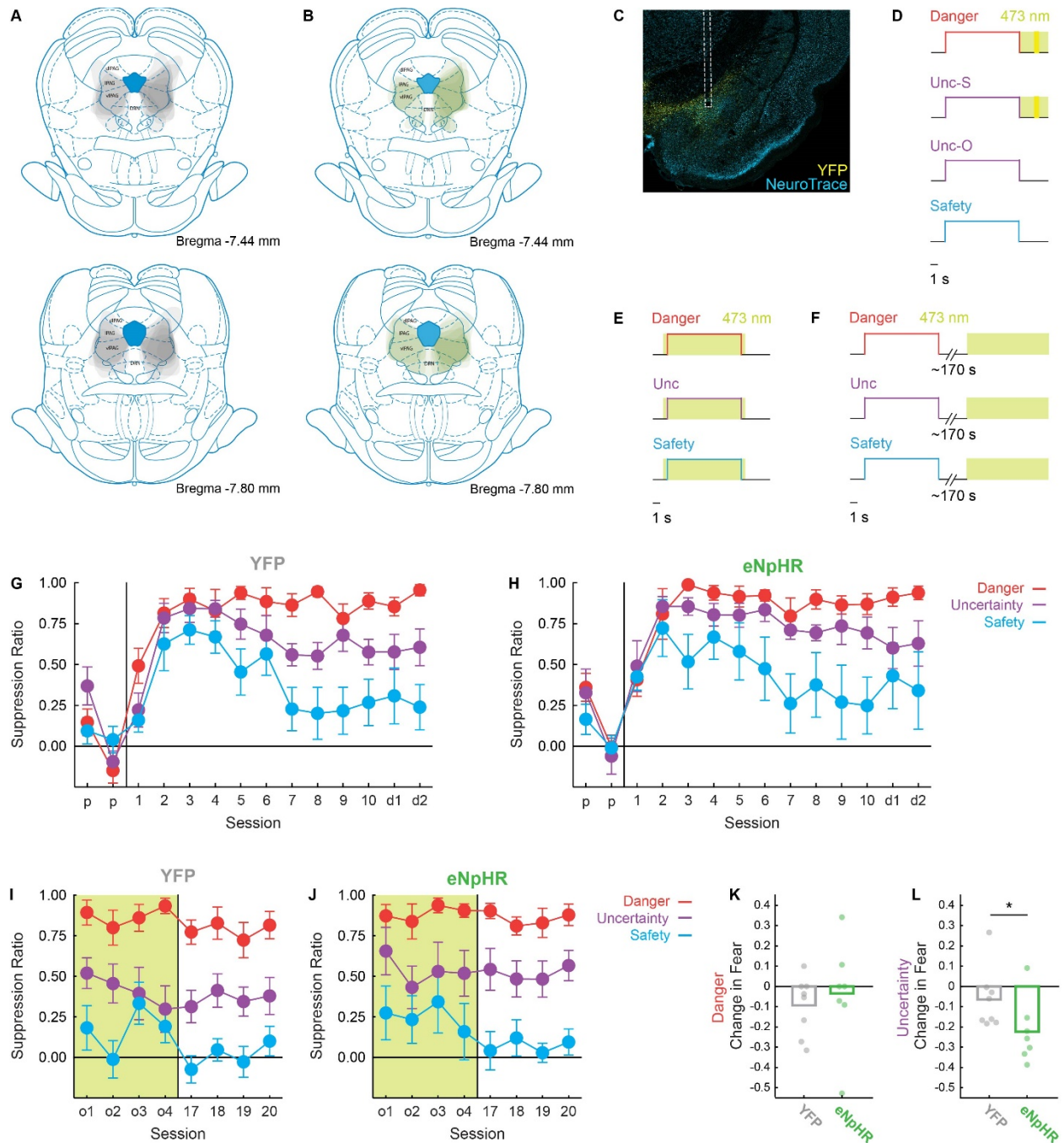


**Figure 3.9 vIPAG-CeM optogenetic inhibition during foot shock decreases fear to uncertainty.** (A) Viral transfection extent was mapped for all YFP rats, and average transfection extent can be seen in their overlaid tracings. (B) Viral transfection extent for eNpHR rats as in A. (C) Representative terminal transfection and ferrule placement is shown with YFP (yellow) and NeuroTrace™ (blue). Fiber optic ferrule placement can be seen in the CeM as denoted by the white dashed outline. Note that virus was infused in the vIPAG and YFP demonstrates terminal expression from vIPAG projections. (D) During the 4 +PE optogenetic sessions, green-light illumination began at cue offset, continued during the 0.5-s shock (yellow period), and lasted 1.5 s after shock for a total of 4 s. (E)

During the Cue optogenetic manipulation, green-light illumination began 0.5 s before cue onset, continued during the 10-s cue, and lasted 0.5 s after cue offset for a total of 11 s. Illumination occurred on all cue trials, and no shocks were given for any cue during this session. **(F)** During the ITI optogenetic manipulation, green-light illumination occurred for a total of 11 s during the ITI period. Illumination occurred between all cue trials, with an average of 170 s between cue presentation and light illumination. No shocks were given for any cue during this session. **(G)** Mean  $\pm$  SEM suppression ratios for YFP rats to danger (red), uncertainty (purple), and safety (blue) are shown for the 2 pre-exposure sessions (p), 12 discrimination (1-10), and 2 'dummy' tethered-only (d1-d2), sessions. **(H)** eNpHR suppression ratio data shown as in G. **(I)** Mean  $\pm$  SEM suppression ratios for YFP rats to danger (red), uncertainty (purple), and safety (blue) are shown for the 4 +PE optogenetic manipulation (o1-o4) and post-illumination discrimination (17-20) sessions. Green background indicates laser illumination occurred during those sessions. **(J)** eNpHR suppression ratio data shown as in I. **(K)** Change in fear to the danger cue between +PE optogenetics sessions 1 and 2 for YFP (grey) and eNpHR (green) rats. Bars show group average and circles indicate individual difference scores. **(L)** Change in fear to the uncertainty cue between +PE optogenetics sessions 1 and 2 for YFP (grey) and eNpHR (green) rats as in K. \* $p < 0.05$  between groups.

To better understand the behavioral change during illumination, difference scores were calculated for danger and uncertainty: (+PE optogenetic manipulation session 2 suppression ratio) - (+PE optogenetic manipulation session 1 suppression ratio). No group differences were observed for the danger difference score (Fig. 3.9K,  $t_{13} = -0.14$ ,  $p = 0.90$ ). For the uncertainty difference score, t-test and bootstrap confidence intervals showed a significantly greater decrease in fear in the eNpHR group compared to YFP (Fig. 3.9L,  $t_{13} = 2.18$ ,  $p = 0.049$ ). These data demonstrate that vIPAG-CeM inhibition during shock periods did not alter fear to danger but did reduce fear to uncertainty.

### 3.3.2.3 vIPAG-CeM Inhibition during Cue or ITI Does Not Alter Cued Fear or Fear Expression

To determine whether vIPAG-CeM signaling may be critical for cued fear or fear expression, rats were also given one session of cue or ITI optogenetic manipulation.

During the cue optogenetic manipulation, illumination occurred during all cues and each was presented 4 times without reinforcement. Cued fear did not differ between YFP (Fig. 3.10A) and eNpHR (Fig. 3.10B) rats due to illumination during cue periods. Repeated measures ANOVA for suppression ratios during the cue session (within factors: cue and trial; between factors: sex, transfection, and group) confirmed these results, demonstrating no effect or interactions of group (all  $F < 2.65$ , all  $p > 0.05$ ). Main effects of cue ( $F_{2,14} = 7.30$ ,  $p = 0.007$ ,  $\eta^2p = 0.51$ , power = 0.87) and trial ( $F_{3,21} = 6.71$ ,  $p = 0.002$ ,  $\eta^2p = 0.49$ , power = 0.94) demonstrated that rats were discriminating between the cues and fear generally decreased over trials, as cues were no longer reinforced.

During the ITI optogenetic manipulation, each cue was presented 4 times without reinforcement and illumination occurred during 12 ITI periods. Cued fear did not differ between YFP (Fig. 3.10C) and eNpHR (Fig. 3.10D) rats during the ITI optogenetic manipulation session, as expected. Repeated measures ANOVA for cue suppression ratios during the ITI session (within factors: cue and trial; between factors: sex, transfection, and group) confirmed these results, demonstrating a group x sex ( $F_{1,7} = 6.75$ ,  $p = 0.036$ ,  $\eta^2p = 0.49$ , power = 0.61) interaction but no main effect or interactions of group with cue or trial (all  $F < 3.12$ , all  $p > 0.05$ ). Main effects of cue ( $F_{2,14} = 6.88$ ,  $p = 0.008$ ,  $\eta^2p = 0.50$ , power = 0.85) and trial ( $F_{3,21} = 9.52$ ,  $p < 0.001$ ,  $\eta^2p = 0.58$ , power = 0.99) once again demonstrated that rats were discriminating between the cues and fear generally decreased over trials, as cues were no longer reinforced.

Further, illumination during ITI periods did not alter immediate fear expression in YFP or eNpHR rats (Fig. 3.10E). This was supported by repeated measures ANOVA for suppression ratios over the laser period (within factor: trial; between factors: sex,

transfection, and group), which demonstrated no significant effects or interactions with group (all  $F < 1.60$ , all  $p > 0.05$ ). Together, these results do not support a role for vIPAG-CeM signaling in cued fear or fear expression in this task.

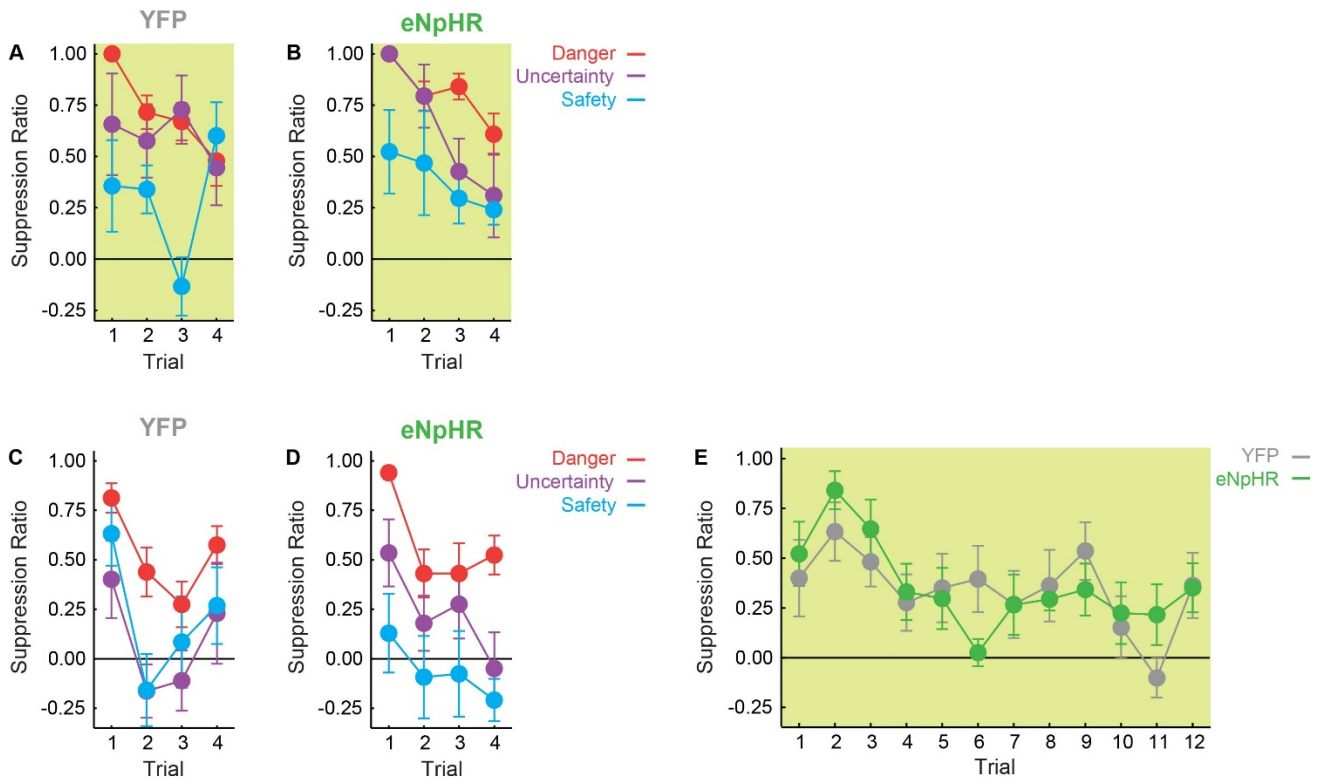


**Figure 3.10 vIPAG-CeM optogenetic inhibition during cue or ITI does not alter fear.** (A) Mean  $\pm$  SEM suppression ratios for YFP rats to danger (red), uncertainty (purple), and safety (blue) are shown for the cue optogenetic manipulation session with individual trials plotted. Green background indicates laser illumination occurred during those trials. (B) eNpHR suppression ratio data shown as in A. (C) Mean  $\pm$  SEM suppression ratios for YFP rats to danger (red), uncertainty (purple), and safety (blue) are shown for the ITI optogenetic manipulation session with individual trials plotted. Illumination did not occur during the cue for this session. (D) eNpHR suppression ratio data shown as in C. (E) Mean  $\pm$  SEM suppression ratios for YFP (grey) and eNpHR (green) rats during the ITI laser period are shown for the ITI optogenetic manipulation session with individual trials plotted. Green background indicates laser illumination occurred during those trials.

### 3.4 Discussion

Experiment 1 used DREADDs paired with *in vivo* recording to demonstrate vIPAG inactivation decreases behavioral fear to uncertainty and reduces discriminative firing in some neuronal populations. CeM single units were best defined by their response to a danger cue, resulting in ‘danger excited’ and ‘danger inhibited’ populations. These populations were differentially impacted by vIPAG inactivation; while danger excited units showed equivalent discriminative firing during saline and J60 sessions, danger inhibited units showed reduced discriminative firing due to J60. This effect was most evident in later cue firing, as no difference was detected at cue onset. These results exhibit CeM involvement in cued fear processing and that this activity is partially dependent on vIPAG input. While CeM-vIPAG projections have previously been the focus in fear settings, these data are some of the first to showcase the importance of information flow from vIPAG-CeM for fear processing and behavior. However, this experiment was not able to tie vIPAG inactivation temporally to +PE periods, so the question still remained whether +PEs are sent to CeM from direct vIPAG projections.

Experiment 2 used pathway specific optical inhibition of vIPAG-CeM to determine whether activity in this pathway is necessary for +PE fear updating. Illumination of vIPAG terminals in the CeM at the time of foot shock selectively decreased fear to the uncertainty cue while leaving fear to danger unaffected, indicating this pathway indeed carries vIPAG +PEs. While this effect was more transient than inhibition of vIPAG cell bodies (Walker et al., 2019), that is not surprising. It is likely that multiple regions receive +PE signals from the vIPAG to carry out appropriate behavioral and neural responses to this updating signal, and there may even be redundancy in these projections. It would then be expected

that the largest behavioral difference would be seen by vIPAG cell body inhibition. Results further suggest that this pathway is specifically activated during +PE periods, as vIPAG-CeM inhibition during cue and ITI periods did not impact cued fear or immediate fear expression. Together these experiments indicate the vIPAG +PEs are sent to the CeM to carry out fear updating.

In considering the implications of these findings, some caveats should be noted. Firstly, DREADD expression in Experiment 1 was not restricted to the vIPAG. Spread outside of vIPAG was mainly seen in IPAG and dIPAG. While expression was greatest and most consistent in vIPAG, effects of IPAG and dIPAG inactivation due to J60 cannot be ruled out and may have contributed to differences in behavioral and/or firing patterns. Ideally, future experiments would use targeted optical inhibition of the vIPAG during +PE periods to more directly tie changes in vIPAG PE signaling to CeM activity.

It is also worth noting that J60 is a relatively novel DREADD agonist, so there are only a couple of published experiments using this agonist (Barbano et al., 2020; Lewis et al., 2020). CNO has been demonstrated as an unreliable ligand that does not directly act on receptors (Manvich et al., 2018), however, and J60 was designed to have higher affinity and potency for hM4Di. Behavioral and firing differences due to J60 administration lend support to its effectiveness and specificity, as fear was impacted but not baseline nose pokes nor baseline firing rate. Further, pilot data show that J60 in the absence of DREADD expression does not disrupt fear discrimination compared to saline in the same task (data not shown). Together these findings indicate J60 is an effective DREADD agonist that does not impact behavior when administered alone.

In Experiment 2, a subset of rats only showed unilateral vIPAG expression of eNpHR. Because of contralateral projections from vIPAG to CeM, there was at least some bilateral terminal expression seen in the CeM of unilaterally expressing rats. To further mitigate the potential effect of expression pattern, expression (bilateral vs. unilateral) was used as a factor in analyses and did not appear to impact the major findings in the experiment. It is possible still that optogenetic illumination may have been more effective with more complete bilateral expression.

Finally, there were a number of significant effects related to biological sex in Experiment 2. Sex differences in baseline behavior (i.e. nose poke rate and absolute fear levels) in the optogenetics results are consistent with previous findings in the same behavioral task (Walker et al., 2018, 2019). While there were some interactions with sex in suppression ratio data, sex was not a significant factor in the main +PE optogenetic finding. While Experiment 1 was conducted solely in females, it seems likely that the regions involved in +PE signaling do not differ between males and females given the results of Experiment 2 and the findings relayed in chapter 2.

Because two functional populations of CeM units were identified in Experiment 1, it raises the question as to whether these may be distinct populations based on neurotransmitter usage. Although there was not a method to identify specific neuron types in the present experiment, baseline firing rates may provide some insight into whether these populations differ on basic unit characteristics. Interestingly, there were no differences in baseline firing rate between populations, suggesting that danger excited and danger inhibited units may have consist of similar neuronal types with functional differences. While not specific to a neurotransmitter population, Experiment 2 was able

to tie effects to those terminals coming from vIPAG. Pathway tracing studies may be helpful in illuminating the neuron types comprising this pathway and uncovering neuronal types would be illuminating in future experiments.

Much is still unknown in +PE circuitry, including what vIPAG and CeM neuron types send and receive +PE signals and what other pathways receive vIPAG +PE information. This chapter identified the vIPAG-CeM as a pathway carrying +PE information used for between session fear updating. Chapter 4 will focus on determining the source of those errors opposing +PE signals: -PEs.

## **Chapter 4: Dorsal Raphe Serotonin Regulation of Fear Updating**

## 4.1 Introduction

Previous research has offered the DRN as the source of aversive –PE generation (Berg et al., 2014). In particular, neurotoxic lesions of the DRN prevented decreases in fear to an uncertain cue (Berg et al., 2014). It left open the question of which subpopulation in the DRN may be involved in computing the error, however, due to the non-specific nature of the lesions. These results suggested a possible impairment in –PE signaling, but the manipulation lacked the temporal and transmitter specificity required to casually implicate DRN 5-HT as the source of –PE generation. Others have suggested the DRN may instead be involved in positive or unsigned prediction errors (Matias et al., 2017). Given the DRN's largest cell population is serotonergic and serotonin has been shown to play a role in fear learning, I hypothesized that this subset of neurons in the DRN generate aversive –PEs.

In this chapter, I sought to uncover a relationship between DRN 5-HT -PE activity and fear updating. To do so, I employed a fear discrimination procedure in which a safety cue predicted shock omission deterministically and an uncertainty cue predicted shock omission probabilistically (Berg et al., 2014; Walker et al., 2018, 2019; Wright et al., 2015). Fear to the uncertainty cue was of particular interest, as this behavior would be reliant on –PE updating. In Experiment 1, I selectively deleted DRN serotonergic neurons to determine whether this impacts fear discrimination or extinction of the uncertain cue. In Experiment 2, I selectively inhibited DRN 5-HT activity around the time of predicted (safety) and surprising (uncertainty) foot shock omission. Inhibition during shock periods was used to test for possible involvement in positive or unsigned PE signaling. Analyses focused on subsequent changes in fear to the safety and uncertainty cues and the

temporal emergence of these changes. These experiments allowed me to determine if DRN 5-HT activity is necessary to update and decrease future fear via -PE.

## **4.2 Materials and Methods**

### *4.2.1 Experimental Subjects*

All rats were maintained on a 12-hour light-dark cycle (lights on 0600 – 1800). Rats were single housed and food restricted to 85% of their free-feeding body weight during Pavlovian fear conditioning with standard laboratory chow (18% Protein Rodent Diet #2018, Harlan Teklad Global Diets, Madison, WI). Water was available *ad libitum* in the home cage but was not available during behavioral testing, at which time only Dustless Precision Test Pellets (Bio-Serv: Cat #F0021) were present. All protocols were approved by the Boston College Animal Care and Use Committee, and all experiments were carried out in accordance with the NIH guidelines regarding the care and use of rats for experimental procedures.

#### 4.2.1.1 Experiment 1

For Experiment 1, final subjects were 14 female and 9 male adult TPH2-cre transgenic rats on the background of Long-Evans born in the laboratory. All rats underwent stereotaxic surgery under isoflurane (Henry Schein, Melville, NY) anesthesia. Rats received 0.75  $\mu$ l bilateral infusions of a 50/50 mixture of cre-caspase (rAAV5-Flex-taCasp3-TEVp) and cre-YFP (rAAV5-Ef1a-DIO-eYFP) to delete serotonergic neurons (Caspase; n=12; 7 females) or cre-YFP only (YFP; n=11; 7 females) in the DRN (-8.00 AP,  $\pm$ 0.40 ML, -6.45 DV from skull). Ten minutes elapsed before the syringe was

withdrawn to allow for viral diffusion. Rats received at least 10 days of undisturbed recovery post-surgery before beginning behavior.

#### 4.2.1.2 Experiment 2

For Experiment 2, final subjects were 14 female and 6 male adult TPH2-cre transgenic rats on the background of Long-Evans born in the laboratory. All rats underwent stereotaxic surgery under isoflurane (Henry Schein, Melville, NY) anesthesia. Rats received 0.75  $\mu$ l bilateral infusions of cre-dependent halorhodopsin (rAAV5-Ef1a-DIO-eNpHR3.0-eYFP; n=10; 7 females) or cre-YFP (rAAV5-Ef1a-DIO-eYFP; n=10; 7 females) in the DRN (-8.00 AP,  $\pm$ 0.40 ML, -6.45 DV from skull). Ten minutes elapsed before the syringe was withdrawn to allow for viral diffusion. Fiber optic ferrules were bilaterally implanted in the DRN (-8.10 AP,  $\pm$ 1.83 ML, -6.35 DV from skull at  $\pm$ 10° angle) to permit 532 nm light illumination. Implants were secured with dental cement surrounded by a cut 50 mL plastic centrifuge tube to protect the implants. Rats received 2 weeks of undisturbed recovery post-surgery with prophylactic antibiotic treatment (cephalexin; Henry Schein) before resuming behavior. In order to be considered for analysis, rats had to maintain a nose poke rate higher than 5 poke/min (low rates make suppression ratios unreliable). One rat was excluded from analyses based on nose poke criteria.

#### *4.2.2 Apparatus*

The apparatus for Pavlovian fear discrimination consisted of eight, individual sound-attenuated enclosures that each housed a behavior chamber with aluminum front and back walls, clear acrylic sides and top, and a metal grid floor. Each grid floor bar was

electrically connected to an aversive shock generator (Med Associates, St. Albans, VT). A single food cup and a central nose poke opening, equipped with infrared photocells, were present on one wall. Auditory stimuli were presented through two speakers mounted on the ceiling of each sound-attenuated enclosure. Behavior chambers were modified to allow for free movement of the optical cables during behavior; plastic funnels were epoxied to the top of the behavior chambers with the larger end facing down, and the tops of the chambers were cut to the opening of the funnel. Green (532 nm, 500 mW) lasers (Shanghai Laser & Optics Century Co., Ltd.; Shanghai, China) were used to illuminate the vIPAG. Optical cables were connected to the lasers via 1X2 fiber optic rotatory joints (Doric; Quebec, Canada). Rats were bilaterally connected to the optical cables by a ceramic sleeve placed over the implanted ferrule and ceramic ferrule end of the cable. Black shrink-wrap was also placed on the ends of the cables to block light emission into the behavioral chamber. A PM160 light meter (Thorlabs; Newton, NJ) was used to measure light output.

#### *4.2.3 Nose Poke Acquisition*

Before behavioral testing began, all rats were given 2 days of pre-exposure in the home cage to the pellets used for rewarded nose poking. Rats were then shaped to nose poke for these pellets in the experimental chamber. During the first session, rats were issued one pellet every 60 seconds with the nose poke port removed for 30 minutes. Rats were then issued pellets on a fixed ratio schedule in which one nose poke yielded one pellet until they reached at least 50 nose pokes (FR1) in a session. Over the next 5 days, rats were reinforced for nose pokes on a variable interval schedule first on average every

30 seconds (VI-30), for one session, then on average every 60 seconds (VI-60), for four sessions. All subsequent conditioning sessions were run with a background VI-60 reinforcement schedule that was completely independent of auditory cue or foot shock presentation on conditioning trials. Rats in Experiment 2 were trained through four VI-60 sessions then underwent surgery and recovery before receiving two reminder VI-60 sessions and beginning pre-exposure.

#### *4.2.4 Pre-Exposure*

In two separate sessions, each rat was pre-exposed to the three 10 s auditory cues to be used in Pavlovian fear discrimination. These 42 min sessions consisted of four presentations of each cue (12 total presentations) with a mean inter-trial interval (ITI) of 3.5 min. The order of trial type presentation was randomly determined by the behavioral program and differed for each rat during each session. Auditory cues consisted of repeating motifs of: broadband click, phaser, or trumpet and can be found here: <http://mcdannaldlab.org/resources/ardbark>. Extensive testing has found these cues to be equally salient, yet discriminable (Berg et al., 2014; Walker et al., 2018, 2019; Wright et al., 2015).

#### *4.2.5 Fear Discrimination*

Rats were exposed to three auditory cues that were 10 s in duration and consisted of repeating motifs of a broadband click, phaser, or trumpet. Every session began with a 5-minute habituation period, and ITIs were 3.5 minutes on average. Each cue was associated with a unique probability of foot shock (0.5 mA, 0.5 s): danger,  $p = 1.00$ ;

uncertainty,  $p = 0.25$ ; and safety,  $p = 0.00$ . Cue identity was counterbalanced within groups. Foot shock was administered 2 s following the termination of the auditory cue on danger and uncertainty-shock trials. There were 16 total trials per session consisting of 4 danger trials, 6 uncertainty-omission trials, 2 uncertainty-shock trials, and 4 safety trials. The order of trial type presentation was randomly determined by the behavioral program, and differed for each rat, each session for both experiments. Rats in Experiment 1 underwent 16 sessions of Pavlovian fear discrimination before moving on to selective extinction. Rats in Experiment 2 underwent 12 sessions of Pavlovian fear discrimination before undergoing optogenetic manipulations. During the last two fear discrimination sessions (11-12), rats were connected to 'dummy' cables like those used during the optogenetic manipulation, but that did not deliver light, to habituate them to the cables.

#### 4.2.6 *Selective Extinction*

Selective extinction sessions resembled fear discrimination sessions but the uncertainty cue was no longer associated with foot shock. The probability of foot shock to the danger and safety cues remained the same as in fear discrimination, meaning the probabilities were now: danger,  $p = 1.00$ ; uncertainty,  $p = 0.00$ ; and safety,  $p = 0.00$ . The order of trial type presentation was randomly determined by the behavioral program, and differed for each rat, each session for both experiments. Rats in Experiment 1 received 8 sessions of selective extinction following their 16 fear discrimination sessions. There were 18 total trials per session consisting of 4 danger trials, 8 uncertainty trials, and 4 safety trials. Rats in Experiment 2 received 8 total sessions of selective extinction, the first 4 during the -PE optogenetic manipulation and the second 4 without any additional

manipulation or cables present. There were 18 total trials per session consisting of 4 danger trials, 8 uncertainty trials, and 6 safety trials.

#### *4.2.7 Optogenetic Manipulations*

Rats in Experiment 2 underwent 8 total sessions, split in two sets of 4, of optogenetic manipulation. The first 4 sessions consisted of a +PE optogenetic manipulation occurring immediately following fear discrimination training. After the +PE optogenetic manipulation, the rats received an additional 2 fear discrimination sessions before beginning the -PE optogenetic manipulation (second set of 4 sessions) to wash out any potential carry over effects of the initial light manipulation.

For both manipulations, optical inhibition was achieved via delivery of 25 mW of 532 nm 'green' light on each side. Light was produced by a DPSS laser connected to an optical commutator attached to a custom-made behavioral cable (Multimode Fiber, 0.22 NA, High-OH, Ø200 µm Core), which connected to the implanted optical ferrule (2.5mm OD, 230 µm Bore Multimode Ceramic Zirconia). Light output of 25 mW was chosen based on calculations the optical fibers will produce ~5 mW/mm<sup>2</sup> of light at distance of 1.2 mm from fiber tip.

##### 4.2.7.1 +PE Optogenetic Manipulation

For the +PE optogenetic manipulation, the DRN was illuminated during the foot shock on uncertainty-shock and danger trials. Illumination on both uncertainty and danger trials occurred for 4 seconds, beginning immediately after auditory cue offset (2 s), continuing during foot shock (0.5 s), and ending 1.5 s after foot shock offset.

#### 4.2.7.2 -PE Optogenetic Manipulation

During the -PE optogenetic manipulation, the uncertainty cue was now selectively extinguished as described above. The DRN was illuminated during the omission period on uncertainty and safety trials. Illumination on both uncertainty and safety trials occurred for 4 seconds, beginning immediately after auditory cue offset.

#### *4.2.8 Histology*

Rats were deeply anesthetized using isoflurane and perfused with 0.9% biological saline and 4% paraformaldehyde in a 0.2 M Potassium Phosphate Buffered Solution. Brains were extracted and post-fixed in a 10% neutral-buffered formalin solution for 24 hrs, stored in 10% sucrose/formalin, frozen at -80°C and sectioned via a sliding microtome. Brains were processed for fluorescent microscopy. Tissue was processed with fluorescent anti-tryptophan hydroxylase immunohistochemistry and NeuroTrace™ (ThermoFisher Scientific, Waltham, MA) in order to ensure deletion of DRN serotonergic neurons (Experiment 1) or transfection of DRN serotonergic neurons (Experiment 2). This tissue was mounted on glass slides with VECTASHIELD HardSet Antifade Mounting Medium (Vector Laboratories, Burlingame, CA). Deletion extent, viral transfection, and optical implant sites were confirmed by comparison to a rat brain atlas (Paxinos & Watson, 2007).

#### *4.2.9 Quantification and Statistical Analysis*

##### 4.2.9.1 Baseline Nose Poke Analyses

The time stamp for every nose poke and event onset (cues and shocks) during each session was recorded automatically. Raw data were processed in MATLAB to extract nose poke rates during three periods: the baseline, which was 20 seconds prior to cue onset; the 10-s cue; and the post-cue period, which was 4 seconds following cue offset. Baseline nose pokes are reported in pokes/min and analyzed with ANOVA.

#### 4.2.9.2 Calculating and Analyzing Suppression Ratios

Suppression of rewarded nose poking was used as the behavioral indicator of fear. Nose poke rates were calculated for two temporal windows. A suppression ratio for total cued fear was calculated from nose poke rates during a 20 s baseline period just prior to cue onset and the 10 s cue period:  $(\text{baseline} - \text{cue} / \text{baseline} + \text{cue})$ . Complete nose poke suppression was signified by a suppression ratio of '1.00' during the cue relative to baseline, indicating a high level of fear. No nose poke suppression was signified by a suppression ratio of '0.00,' indicating no fear. Intermediate values indicated graded levels of fear.

#### 4.2.9.3 Session-by-Session Analyses

In Experiment 1, repeated measures ANOVA for suppression ratios with between factors of group (Caspase vs. YFP) and sex (female vs. male), plus within factors of session (2 pre-exposure and 16 discrimination) and cue (danger vs. uncertainty vs. safety) were used compare behavior during fear discrimination. Similar ANOVAs over the last day of discrimination plus 8 sessions of selective extinction (9 total sessions)

compared fear levels to each cue to determine the effects of 5-HT deletion during selective extinction.

In Experiment 2, repeated measures ANOVA for suppression ratios with between factors of group (YFP vs. eNpHR) and sex (female vs. male), plus within factors of session (2 pre-exposure and 12 discrimination) and cue (danger vs. uncertainty vs. safety) were used compare behavior during fear discrimination. Similar ANOVAs were run for the +PE optogenetic manipulation and –PE optogenetic manipulation/selective extinction sessions to determine the impact of light illumination.

#### 4.2.9.4 Trial-by-Trial Analyses

In order to determine whether changes in fear were due to within- or between-session fear updating, the first selective extinction session post-optogenetics was isolated. The uncertainty cue was no longer paired with shock on any trials in this session. Six uncertainty cue trials were sampled during this session to look at fear at the trial level. Repeated measures ANOVA for suppression ratios with between subjects factor of group (eNpHR vs. YFP) and within factor of trial was used to compare fear within-session.

### **4.3 Summary of Experiments and Results**

#### *4.3.1 Experiment 1*

##### 4.3.1.1 Baseline Nose Poke Rates

Repeated measures ANOVA for baseline nose poke rate (within factor: session; between factors: sex and group) revealed main effects of session ( $F_{25,475} = 31.57$ ,  $p < 0.001$ ,  $\eta^2p = 0.62$ , power = 1.00), sex ( $F_{1,19} = 23.20$ ,  $p < 0.001$ ,  $\eta^2p = 0.55$ , power = 0.99),

and a sex x session interaction ( $F_{25,475} = 6.84$ ,  $p < 0.001$ ,  $\eta^2p = 0.27$ , power = 1.00). Sex effects were driven by higher poke rates in males compared to females, an effect consistent with previous behavioral findings in this task (Walker et al., 2018, 2019). Importantly, there were no effects or interactions with group throughout behavioral testing (all  $F < 0.91$ , all  $p > 0.05$ ), indicating YFP and Caspase groups poked a similar rates (Fig. 4.1).

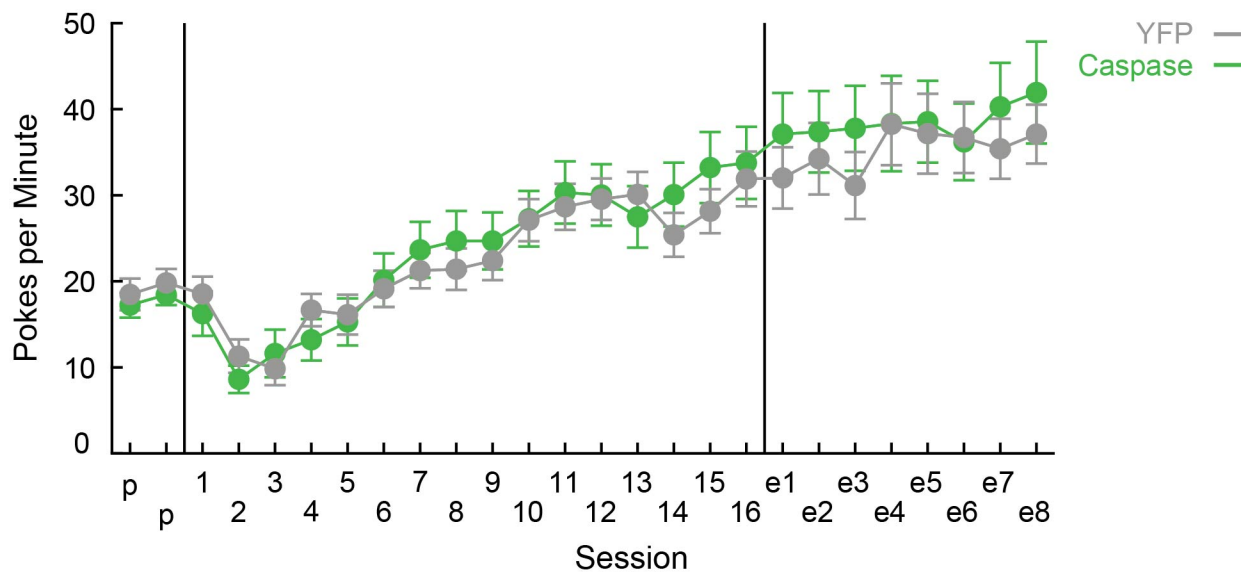


**Figure 4.1 YFP vs. Caspase baseline nose poke rates.** Mean  $\pm$  SEM baseline nose poke rates for YFP (gray) and caspase rats (green) are plotted for the two pre-exposure (p), 16 discrimination (1-16), and 8 selective extinction sessions (e1-e8). No group differences were detected in baseline nose poke behavior.

#### 4.3.1.2 Deletion of DRN 5-HT Does Not Impact Fear Discrimination

If DRN 5-HT neurons are required for  $-PE$  signaling, then deletion of these neurons would be expected to interfere with fear discrimination, particularly in the ability to decrease fear. Deletion would not be expected to interfere with expression of high levels of fear to a deterministic cue, like that usually seen to a danger cue.

TPH2-cre rats received bilateral infusions of either cre-caspase (Caspase; n=12; 7 females) or cre-YFP (YFP; n=11; 7 females) to allow for comparison of fear discrimination with DRN 5-HT selectively deleted or intact. Rats in the Caspase group showed robust deletion of 5-HT throughout the DRN, while rats in the YFP group showed 5-HT intact, as verified by anti-tph2 immunohistochemistry (Fig. 4.2A, B). Rats received two sessions of pre-exposure to the three auditory cues before undergoing 16 sessions of fear discrimination testing. As expected, rats in the YFP group with DRN 5-HT intact showed the typical pattern of behavior during discrimination sessions: high fear to danger, intermediate fear to uncertainty, and low fear to safety (Fig. 4.2C). Somewhat surprisingly, the Caspase group demonstrated a similar pattern of fear behavior during discrimination (Fig. 4.2D). These results were confirmed by ANOVA finding no effects of or interactions with group during pre-exposure or discrimination (all  $F < 1.90$ , all  $p > 0.05$ ), but significant effects of cue ( $F_{2,38} = 48.86$ ,  $p < 0.001$ ,  $\eta^2p = 0.72$ , power = 1.00), session ( $F_{15,285} = 14.92$ ,  $p < 0.001$ ,  $\eta^2p = 0.44$ , power = 1.00), and a cue x session interaction ( $F_{30,570} = 6.91$ ,  $p < 0.001$ ,  $\eta^2p = 0.27$ , power = 1.00). A main effect of sex was also present during discrimination sessions ( $F_{1,19} = 4.49$ ,  $p = 0.048$ ,  $\eta^2p = 0.19$ , power = 0.52) due to higher average suppression ratios in females (mean = 0.72) compared to males (mean = 0.58). These findings demonstrated that both YFP and Caspase rats learned to differentiate the three auditory cues and the two groups began selective extinction with equivalent levels of fear discrimination.

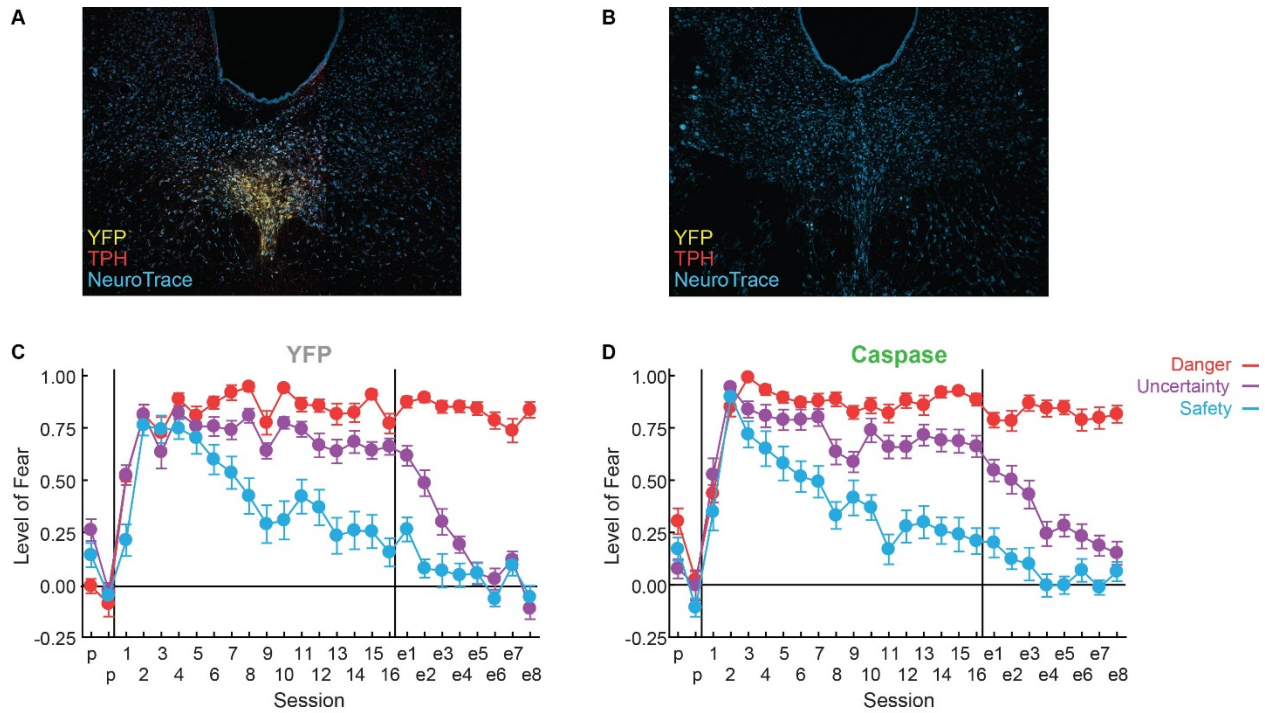


**Figure 4.2 DRN 5-HT deletion does not impact discrimination but impairs extinction of uncertainty.** (A) Representative image shows cre-YFP (yellow) labeling of 5-HT neurons in the DRN against tph2 immunohistochemistry (red). Fluorescent Nissl staining (NeuroTrace™) shows neuronal cell bodies (blue). (B) Representative image shows 5-HT deletion via cre-caspase in the DRN as in A. (C) Mean  $\pm$  SEM suppression ratios for YFP rats to danger (red), uncertainty (purple), and safety (blue) are shown for the 2 pre-exposure sessions (p), 16 discrimination sessions (1-16), and 8 selective extinction sessions (e1-e8). (D) Caspase suppression ratio data shown as in A.

#### 4.3.1.3 Deletion of DRN 5-HT Impairs Extinction of Uncertainty

After fear discrimination, all rats underwent 8 sessions during which the uncertainty cue was now selectively extinguished. YFP rats extinguished fear to the uncertainty cue over these 8 sessions, resulting in a fear level equivalent to that of the safety cue (Fig. 4.2C). Caspase rats, however, extinguished fear to uncertainty more slowly and did not achieve the same level of extinction as the YFP group (Fig. 4.2D). These results were supported by a repeated measures ANOVA demonstrating a significant session  $\times$  group interaction ( $F_{8,152} = 2.07$ ,  $p = 0.042$ ,  $\eta^2_p = 0.098$ , power = 0.82) for the uncertainty cue. A

session x sex interaction was also present ( $F_{8,152} = 2.58$ ,  $p = 0.011$ ,  $\eta^2p = 0.12$ , power = 0.91) during these sessions. There were no group differences in fear to the danger or safety cues during selective extinction (all  $F < 2.82$ , all  $p > 0.05$ ), as expected since they maintained their contingencies.

## 4.3.2 Experiment 2

### 4.3.2.1 Baseline Nose Poke Rates

Repeated measures ANOVA for baseline nose poke rate (within factor: session; between factors: sex and group) revealed main effects of session ( $F_{27,432} = 12.92$ ,  $p < 0.001$ ,  $\eta^2p = 0.45$ , power = 1.00), sex ( $F_{1,16} = 24.66$ ,  $p < 0.001$ ,  $\eta^2p = 0.61$ , power = 0.99), and group ( $F_{1,16} = 5.72$ ,  $p = 0.029$ ,  $\eta^2p = 0.26$ , power = 0.61). Interactions of group x sex ( $F_{1,16} = 7.62$ ,  $p = 0.014$ ,  $\eta^2p = 0.32$ , power = 0.74), group x session ( $F_{27,432} = 1.66$ ,  $p = 0.021$ ,  $\eta^2p = 0.094$ , power = 0.99), and session x sex ( $F_{27,432} = 3.53$ ,  $p < 0.001$ ,  $\eta^2p = 0.18$ , power = 1.00) also reached significance. eNpHR rats exhibited higher nose poke rates compared to YFP in pre-illumination fear discrimination sessions (Fig. 4.3A). Sex effects were driven by higher poke rates in males compared to females, an effect consistent with previous behavioral findings in this task (Walker et al., 2018, 2019). Importantly, there were no effects or interactions with group during either optogenetic manipulation period when these sessions were considered separately (Fig. 4.3A, B; all  $F < 2.87$ , all  $p > 0.05$ ).

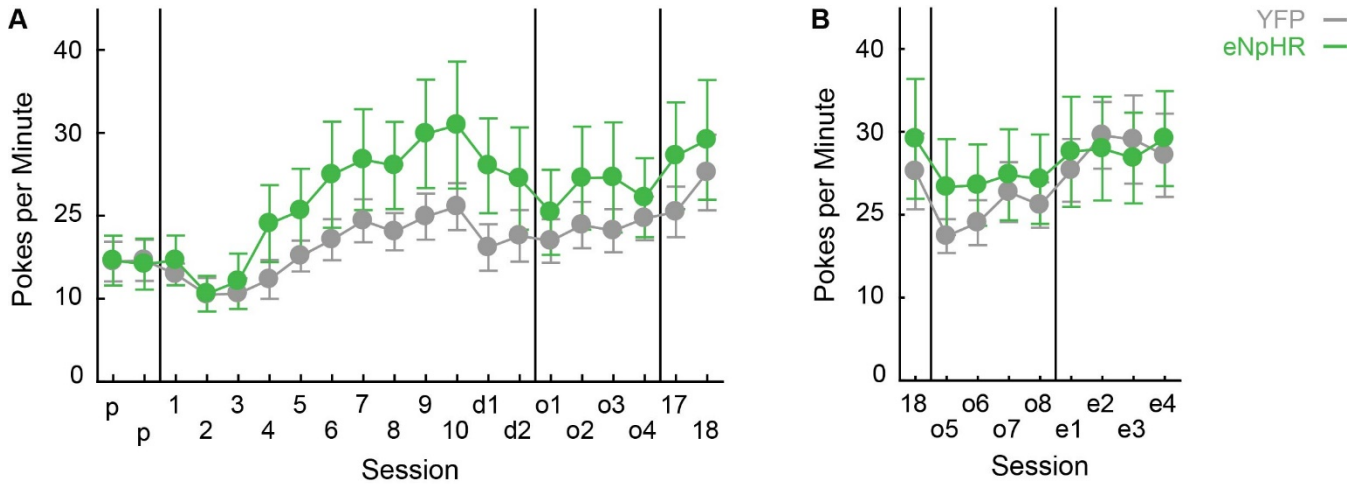


**Figure 4.3 YFP vs. eNpHR baseline nose poke rates. (A)** Mean  $\pm$  SEM baseline nose poke rates for YFP (gray) and eNpHR rats (green) are plotted for the two pre-exposure (p), 12 discrimination (1-10; 17-18), 2 ‘dummy’ tethered-only (d1-d2), and 4 +PE optogenetic manipulation sessions (o1-o4). **(B)** Mean  $\pm$  SEM baseline nose poke rates are plotted for the last fear discrimination (18), 4 –PE optogenetic manipulation (o5-o8), and 4 post-illumination selective extinction sessions (e1-e4) for YFP (gray) and eNpHR (green) rats.

#### 4.3.2.2 Inhibition of DRN 5-HT during +PE Does Not Impact Fear Discrimination

TPH2-cre rats received bilateral DRN transfection with cre-dependent halorhodopsin (eNpHR; n=10; 7 females) or cre-YFP (YFP; n=10; 7 females) and bilateral implantation of optical ferrules over the DRN. All rats showed transfection in 5-HT neurons in the DRN with ferrules tips inside the DRN boundary (representative image Fig. 4.4A). Rats were trained on the fear discrimination procedure before undergoing the +PE (Fig. 4.4B) and –PE (Fig. 4.4C) optogenetic manipulations. If DRN 5-HT neurons are involved in positive or unsigned errors, then inhibition of neural activity at the time of surprising foot shock should alter fear to uncertainty, but have no effect on fear to danger.

Both YFP and eNpHR rats learned to discriminate between the three auditory cues, as indicated by significant effects of cue ( $F_{2,32} = 74.45$ ,  $p < 0.001$ ,  $\eta^2p = 0.82$ , power = 1.00), session ( $F_{13,208} = 40.23$ ,  $p < 0.001$ ,  $\eta^2p = 0.71$ , power = 1.00), and cue x session

( $F_{26,416} = 9.46$ ,  $p < 0.001$ ,  $\eta^2p = 0.37$ , power = 1.00). No effects of or interactions with group were found during pre-exposure or discrimination (all  $F < 0.97$ , all  $p > 0.05$ ), indicating YFP (Fig. 4.4D) and eNpHR (Fig. 4.4E) rats showed equivalent levels of pre-optogenetic manipulation discrimination. There were no effects of sex during fear discrimination (all  $F < 2.29$ , all  $p > 0.05$ ).

Importantly, no significant group effects were present during the +PE manipulation sessions (Fig. 4.4D, E green boxes, all  $F < 1.81$ , all  $p > 0.05$ ), indicating light illumination during foot shock did not alter fear behavior in eNpHR rats. Again, there were no effects of sex during these sessions (all  $F < 1.71$ , all  $p > 0.05$ ). This pattern of behavior stayed consistent in the post-optogenetics discrimination sessions, with no significant effects of group (all  $F < 3.14$ , all  $p > 0.05$ ). Thus, at the start of the –PE optogenetic manipulation, eNpHR and YFP rats showed equivalent fear discrimination.

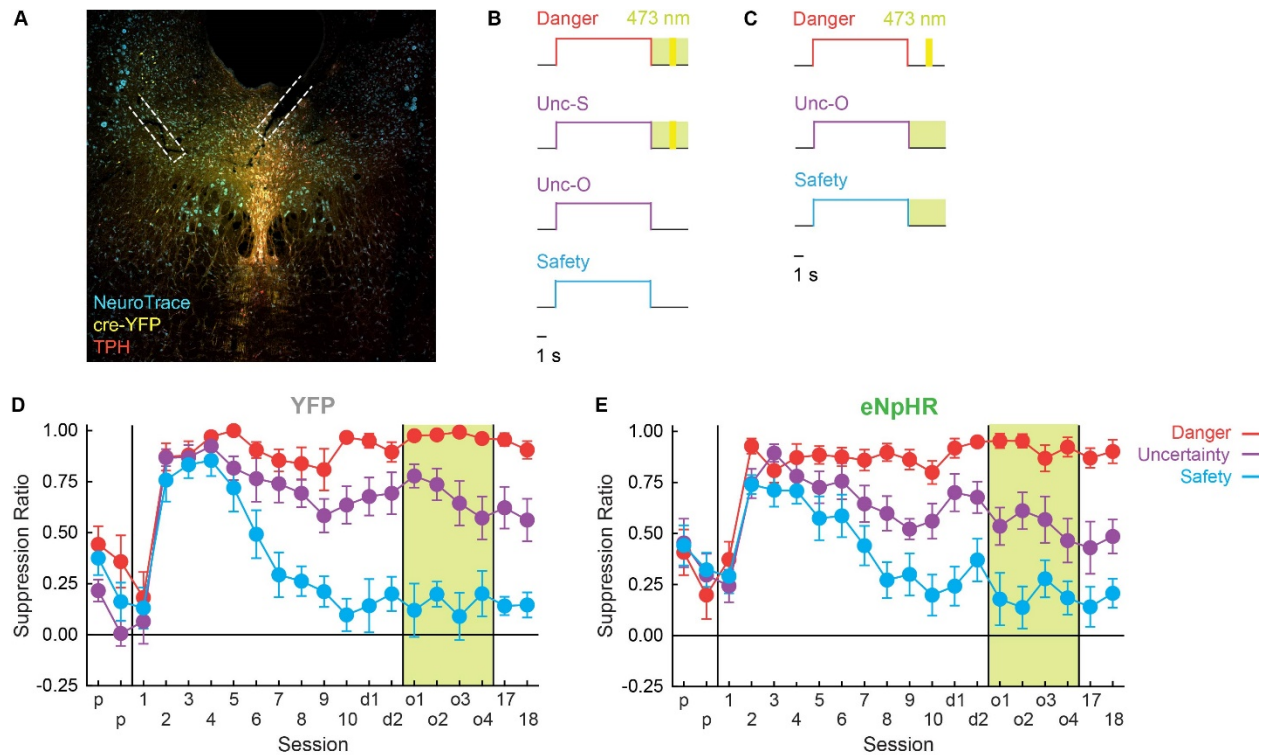


**Figure 4.4 Inhibition of DRN 5-HT does not impact +PE-mediated fear discrimination.** (A) Representative image shows ferrule implant sites (white dashes outlines) and viral transfection in 5-HT neurons in the DRN (YFP, yellow) against *tph2* immunohistochemistry (red). Fluorescent Nissl staining (NeuroTrace™) shows neuronal cell bodies (blue). (B) During the +PE optogenetic manipulation, green-light illumination began at danger and uncertainty-shock cue offset, continued during the 0.5-s shock (yellow period), and lasted 1.5 s after shock for a total of 4 s. Note illumination never occurred during cue periods. (C) During the -PE optogenetic manipulation, green-light illumination began at uncertainty and safety cue offset for a total of 4 s. The uncertainty cue was selectively extinguished during these sessions. Note illumination never occurred during cue periods. (D) Mean  $\pm$  SEM suppression ratios for YFP rats to danger (red), uncertainty (purple), and safety (blue) are shown for the two pre-exposure (p), 12 discrimination (1-10; 17-18), 2 ‘dummy’ tethered-only (d1-d2), and 4 +PE optogenetic manipulation sessions (o1-o4). (E) eNpHR suppression ratio data shown as in B. Both groups achieved discrimination, and light illumination during foot shock did not impact fear behavior.

#### 4.3.2.3 Inhibition of DRN 5-HT during -PE Alters Extinction of Uncertainty

A repeated measures ANOVA for the uncertainty and safety cues revealed no significant effects of or interactions with group during the 4 -PE optogenetic sessions (all  $F < 1.51$ , all  $p > 0.05$ ), but main effects of group ( $F_{1,16} = 4.60$ ,  $p = 0.048$ ,  $\eta^2_p = 0.22$ , power

= 0.52) and sex ( $F_{1,16} = 6.57$ ,  $p = 0.021$ ,  $\eta^2p = 0.29$ , power = 0.67) emerged in the 4 selective extinction sessions (Fig. 4.5A, B). Fear to danger did not change for either group during these sessions (all  $F < 1.17$ , all  $p > 0.05$ ). These results indicated that DRN illumination did not impact fear behavior during illumination sessions, but instead produced a post-illumination decrease in fear to uncertainty.

To better understand the behavioral change during and following illumination, difference scores were calculated for uncertainty and safety: (mean suppression ratio during the 4 post-illumination sessions) - (mean suppression ratio during the 4 illumination sessions). For the uncertainty difference score, t-test and bootstrap confidence intervals showed a significantly greater post-illumination decrease in fear in the eNpHR group compared to YFP (Fig. 4.5C,  $t_{18} = 2.36$ ,  $p = 0.030$ ). No group differences were observed for the safety difference score (Fig. 4.5D,  $t_{18} = 0.12$ ,  $p = 0.90$ ).

To determine whether changes in fear occurred within- or between-session, the first post-illumination session was isolated, and six uncertainty cue trials were sampled during this session. While there was a significant main effect of group, reflecting the between-session effect above, there was no trial x group interaction ( $F_{5,90} = 0.57$ ,  $p = 0.72$ ,  $\eta^2p = 0.031$ , power = 0.20). These results reveal that reduced fear to uncertainty was present on the first trial and thus emerged between sessions, rather than within session. These results demonstrate that inhibition of DRN 5-HT during omission periods did not immediately alter subsequent fear levels but rather impacts post-inhibition fear to uncertainty.



in Experiment 2 selective inhibition of DRN 5-HT neurons during shock and omission periods tested whether activity in these neurons were necessary for +PE or –PE fear updating. There were no immediate effects of inhibition, however, fear to uncertainty significantly decreased in the sessions immediately following the –PE optogenetic manipulation. These findings are not consistent with the theoretical framework that DRN 5-HT generates –PEs, instead indicating that DRN 5-HT is involved in –PE fear updating but is likely not the source of these neural signals.

Taking a closer look at the implications of these results, Experiment 1 indicated that deletion of DRN 5-HT does not impact the ability to learn to discriminate between danger, uncertainty, and safety cues. These results may seem surprising because if DRN 5-HT was necessary to generate –PEs, as I initially hypothesized, then it would be expected that fear discrimination would be impacted. Results were consistent, however, with previous findings showing rats with global DRN neurotoxic lesions could acquire fear but were slower to extinguish fear to uncertain and danger cues (Berg et al., 2014). Given that the deletion occurred prior to any training and was not temporally tied to –PE periods, it was possible that a compensatory mechanism obfuscated a deficit from the lack of DRN 5-HT such that no behavioral differences could be seen during fear discrimination and only became visible during extinction of the uncertainty cue.

Experiment 2 ruled out DRN 5-HT contribution to positive or unsigned PE signaling, as inhibition during shock periods had no effect on behavior during +PE optogenetic manipulation sessions or the subsequent non-illumination discrimination sessions. Further, behavioral results during the –PE optogenetic manipulation unexpectedly showed no impact of DRN 5-HT inhibition. If DRN 5-HT is necessary for –

PE generation, inhibition during shock omission periods would be expected to have prevented decreases in fear to the uncertainty cue in eNpHR rats compared to YFP. Greater post-optogenetics extinction of uncertainty but no change in fear to safety suggested that while –PEs may still have been generated, DRN 5-HT plays a role in use of this error. As soon as DRN 5-HT came back online, fear to uncertainty decreased, suggesting updating of the neural representation of shock expectancy was occurring. Differences in fear to uncertainty also manifested between, not within sessions, providing further support to the idea that DRN 5-HT is not computing –PE, only utilizing it.

DRN 5-HT contribution to –PE fear updating also does not appear to vary by sex. While there were a few significant results with sex as a factor in Experiments 1 and 2, none of the critical findings related to fear updating were impacted by sex, indicated by a lack of sex x group or sex x group x session interactions. Baseline nose poke behavior was generally higher in males, but this effect is consistent with previous findings in the same task (Walker et al., 2018, 2019) and was not significant during optogenetics sessions. Overall, these findings support the idea that PEs likely function similarly in males and females, but sex is still an important factor to consider in analyses.

If DRN 5-HT does not generate, but rather receives, –PE signals then the question arises as to where the signal *is* generated. Based on the present findings, the source is likely to directly impact DRN 5-HT signaling, suggesting it is a population synapsing onto serotonergic neurons in the DRN. This leaves open not only the possibility that this signal is generated elsewhere in the brain, but also that it could arise from another cell type with in the DRN itself. Future studies should focus on tracking where the –PE is generated *de*

*novo*. This chapter identified DRN 5-HT not as the source of –PE generation but as a probable node of –PE-mediated fear updating.

## Chapter 5: Discussion

## 5.1 Summary of Findings

The goals of this dissertation were to test the hypotheses that 1) the vIPAG generates aversive +PEs and 2) sends these signals to CeM to update future fear while 3) serotonergic neurons in the DRN generate aversive –PEs. Chapter 2 tested this first hypothesis. Using optogenetics, vIPAG activity was inhibited precisely at the time of +PE (during and following foot shock receipt) to determine whether this region is necessary for +PE signaling. Using Long-Evans male and female rats, halorhodopsin or YFP control fluorophore was infused into the vIPAG and optical ferrules were bilaterally implanted to allow for delivery of 532 nm light. Rats underwent 16 sessions of fear discrimination training during which three cues were associated with different probabilities of foot shock: safety  $p = 0.00$ , uncertainty  $p = 0.375$ , and danger  $p = 1.00$ . After fear discrimination, all rats received 3 sessions of vIPAG illumination via optical cables followed by 3 sessions without illumination or cables. The vIPAG was illuminated during the foot shock on uncertainty-shock (+PE period) and danger (control, no +PE period) trials.

Fear, as indicated by nose poke suppression, decreased selectively to uncertainty in halorhodopsin rats receiving vIPAG inhibition. Fear did not change to the fully predicted danger cue for halorhodopsin rats or to any cue for YFP control rats. Importantly, fear response to foot shock did not change due to the optogenetic manipulation, indicating these findings are not due to impaired processing of the shock. These results are especially convincing, as light manipulations occur during shock periods after the cue, but fear changes during the cue period itself on future cue presentations. This was the first evidence demonstrative of a casual role for vIPAG activity precisely at the time of +PE.

Chapter 3 provided a test of the second hypothesis building off of the findings in chapter 2. Using Long-Evans female rats, vIPAG activity was first reversibly silenced using an inhibitory DREADD while single-unit activity was recorded in the CeM in Experiment 1. Rats were first trained to discriminate between safety ( $p = 0.00$ ), uncertainty ( $p = 0.33$ ), and danger ( $p = 1.00$ ) cues before chemogenetic manipulation. Comparisons of CeM activity when the vIPAG was active and inactivated by a DREADD agonist demonstrated CeM units show discriminative firing to cues predicting shock at different probabilities and that this activity is at least partially dependent on vIPAG input. Behavioral fear to uncertainty was also decreased due to vIPAG silencing. Because DREADD inactivation could not be tied to the +PE period specifically, Experiment 2 used optogenetics to inhibit the vIPAG-CeM pathway at temporally precise periods during fear discrimination.

As in chapter 2, halorhodopsin or YFP control fluorophore was infused into the vIPAG and but now optical ferrules were bilaterally implanted in the CeM to allow for delivery of 532 nm light in Long-Evans male and female rats. After fear discrimination training, rats underwent the same optogenetic manipulation only with CeM illumination during the foot shock on uncertainty-shock (+PE period) and danger (control, no +PE period) trials. Fear decreased selectively to uncertainty in halorhodopsin rats receiving vIPAG-CeM inhibition, but this effect was more transient and occurred within session in comparison to cell body inhibition. Fear did not change to the fully predicted danger cue for eNpHR rats or to any cue for YFP control rats. Additional optogenetic manipulations targeting the cue and ITI periods demonstrated that the vIPAG-CeM pathway is not critical

for cued or immediate non-cued fear expression, suggesting these projections are mainly involved in +PE signaling.

To investigate the origin of –PEs, DRN serotonergic neurons were manipulated during fear conditioning in chapter 4. Of the molecularly distinct neuron types within the DRN, serotonergic neurons are the most abundant (Huang et al., 2019), and given the widespread projections of these cells, it was hypothesized that this specific DRN subpopulation generates aversive –PEs. Using Tph2-cre rats bred on a Long-Evans background, DRN serotonergic neurons were selectively deleted via cre-caspase or labeled with a cre-YFP control fluorophore. Rats underwent 16 sessions of fear discrimination training during which three cues were associated with different probabilities of foot shock: safety  $p=0.00$ , uncertainty  $p=0.25$ , and danger  $p=1.00$ . This task was designed such that it requires the use of prediction errors to demonstrate appropriate fear, specifically for the uncertainty cue. After fear discrimination, rats underwent 8 sessions of selective extinction, during which the uncertainty cue was no longer paired with shock. Results indicated that DRN serotonin is needed to accurately decrease fear to uncertainty during extinction, as rats with serotonin depletion were slower to extinguish fear to the uncertainty cue and did not extinguish to the same extent as YFP controls. While these results indicated some possible –PE involvement, they are not causally implicating and compensatory mechanisms cannot be ruled out due to the nature of the deletion.

To causally examine the role of DRN serotonergic neurons in prediction error signaling, this subpopulation was next optically inhibited at the time of –PE. Again using Tph2-cre rats, cre-dependent halorhodopsin or a cre-YFP control fluorophore was infused into the DRN and optical ferrules were bilaterally implanted to allow for delivery of 532 nm

light. This experiment was devised to assess –PE involvement as well as the possibility of alternate outcomes, such as involvement in general fear expression or positive or unsigned errors. Using the same task as above with safety  $p=0.00$ , uncertainty  $p=0.25$  and danger  $p=1.00$  cues, all rats underwent 12 sessions of Pavlovian fear discrimination, 4 sessions of +PE optogenetic manipulation, and 2 additional sessions of fear discrimination. The +PE optogenetic manipulation consisted of illumination at the time of shock receipt to the uncertainty cue (when +PEs would be generated) as well as shock receipt for a fully predicted danger cue (when no +PEs should be generated) to assess possible illumination effects on general fear expression. Rats then underwent extinction of the uncertainty cue with 4 sessions of –PE optogenetic manipulation and 4 post-illumination selective extinction sessions. Inhibition of serotonergic neurons was achieved by delivering light at the time of shock omission to the uncertainty cue during selective extinction in order to target the time of –PE. During this –PE optogenetic manipulation, illumination also occurred during omission periods for the safety cue in order to assess possible illumination effects on general fear expression. The –PE optogenetic manipulation was the period of interest, while the +PE optogenetic manipulation served as a control to rule out DRN 5-HT involvement in +PE or unsigned prediction error signaling.

Results indicated that inhibition at the time of shock omission led to immediate post-optogenetics extinction to the uncertainty cue and no change in fear to a safety cue in the halorhodopsin group compared to YFP controls. Fear did not change due to light delivery during omission on safety cue trials or during +PE periods for either group, indicating the effects were specific to –PE related signaling. These results indicate that

DRN serotonergic neurons are involved in –PE fear updating but are likely not the source of these neural signals, as post-illumination extinction was bolstered. Together, these experiments demonstrate a role for DRN serotonergic neurons in fear updating, particularly via involvement in –PE processing, but fail to identify the neural locus of –PE generation. Future studies should determine whether other cell types within the DRN or regions projecting onto DRN serotonergic neurons might be involved in –PE signaling.

## **5.2 Additional Experimental Findings**

Other findings from our lab and recent publications outside the lab have provided further support for the present experimental findings, particularly related to +PEs. Additional evidence supports the causal mechanism of vIPAG +PE generation, with work from our lab finding that shock-responsive vIPAG neurons show +PE signaling. *In vivo* recordings during the same fear discrimination paradigm show neurons selected generally for their responsiveness to foot shock (increased firing compared to baseline) fired most to surprising shock receipt on uncertainty trials (Walker et al., 2019). Increased activity over danger trials was most evident in the 500ms post-shock, indicating this is the period when +PE signal is maximal. Trial-by-trial fluctuations in single-unit firing predicted subsequent changes in fear to uncertainty, as would be expected of a PE signal. Further, the time scale of this endogenous updating matches the emergence of the effects due to optical inhibition of vIPAG cell bodies, with behavioral effects seen after ~3 trials. Given that the optogenetic procedure utilized only 3 uncertainty-shock trials per session, this would explain why no change in fear was observed during the first illumination session. Instead, optogenetic inhibition would be expected to block +PE fear updating to

uncertainty *within* the second illumination session, as results demonstrated. *In vivo* findings also confirmed that vIPAG activity to foot shock is better captured by +PE, rather than a more general biological salience signal. While shock-responsive vIPAG neurons were cue-responsive in a manner that resembles prediction, there was no relationship between +PE activity and predictive signaling (Walker et al., 2019). Signals for prediction are then very likely to arise from distal brain regions. The central amygdala may provide such an input (Ozawa et al., 2017), but additional brain regions are likely involved.

These results are particularly relevant to those from recent study by Assareh and colleagues (Assareh et al., 2017). In this study, the l/vIPAG was photo inhibited during acquisition of a new cue-shock association, specifically at the time of foot shock. They found that in a subsequent extinction test rats that had received foot shock photo inhibition showed *greater* fear to the conditioned cue. This would appear to directly oppose the above findings. Recall that prediction error is the discrepancy between predicted and received shock. Assareh and colleagues (2017) argue that inhibiting vIPAG during the time of foot shock effectively blocked the prediction signal. The result was a larger, positive discrepancy between the predicted and actual shock, producing a larger +PE and further strengthening the cue-shock association. In reality, my results are consistent with those of Assareh in colleagues (2017). Our lab observes vIPAG signals for ‘prediction’ prior to shock delivery and critically, even during shock presentation (Walker et al., 2019). A vIPAG signal for ‘+PE’ – the discrepancy – is not maximal until the 500ms following shock offset. The optogenetic manipulation used in my experiments was designed to inhibit during this post-shock period, as well as the pre-shock period. Thus, inhibiting vIPAG activity only during the pre-shock or shock period would be expected to strengthen

cue-shock associations, while inhibiting during the post-shock period would be expected to weaken cue-shock associations.

Another question that these results raise is: which cells within the vIPAG are responsible for +PE generation? Tyrosine hydroxylase positive (TH+), a dopamine/norepinephrine neuron marker, vIPAG neurons are shock-responsive and show learning-related changes in firing consistent with +PE. These TH+ neurons also typically contain the vesicular glutamate transporter 2 (vGluT2), a glutamatergic marker (C. Li et al., 2016; Matthews et al., 2016). However, a separate TH+/VgluT2+ population is primarily cue onset-responsive (Groessl et al., 2018). This population also shows learning-related changes in firing, but is largely distinct from the shock population. Shock-responsive vIPAG neurons found in the present fear discrimination task are not strongly cue onset-responsive (Walker et al., 2019). These populations must then be separated by additional genetic markers or perhaps by their connectivity, for example, those with innervation by dorsal horn nociceptive inputs (shock-responsive) versus central auditory inputs (cue-responsive). The development of increasingly advanced labelling systems that can be used to differentiate cellular activity in relation to stimuli will help to fully determine the specific neuronal population generating +PEs in the vIPAG.

The present findings also demonstrated vIPAG-CeM is an essential pathway for behavioral updating due to +PE, but it is likely that vIPAG +PEs are sent to a number of brain regions. In initial research on the neural targets of vIPAG +PEs, I previously hypothesized that the midline/intralaminar thalamus (MIT) was the target of vIPAG +PEs. The MIT receives projections from the vIPAG and projects to a host of brain regions in a greater fear network including the basolateral amygdala, prelimbic cortex, insular cortex

and infralimbic cortex (Van der Werf et al., 2002) and this region has been suggested to receive vIPAG +PEs (McNally et al., 2011; A. Sengupta & McNally, 2014). Employing the same optogenetics procedure used for vIPAG cell body inhibition, I inhibited terminals from the vIPAG in the MIT during +PE. MIT terminal inhibition did not alter fear to uncertainty (data not shown). This suggests that vIPAG +PE signals likely target the fear circuit more directly, and results from chapter 3 indeed support this idea with evidence that CeM receives vIPAG +PEs. Although the present results indicate CeM as a major +PE receiving area, experimentally untested areas may yet be identified as major +PE receiving areas.

While evidence did not support DRN 5-HT -PE generation, it is notable that a correlate for negative prediction error (increased firing to shock omission on uncertainty trials) was not observed in vIPAG single-units during fear discrimination (Walker et al., 2019). Optogenetic inhibition of vIPAG was therefore not targeted at -PE periods. Unlike VTA dopamine neurons that can produce positively and negatively signed reward prediction errors (Roesch et al., 2007; Schultz, 1997), vIPAG neurons only appear to produce a +PE. Of course, reward settings permit many more trials per sessions, allowing for greater observation of a variety of prediction errors signals within a single session (Calu et al., 2010; Roesch et al., 2010). Still, these results rule out vIPAG generation of -PE and suggest that the source of generation is one with projections to DRN serotonergic neurons.

Recently, one other area has been put forth as a potential source of -PE: the VTA. VTA DA neurons were shown to be activated by surprising shock omission, and fear extinction was dependent on VTA DA (Salinas-Hernandez et al., 2018). Another group

similarly demonstrated extinction dependence on VTA DA (R. Luo et al., 2018), and these neurons provide input to the DRN (Christelle Peyron et al., 2018), which the present results suggest receive -PE signals. Further, DRN 5-HT neurons have been shown to express D1 and D2 dopamine receptors (Niederkofler et al., 2016; Okaty et al., 2019), indicating VTA inputs may even directly act on this population. VTA generation of -PE would be particularly interesting given its involvement in reward prediction errors. Still, causal evidence targeting the -PE period is lacking, especially outside the context of extinction. Experimental evidence presented here also does not preclude the possibility that other DRN population could generate -PEs, and DRN DA is one such possibility. With direct projections to the lateral central amygdala (Matthews et al., 2016), DRN DA would be well-positioned to influence the broader fear network and could interact with DRN 5-HT through local modulation. Further testing is necessary to determine which, if any, of these populations generate -PEs. Despite many questions surrounding aversive PEs remaining unanswered, these experiments provide novel insights into how signed PEs are generated.

### **5.3 Consideration of Biological Sex in Prediction Error Signaling**

While considering the neural mechanisms of prediction errors, it is important to investigate possible sex differences not only in these mechanisms but also in the behavioral responses used to measure fear. Fear conditioning data has historically ignored contributions of sex, leaving open the possibility of untested differences (Foilb et al., 2018; Lebron-Milad & Milad, 2012; Tronson, 2018). Additionally, behavioral tasks used to assess prediction error signaling vary, and some tasks may tap into sex

differences while females and males may behave similarly on other tasks (Fernandes et al., 1999; Gruene et al., 2015; Maren et al., 1994; Voulo & Parsons, 2017). In particular, females may in some situations exhibit lower levels of freezing compared to males (Pryce et al., 1999), instead favoring more active responses (Gruene et al., 2015).

In the fear discrimination task employed for the experiments detailed above, conditioned suppression was used to behaviorally assess fear. Lower baseline nose poke behavior, which is used to calculate suppression ratios, has been consistently found in females in this task (Walker et al., 2018, 2019) and this effect was again seen in the present experiments. Females have also demonstrated generally heightened cued fear compared to males in some instances (Walker et al., 2018, 2019), and fear discrimination in females, but not males, is sensitive to early adolescent adversity (Walker et al., 2018). Recent evidence in another discrimination task has shown that females tend to overgeneralize fear to safety cues compared to males (H. L. L. Day et al., 2016) and this sex effect was correlated with differences in medial prefrontal cortex (mPFC) activity (Harriet L. L. Day et al., 2020). Even when exhibiting heightened fear, however, females still display behavioral fear discrimination in the present task, suggesting manipulations expected to change fear discrimination are still valid tests in this paradigm. Sex differences related to the findings presented here may then be less reflective of differences in neural generation of prediction errors but rather behavioral expression of their effects. Given these findings, it is critical to consider sex as a variable in analyses and the potential impact of sex when designing experiments.

In the present chapters, all experiments included both male and female subjects with the exception of the DREADD/recording experiment in chapter 3, which used only

females. Related findings demonstrating endogenous vIPAG +PE signaling in single-units used only male subjects (Walker et al., 2019). Given that optogenetic and DREADD/recording findings related to +PE are seen in females, however, PEs in females appear to be generated through the same neural mechanisms as in males. Further, fear updating effects appear similarly PE-dependent in males and females based on the present findings. Previous literature related to aversive prediction error signaling using rodents has only employed male subjects (Assareh et al., 2017; Cole & McNally, 2009; Groessl et al., 2018; Johansen et al., 2010; McNally & Cole, 2006; Ozawa et al., 2017), and one study in humans used both males and females but did not consider sex as a factor in their analyses (Roy et al., 2014).

Even if typical prediction error function does not differ between the sexes, it is possible that other factors, such as early experience, stress, and genetic differences, could interact with sex to produce differences in signaling or expression. Sex differences in rates of clinical disorders, the understanding of which may be informed by these findings, further highlight the importance of employing males and females in future studies and considering sex in analyses.

#### **5.4 Relevance to Clinical Research**

Understanding how the brain formulates fear responses, including through use of prediction errors, is important for informing our knowledge of psychiatric disorders. Exaggerated fear responses are a hallmark of Post-Traumatic Stress Disorder (PTSD) and anxiety disorders (American Psychiatric Association. DSM-5 Task Force & American Psychiatric Association, 2013) and may be due in part to aberrant processing of uncertain

threats (Grupe & Nitschke, 2013). Such disorders can lead to physically, mentally, emotionally, and socially disadvantageous behaviors, however, excessive threat processing is not limited to disorders of anxiety. Adults maltreated as children show exaggerated neural responses to threatening stimuli despite the lack of any clinical diagnosis (Dannlowski et al., 2012), and I have previously shown that early adolescent adversity inflates fear to uncertainty in rodents (Walker et al., 2018; Wright et al., 2015).

Notably, PTSD and anxiety disorder rates are much higher in females (Kessler et al., 1995, 2006; Tolin & Foa, 2006), and females may be more likely to develop comorbid disorders as well as demonstrate higher disorder burden (McLean et al., 2011). Females are more likely to develop PTSD after exposure to a traumatic event compared to males (Breslau et al., 1997), despite males receiving more exposure to traumatic events (Kessler et al., 1995; Tolin & Foa, 2006). These findings indicate that exposure does not account for differences in disorder rates. While estrogen has been shown to regulate stress and fear responding, the mechanisms behind sex differences in stress and anxiety disorders are not fully understood (Maeng & Milad, 2015). While the present findings do not point toward substantial sex differences in PE generation, disparities in disorder rates highlight the importance of using sex as a factor in experiments related to the neural basis of fear.

While speculative, the current results offer a potential mechanism by which exaggerated +PE activity in vIPAG neurons could drive excessive fear to ambiguous, threatening cues. There are currently no experiments, however, linking dysregulated prediction error signaling to disordered fear behavior. Manipulating aversive prediction error signaling could be highly valuable to treating excessive fear responding, but before

we can hope to harness the power of these neural signals, we need to understand the circuitry behind them. Future studies examining prediction error signaling may then provide insight into a more complete neural circuit for normal and aberrant threat processing.

## **5.5 Revision of Initial Hypotheses**

As previously stated, this work aimed to explicitly test the hypotheses that 1) the vIPAG generates aversive +PEs and 2) sends these signals to CeM to update future fear while 3) serotonergic neurons in the DRN generate aversive –PEs. Experimental results confirm the hypotheses that vIPAG generates +PEs and sends them to the CeM to carry out fear updating. Because the effects vIPAG-CeM terminal inhibition did not completely recapitulate the behavioral pattern caused by vIPAG cell body inhibition, it is likely that vIPAG +PEs are sent to multiple targets. The relevant question then may not be which vIPAG projection carries +PE, but rather how does each vIPAG +PE projection affect aversive cue signaling in each target region. In humans, orbitofrontal, anterior mid-cingulate, and dorsomedial prefrontal cortex activation has been detected after PAG +PE (Roy et al., 2014), suggesting these as another potential target. vIPAG does not provide direct input to cortical regions (Vianna & Brandão, 2003), however, indicating an indirect pathway would have to be responsible for this activation. Outside of CeM, vIPAG sends direct projections to the major dopamine-containing regions (A8 retrorubral field, A9 substantia nigra, and A10 ventral tegmental area) (Watabe-Uchida et al., 2012); the diagonal band and the lateral bed nucleus of the stria terminalis (Beitz, 1982); and caudal DRN and thalamic nuclei (Vianna & Brandão, 2003). vIPAG projections to the thalamus

could act as a relay for +PEs to reach the cortex (Fig. 5.1) given its dense cortical innervation, but presently there is no experimental evidence to confirm this idea.

Considering the final hypothesis tested through these experiments, DRN 5-HT generation of -PEs was not confirmed by experimental evidence. Results suggest that these neurons receive -PE signals rather than acting as the source, which remains unknown. Here it is speculated that VTA DA neurons could be responsible for -PE generation and sends these errors to the DRN (Fig. 5.1). The presence of dopamine receptors, D1 and D2, on some 5-HT neurons adds plausibility to direct action of VTA on DRN 5-HT (Niederkofler et al., 2016; Okaty et al., 2019). It is further suggested that DRN 5-HT neurons subsequently send error related information on to the BLA. It is also possible that another neuronal group within the DRN may be responsible for -PE generation. DA neurons are one such prospective cell type, with these neurons having direct projections to the lateral central amygdala (Matthews et al., 2016). These new ideas await scientific testing.

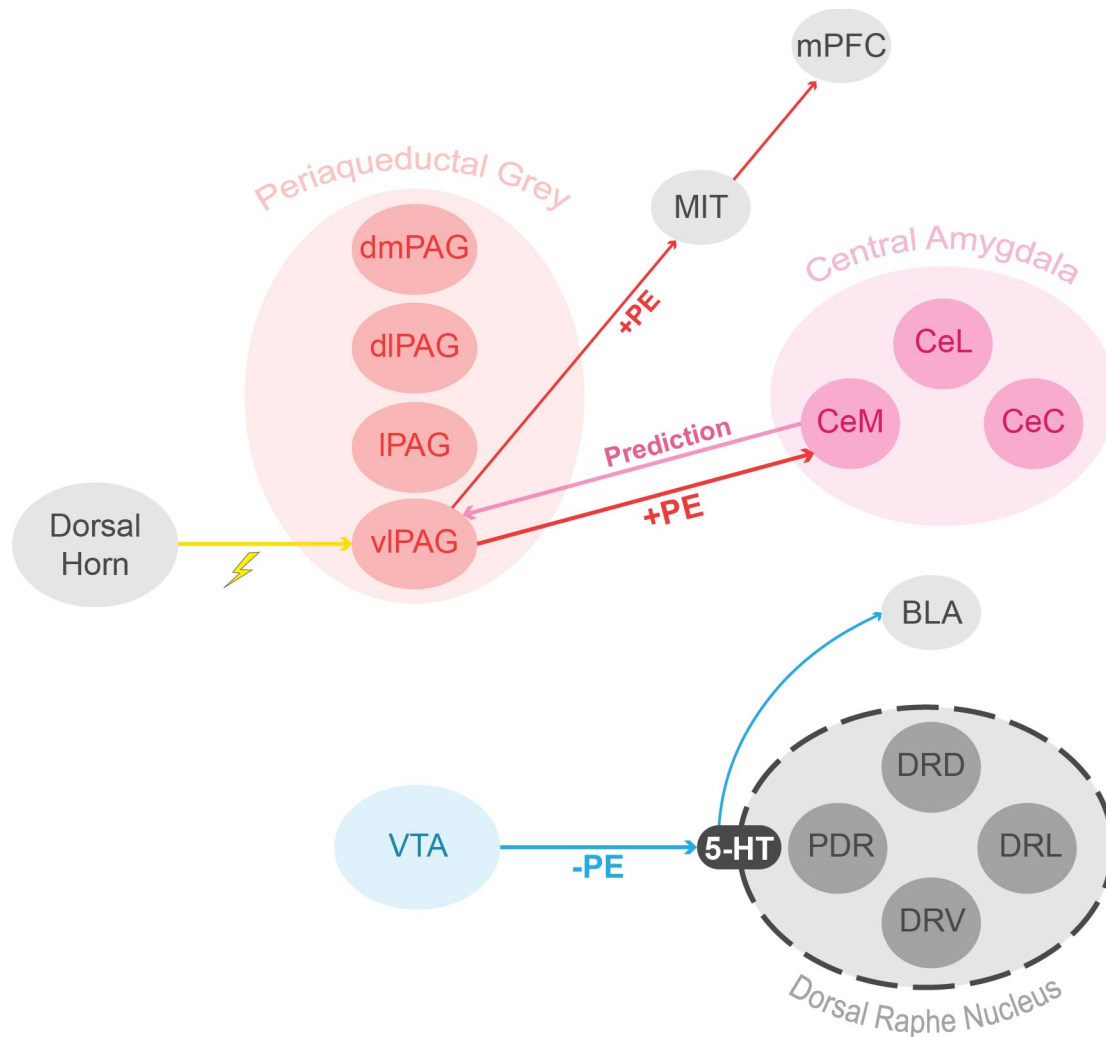


**Figure 5.1 Revised schematic of sources of aversive prediction error.** Experimental evidence confirmed the hypotheses that vIPAG generates +PEs and sends these signals to CeM for fear updating. It is likely that other regions also receive +PEs, but this may also occur through indirect pathways. DRN 5-HT generation of -PEs was not confirmed by experimental evidence. Results suggest that these neurons receive -PE signals rather than acting as the source, which remains unknown but is here hypothesized to be the VTA. It is further suggested that DRN 5-HT neurons receiving VTA -PEs pass prediction error related information on to the BLA. Abbreviations: **BLA**: basolateral amygdala; **dmPAG**: dorsomedial periaqueductal grey; **dlPAG**: dorsolateral periaqueductal grey; **IPAG**: lateral periaqueductal grey; **vIPAG**: ventrolateral periaqueductal grey; **CeC**: central amygdala, capsular; **CeL**: central amygdala, lateral; **CeM**: central amygdala, medial; **DRD**: dorsal raphe nucleus, dorsal; **DRL**: dorsal raphe nucleus, lateral; **DRV**: dorsal raphe nucleus, ventral; **MIT**: midline intralaminar thalamus; **mPFC**: medial prefrontal cortex; **PDR**: posterodorsal raphe nucleus; **VTA**: ventral tegmental area; **5-HT**: serotonin.

## **5.6 Conclusion**

This work sought to uncover the neural basis of aversive prediction error generation. The findings presented here are the first causal evidence of vIPAG +PE generation and demonstration of CeM receipt of these signals for fear updating. While the source of -PE was not identified by this work, DRN serotonin involvement in -PE fear updating was revealed. Further research is needed to describe a full aversive prediction error network, but these results provide a strong foundation for future experiments on prediction errors.

## References

- American Psychiatric Association. DSM-5 Task Force, & American Psychiatric Association. (2013). *Diagnostic and statistical manual of mental disorders: DSM-5* (5th ed.). American Psychiatric Association.
- Assareh, N., Bagley, E. E., Carrive, P., & McNally, G. P. (2017). Brief optogenetic inhibition of rat lateral or ventrolateral periaqueductal gray augments the acquisition of Pavlovian fear conditioning. *Behav Neurosci*, *131*(6), 454–459. <https://doi.org/10.1037/bne0000217>
- Assareh, N., Sarrami, M., Carrive, P., & McNally, G. P. (2016). The Organization of Defensive Behavior Elicited by Optogenetic Excitation of Rat Lateral or Ventrolateral Periaqueductal Gray. *Behavioral Neuroscience*, *130*(4), 406–414. <https://doi.org/10.1037/bne0000151>
- Baker, K. G., Halliday, G. M., Hornung, J.-P., Geffen, L. B., Cotton, R. G. H., & Törk, I. (1991). Distribution, morphology and number of monoamine-synthesizing and substance P-containing neurons in the human dorsal raphe nucleus. *Neuroscience*, *42*(3), 757–775. [https://doi.org/10.1016/0306-4522\(91\)90043-N](https://doi.org/10.1016/0306-4522(91)90043-N)
- Bandler, R., & Shipley, M. T. (1994). Columnar Organization in the Midbrain Periaqueductal Gray—Modules for Emotional Expression. *Trends in Neurosciences*, *17*(9), 379–389. [https://doi.org/10.1016/0166-2236\(94\)90047-7](https://doi.org/10.1016/0166-2236(94)90047-7)
- Barbano, M. F., Wang, H.-L., Zhang, S., Miranda-Barrientos, J., Estrin, D. J., Figueroa-González, A., Liu, B., Barker, D. J., & Morales, M. (2020). VTA Glutamatergic Neurons Mediate Innate Defensive Behaviors. *Neuron*, *107*(2), 368-382.e8. <https://doi.org/10.1016/j.neuron.2020.04.024>

- Behbehani, M. M., & Fields, H. L. (1979). Evidence that an excitatory connection between the periaqueductal gray and nucleus raphe magnus mediates stimulation produced analgesia. *Brain Research*, *170*(1), 85–93. [https://doi.org/10.1016/0006-8993\(79\)90942-9](https://doi.org/10.1016/0006-8993(79)90942-9)
- Behrens, T. E. J., Woolrich, M. W., Walton, M. E., & Rushworth, M. F. S. (2007). Learning the value of information in an uncertain world. *Nature Neuroscience*, *10*(9), 1214–1221. <https://doi.org/10.1038/nn1954>
- Beitz, A. J. (1982). The organization of afferent projections to the midbrain periaqueductal gray of the rat. *Neuroscience*, *7*(1), 133–159.
- Belova, M. A., Paton, J. J., Morrison, S. E., & Salzman, C. D. (2007). Expectation modulates neural responses to pleasant and aversive stimuli in primate amygdala. *Neuron*, *55*(6), 970–984. <https://doi.org/10.1016/j.neuron.2007.08.004>
- Berg, B. A., Schoenbaum, G., & McDannald, M. A. (2014). The dorsal raphe nucleus is integral to negative prediction errors in Pavlovian fear. *European Journal of Neuroscience*, *40*(7), 3096–3101.
- Bertoglio, L. J., & Zangrossi, H., Jr. (2005). Involvement of dorsolateral periaqueductal gray cholecystokinin-2 receptors in the regulation of a panic-related behavior in rats. *Brain Res*, *1059*(1), 46–51. <https://doi.org/10.1016/j.brainres.2005.08.006>
- Boatman, J. A., & Kim, J. J. (2006). A thalamo-cortico-amygdala pathway mediates auditory fear conditioning in the intact brain. *The European Journal of Neuroscience*, *24*(3), 894–900. <https://doi.org/10.1111/j.1460-9568.2006.04965.x>

- Breslau, N., Davis, G. C., Andreski, P., Peterson, E. L., & Schultz, L. R. (1997). Sex Differences in Posttraumatic Stress Disorder. *Archives of General Psychiatry*, 54(11), 1044–1048. <https://doi.org/10.1001/archpsyc.1997.01830230082012>
- Bukalo, O., Pinard, C. R., Silverstein, S., Brehm, C., Hartley, N. D., Whittle, N., Colacicco, G., Busch, E., Patel, S., Singewald, N., & Holmes, A. (2015). Prefrontal inputs to the amygdala instruct fear extinction memory formation. *Science Advances*, 1(6), e1500251. <https://doi.org/10.1126/sciadv.1500251>
- Bush, R. R., & Mosteller, F. (1951). A mathematical model for simple learning. *Psychological Review*, 58(5), 313–323. <http://dx.doi.org/10.1037/h0054388>
- Calu, D. J., Roesch, M. R., Haney, R. Z., Holland, P. C., & Schoenbaum, G. (2010). Neural correlates of variations in event processing during learning in central nucleus of amygdala. *Neuron*, 68(5), 991–1001.
- Campeau, S., & Davis, M. (1995). Involvement of the central nucleus and basolateral complex of the amygdala in fear conditioning measured with fear-potentiated startle in rats trained concurrently with auditory and visual conditioned stimuli. *J Neurosci*, 15(3 Pt 2), 2301–2311.
- Carrive, P. (1993). The periaqueductal gray and defensive behavior: Functional representation and neuronal organization. *Behavioural Brain Research*, 58(1–2), 27–47. [https://doi.org/10.1016/0166-4328\(93\)90088-8](https://doi.org/10.1016/0166-4328(93)90088-8)
- Cassell, M. D., & Gray, T. S. (1989). Morphology of peptide-immunoreactive neurons in the rat central nucleus of the amygdala. *Journal of Comparative Neurology*, 281(2), 320–333. <https://doi.org/10.1002/cne.902810212>

- Challis, C., Boulden, J., Veerakumar, A., Espallergues, J., Vassoler, F. M., Pierce, R. C., Beck, S. G., & Berton, O. (2013). Raphe GABAergic neurons mediate the acquisition of avoidance after social defeat. *J Neurosci*, *33*(35), 13978–13988, 13988a. <https://doi.org/10.1523/JNEUROSCI.2383-13.2013>
- Cho, J. R., Treweek, J. B., Robinson, J. E., Xiao, C., Bremner, L. R., Greenbaum, A., & Gradinaru, V. (2017). Dorsal Raphe Dopamine Neurons Modulate Arousal and Promote Wakefulness by Salient Stimuli. *Neuron*, *94*(6), 1205-1219 e8. <https://doi.org/10.1016/j.neuron.2017.05.020>
- Ciocchi, S., Herry, C., Grenier, F., Wolff, S. B. E., Letzkus, J. J., Vlachos, I., Ehrlich, I., Sprengel, R., Deisseroth, K., Stadler, M. B., Müller, C., & Lüthi, A. (2010). Encoding of conditioned fear in central amygdala inhibitory circuits. *Nature*, *468*(7321), 277–282. <https://doi.org/10.1038/nature09559>
- Cole, S., & McNally, G. P. (2009). Complementary roles for amygdala and periaqueductal gray in temporal-difference fear learning. *Learn Mem*, *16*(1), 1–7. <https://doi.org/10.1101/lm.1120509>
- Collins, D. R., & Pare, D. (2000). Differential fear conditioning induces reciprocal changes in the sensory responses of lateral amygdala neurons to the CS+ and CS-. *Learning & Memory*, *7*(2), 97–103.
- Dannlowski, U., Stuhrmann, A., Beutelmann, V., Zwanzger, P., Lenzen, T., Grotegerd, D., Domschke, K., Hohoff, C., Ohrmann, P., Bauer, J., Lindner, C., Postert, C., Konrad, C., Arolt, V., Heindel, W., Suslow, T., & Kugel, H. (2012). Limbic scars: Long-term consequences of childhood maltreatment revealed by functional and

- structural magnetic resonance imaging. *Biol Psychiatry*, 71(4), 286–293.  
<https://doi.org/10.1016/j.biopsych.2011.10.021>
- Daw, N. D., Kakade, S., & Dayan, P. (2002). Opponent interactions between serotonin and dopamine. *Neural Networks*, 15(4–6), 603–616.
- Day, H. L. L., Reed, M. M., & Stevenson, C. W. (2016). Sex differences in discriminating between cues predicting threat and safety. *Neurobiology of Learning and Memory*, 133, 196–203. <https://doi.org/10.1016/j.nlm.2016.07.014>
- Day, Harriet L. L., Suwansawang, S., Halliday, D. M., & Stevenson, C. W. (2020). Sex differences in auditory fear discrimination are associated with altered medial prefrontal cortex function. *Scientific Reports*, 10(1), 6300.  
<https://doi.org/10.1038/s41598-020-63405-w>
- Diederer, K. M. J., Spencer, T., Vestergaard, M. D., Fletcher, P. C., & Schultz, W. (2016). Adaptive Prediction Error Coding in the Human Midbrain and Striatum Facilitates Behavioral Adaptation and Learning Efficiency. *Neuron*, 90(5), 1127–1138.  
<https://doi.org/10.1016/j.neuron.2016.04.019>
- Duvarci, S., Popa, D., & Paré, D. (2011). Central Amygdala Activity during Fear Conditioning. *Journal of Neuroscience*, 31(1), 289–294.  
<https://doi.org/10.1523/JNEUROSCI.4985-10.2011>
- Faull, O. K., Jenkinson, M., Ezra, M., & Pattinson, Kt. (2016). Conditioned respiratory threat in the subdivisions of the human periaqueductal gray. *Elife*, 5.  
<https://doi.org/10.7554/eLife.12047>
- Fernandes, C., González, M. I., Wilson, C. A., & File, S. E. (1999). Factor Analysis Shows That Female Rat Behaviour Is Characterized Primarily by Activity, Male Rats Are

- Driven by Sex and Anxiety. *Pharmacology Biochemistry and Behavior*, 64(4), 731–736. [https://doi.org/10.1016/S0091-3057\(99\)00139-2](https://doi.org/10.1016/S0091-3057(99)00139-2)
- Floyd, N. S., Price, J. L., Ferry, A. T., Keay, K. A., & Bandler, R. (2000). Orbitomedial prefrontal cortical projections to distinct longitudinal columns of the periaqueductal gray in the rat. *J Comp Neurol*, 422(4), 556–578.
- Foib, A. R., Bals, J., Sarlitto, M. C., & Christianson, J. P. (2018). Sex differences in fear discrimination do not manifest as differences in conditioned inhibition. *Learning & Memory*, 25(1), 49–53. <https://doi.org/10.1101/lm.045500.117>
- Geddes, S. D., Assadzada, S., Lemelin, D., Sokolovski, A., Bergeron, R., Haj-Dahmane, S., & Béique, J.-C. (2016). Target-specific modulation of the descending prefrontal cortex inputs to the dorsal raphe nucleus by cannabinoids. *Proceedings of the National Academy of Sciences*, 113(19), 5429–5434. <https://doi.org/10.1073/pnas.1522754113>
- Goosens, K. A., & Maren, S. (2001). Contextual and auditory fear conditioning are mediated by the lateral, basal, and central amygdaloid nuclei in rats. *Learning & Memory*, 8(3), 148–155.
- Graeff, F. G. (2004). Serotonin, the periaqueductal gray and panic. *Neurosci Biobehav Rev*, 28(3), 239–259. <https://doi.org/10.1016/j.neubiorev.2003.12.004>
- Grahn, R. E., Will, M. J., Hammack, S. E., Maswood, S., McQueen, M. B., Watkins, L. R., & Maier, S. F. (1999). Activation of serotonin-immunoreactive cells in the dorsal raphe nucleus in rats exposed to an uncontrollable stressor. *Brain Res*, 826(1), 35–43.

- Gray, T. S., & Magnuson, D. J. (1987). Neuropeptide neuronal efferents from the bed nucleus of the stria terminalis and central amygdaloid nucleus to the dorsal vagal complex in the rat. *Journal of Comparative Neurology*, 262(3), 365–374. <https://doi.org/10.1002/cne.902620304>
- Groessl, F., Munsch, T., Meis, S., Griessner, J., Kaczanowska, J., Pliota, P., Kargl, D., Badurek, S., Kraitsy, K., Rassoulpour, A., Zuber, J., Lessmann, V., & Haubensak, W. (2018). Dorsal tegmental dopamine neurons gate associative learning of fear. *Nat Neurosci*, 21(7), 952–962. <https://doi.org/10.1038/s41593-018-0174-5>
- Gruene, T. M., Flick, K., Stefano, A., Shea, S. D., & Shansky, R. M. (2015). Sexually divergent expression of active and passive conditioned fear responses in rats. *Elife*, 4. <https://doi.org/10.7554/eLife.11352>
- Grupe, D. W., & Nitschke, J. B. (2013). Uncertainty and anticipation in anxiety: An integrated neurobiological and psychological perspective. *Nat Rev Neurosci*, 14(7), 488–501. <https://doi.org/10.1038/nrn3524>
- Halberstadt, A. L., & Balaban, C. D. (2008). Selective anterograde tracing of nonserotonergic projections from dorsal raphe nucleus to the basal forebrain and extended amygdala. *Journal of Chemical Neuroanatomy*, 35(4), 317–325. <https://doi.org/10.1016/j.jchemneu.2008.02.006>
- Holland, P. C., & Gallagher, M. (2006). Different roles for amygdala central nucleus and substantia innominata in the surprise-induced enhancement of learning. *Journal of Neuroscience*, 26(14), 3791–3797. <https://doi.org/10.1523/JNEUROSCI.0390-06.2006>

- Hopkins, D. A., & Holstege, G. (1978). Amygdaloid projections to the mesencephalon, pons and medulla oblongata in the cat. *Experimental Brain Research*, 32(4), 529–547. <https://doi.org/10.1007/BF00239551>
- Huang, K. W., Ochandarena, N. E., Philson, A. C., Hyun, M., Birnbaum, J. E., Cicconet, M., & Sabatini, B. L. (2019). Molecular and anatomical organization of the dorsal raphe nucleus. *Elife*, 8. <https://doi.org/10.7554/eLife.46464>
- Jansen, A. S. P., Farkas, E., Mac Sams, J., & Loewy, A. D. (1998). Local connections between the columns of the periaqueductal gray matter: A case for intrinsic neuromodulation. *Brain Research*, 784(1), 329–336. [https://doi.org/10.1016/S0006-8993\(97\)01293-6](https://doi.org/10.1016/S0006-8993(97)01293-6)
- Johansen, J. P., Tarpley, J. W., LeDoux, J. E., & Blair, H. T. (2010). Neural substrates for expectation-modulated fear learning in the amygdala and periaqueductal gray. *Nat Neurosci*, 13(8), 979–986. <https://doi.org/10.1038/nn.2594>
- Kalén, P., Karlson, M., & Wiklund, L. (1985). Possible excitatory amino acid afferents to nucleus raphe dorsalis of the rat investigated with retrograde wheat germ agglutinin and D-[3H]aspartate tracing. *Brain Research*, 360(1–2), 285–297. [https://doi.org/10.1016/0006-8993\(85\)91244-2](https://doi.org/10.1016/0006-8993(85)91244-2)
- Kamin, L. J. (1969). Predictability, Surprise, Attention and Conditioning. In B. A. Cambell & R. M. Church (Eds.), *Punishment Aversive Behavior* (pp. 279–296). Appleton-Century-Crofts.
- Kamin, Leon J. (1967). *Attention-like processes in classical conditioning*.
- Kessler, R. C., Chiu, W. T., Jin, R., Ruscio, A. M., Shear, K., & Walters, E. E. (2006). The epidemiology of panic attacks, panic disorder, and agoraphobia in the National

- Comorbidity Survey Replication. *Archives of General Psychiatry*, 63(4), 415–424.  
<https://doi.org/10.1001/archpsyc.63.4.415>
- Kessler, R. C., Sonnega, A., Bromet, E., Hughes, M., & Nelson, C. B. (1995). Posttraumatic Stress Disorder in the National Comorbidity Survey. *Archives of General Psychiatry*, 52(12), 1048–1060.  
<https://doi.org/10.1001/archpsyc.1995.03950240066012>
- Krout, K. E., & Loewy, A. D. (2000). Periaqueductal gray matter projections to midline and intralaminar thalamic nuclei of the rat. *J Comp Neurol*, 424(1), 111–141.
- Lebron-Milad, K., & Milad, M. R. (2012). Sex differences, gonadal hormones and the fear extinction network: Implications for anxiety disorders. *Biol Mood Anxiety Disord*, 2, 3. <https://doi.org/10.1186/2045-5380-2-3>
- LeDoux, J. E., Cicchetti, P., Xagoraris, A., & Romanski, L. M. (1990). The lateral amygdaloid nucleus: Sensory interface of the amygdala in fear conditioning. *Journal of Neuroscience*, 10(4), 1062–1069.
- LeDoux, J. E., Farb, C., & Ruggiero, D. A. (1990). Topographic organization of neurons in the acoustic thalamus that project to the amygdala. *The Journal of Neuroscience: The Official Journal of the Society for Neuroscience*, 10(4), 1043–1054.
- LeDoux, J. E., Iwata, J., Cicchetti, P., & Reis, D. J. (1988). Different projections of the central amygdaloid nucleus mediate autonomic and behavioral correlates of conditioned fear. *Journal of Neuroscience*, 8(7), 2517–2529.
- LeDoux, J. E., Ruggiero, D. A., & Reis, D. J. (1985). Projections to the subcortical forebrain from anatomically defined regions of the medial geniculate body in the

- rat. *The Journal of Comparative Neurology*, 242(2), 182–213.  
<https://doi.org/10.1002/cne.902420204>
- Lee, H. J., Gallagher, M., & Holland, P. C. (2010). The central amygdala projection to the substantia nigra reflects prediction error information in appetitive conditioning. *Learn Mem*, 17(10), 531–538. <https://doi.org/10/531>
- Lewis, R. G., Serra, M., Radl, D., Gori, M., Tran, C., Michalak, S. E., Vanderwal, C. D., & Borrelli, E. (2020). Dopaminergic Control of Striatal Cholinergic Interneurons Underlies Cocaine-Induced Psychostimulation. *Cell Reports*, 31(3), 107527. <https://doi.org/10.1016/j.celrep.2020.107527>
- Li, C., Sugam, J. A., Lowery-Gionta, E. G., McElligott, Z. A., McCall, N. M., Lopez, A. J., McKlveen, J. M., Pleil, K. E., & Kash, T. L. (2016). Mu Opioid Receptor Modulation of Dopamine Neurons in the Periaqueductal Gray/Dorsal Raphe: A Role in Regulation of Pain. *Neuropsychopharmacology*, 41(8), 2122–2132. <https://doi.org/10.1038/npp.2016.12>
- Li, S. S., & McNally, G. P. (2014). The conditions that promote fear learning: Prediction error and Pavlovian fear conditioning. *Neurobiol Learn Mem*, 108, 14–21. <https://doi.org/10.1016/j.nlm.2013.05.002>
- Li, S. S. Y., & McNally, G. P. (2015). A Role of Nucleus Accumbens Dopamine Receptors in the Nucleus Accumbens Core, but Not Shell, in Fear Prediction Error. *Behavioral Neuroscience*, 129(4), 450–456. <https://doi.org/10.1037/bne0000071>
- Li, Y., Zhong, W., Wang, D., Feng, Q., Liu, Z., Zhou, J., Jia, C., Hu, F., Zeng, J., Guo, Q., Fu, L., & Luo, M. (2016). Serotonin neurons in the dorsal raphe nucleus encode

- reward signals. *Nature Communications*, 7, 10503.  
<https://doi.org/10.1038/ncomms10503>
- Loyd, D. R., Wang, X., & Murphy, A. Z. (2008). Sex differences in micro-opioid receptor expression in the rat midbrain periaqueductal gray are essential for eliciting sex differences in morphine analgesia. *The Journal of Neuroscience: The Official Journal of the Society for Neuroscience*, 28(52), 14007–14017.  
<https://doi.org/10.1523/JNEUROSCI.4123-08.2008>
- Luo, M., Zhou, J., & Liu, Z. (n.d.). Reward processing by the dorsal raphe nucleus: 5-HT and beyond. *Learning & Memory*, 22(9), 452.  
<https://doi.org/10.1101/lm.037317.114>
- Luo, R., Uematsu, A., Weitemier, A., Aquili, L., Koivumaa, J., McHugh, T. J., & Johansen, J. P. (2018). A dopaminergic switch for fear to safety transitions. *Nature Communications*, 9. <https://doi.org/10.1038/s41467-018-0478-7>
- Maeng, L. Y., & Milad, M. R. (2015). Sex Differences in Anxiety Disorders: Interactions between Fear, Stress, and Gonadal Hormones. *Hormones and Behavior*, 76, 106–117. <https://doi.org/10.1016/j.yhbeh.2015.04.002>
- Manvich, D. F., Webster, K. A., Foster, S. L., Farrell, M. S., Ritchie, J. C., Porter, J. H., & Weinshenker, D. (2018). The DREADD agonist clozapine N -oxide (CNO) is reverse-metabolized to clozapine and produces clozapine-like interoceptive stimulus effects in rats and mice. *Scientific Reports*, 8(1), 3840.  
<https://doi.org/10.1038/s41598-018-22116-z>

- Maren, S., De Oca, B., & Fanselow, M. S. (1994). Sex differences in hippocampal long-term potentiation (LTP) and Pavlovian fear conditioning in rats: Positive correlation between LTP and contextual learning. *Brain Res*, *661*(1–2), 25–34.
- Mascagni, F., McDonald, A. J., & Coleman, J. R. (1993). Corticoamygdaloid and corticocortical projections of the rat temporal cortex: APhaseolus vulgaris leucoagglutinin study. *Neuroscience*, *57*(3), 697–715. [https://doi.org/10.1016/0306-4522\(93\)90016-9](https://doi.org/10.1016/0306-4522(93)90016-9)
- Matias, S., Lottem, E., Dugué, G. P., & Mainen, Z. F. (2017). Activity patterns of serotonin neurons underlying cognitive flexibility. *ELife*, *6*, e20552. <https://doi.org/10.7554/eLife.20552>
- Matsumoto, M., Matsumoto, K., Abe, H., & Tanaka, K. (2007). Medial prefrontal cell activity signaling prediction errors of action values. *Nature Neuroscience*, *10*(5), 647–656. <https://doi.org/10.1038/nn1890>
- Matthews, G. A., Nieh, E. H., Vander Weele, C. M., Halbert, S. A., Pradhan, R. V., Yosafat, A. S., Glober, G. F., Izadmehr, E. M., Thomas, R. E., Lacy, G. D., Wildes, C. P., Ungless, M. A., & Tye, K. M. (2016). Dorsal Raphe Dopamine Neurons Represent the Experience of Social Isolation. *Cell*, *164*(4), 617–631. <https://doi.org/10.1016/j.cell.2015.12.040>
- McDonald, A. J. (1998). Cortical pathways to the mammalian amygdala. *Progress in Neurobiology*, *55*(3), 257–332. [https://doi.org/10.1016/s0301-0082\(98\)00003-3](https://doi.org/10.1016/s0301-0082(98)00003-3)
- McHugh, S. B., Barkus, C., Huber, A., Capitaio, L., Lima, J., Lowry, J. P., & Bannerman, D. M. (2014). Aversive prediction error signals in the amygdala. *J Neurosci*, *34*(27), 9024–9033. <https://doi.org/10.1523/JNEUROSCI.4465-13.2014>

- McLean, C. P., Asnaani, A., Litz, B. T., & Hofmann, S. G. (2011). Gender differences in anxiety disorders: Prevalence, course of illness, comorbidity and burden of illness. *Journal of Psychiatric Research*, 45(8), 1027–1035. <https://doi.org/10.1016/j.jpsychires.2011.03.006>
- McNally, G. P., & Cole, S. (2006). Opioid receptors in the midbrain periaqueductal gray regulate prediction errors during pavlovian fear conditioning. *Behav Neurosci*, 120(2), 313–323. <https://doi.org/10.1037/0735-7044.120.2.313>
- McNally, G. P., Johansen, J. P., & Blair, H. T. (2011). Placing prediction into the fear circuit. *Trends Neurosci*, 34(6), 283–292. <https://doi.org/10.1016/j.tins.2011.03.005>
- Mendes-Gomes, J., Amaral, V. C., & Nunes-de-Souza, R. L. (2011). Ventrolateral periaqueductal gray lesion attenuates nociception but does not change anxiety-like indices or fear-induced antinociception in mice. *Behav Brain Res*, 219(2), 248–253. <https://doi.org/10.1016/j.bbr.2011.01.012>
- Michelsen, K. A., Schmitz, C., & Steinbusch, H. W. (2007). The dorsal raphe nucleus—From silver stainings to a role in depression. *Brain Res Rev*, 55(2), 329–342. <https://doi.org/10.1016/j.brainresrev.2007.01.002>
- Miller, R. R., Barnet, R. C., & Grahame, N. J. (1995). Assessment of the Rescorla-Wagner model. *Psychological Bulletin*, 117(3), 363–386. APA PsycArticles®. <https://doi.org/10.1037/0033-2909.117.3.363>
- Montague, P. R., Dayan, P., & Sejnowski, T. J. (1996). A framework for mesencephalic dopamine systems based on predictive Hebbian learning. *Journal of*

- Neuroscience*, 16(5), 1936–1947. <https://doi.org/10.1523/JNEUROSCI.16-05-01936.1996>
- Mouton, L. J., & Holstege, G. (1994). The periaqueductal gray in the cat projects to lamina VIII and the medial part of lamina VII throughout the length of the spinal cord. *Experimental Brain Research*, 101(2), 253–264. <https://doi.org/10.1007/BF00228745>
- Niederkofler, V., Asher, T. E., Okaty, B. W., Rood, B. D., Narayan, A., Hwa, L. S., Beck, S. G., Miczek, K. A., & Dymecki, S. M. (2016). Identification of serotonergic neuronal modules that affect aggressive behavior. *Cell Reports*, 17(8), 1934–1949. <https://doi.org/10.1016/j.celrep.2016.10.063>
- Okaty, B. W., Commons, K. G., & Dymecki, S. M. (2019). Embracing diversity in the 5-HT neuronal system. *Nat Rev Neurosci*. <https://doi.org/10.1038/s41583-019-0151-3>
- Olucha-Bordonau, F. E., Fortes-Marco, L., Otero-García, M., Lanuza, E., & Martínez-García, F. (2015). Chapter 18 - Amygdala: Structure and Function. In G. Paxinos (Ed.), *The Rat Nervous System (Fourth Edition)* (pp. 441–490). Academic Press. <https://doi.org/10.1016/B978-0-12-374245-2.00018-8>
- Ozawa, T., Ycu, E. A., Kumar, A., Yeh, L. F., Ahmed, T., Koivumaa, J., & Johansen, J. P. (2017). A feedback neural circuit for calibrating aversive memory strength. *Nature Neuroscience*, 20(1), 90–97. <https://doi.org/10.1038/nn.4439>
- Pare, D., Smith, Y., & Pare, J. F. (1995). Intra-Amygdaloid Projections of the Basolateral and Basomedial Nuclei in the Cat—Phaseolus-Vulgaris-Leukoagglutinin

- Anterograde Tracing at the Light and Electron-Microscopic Level. *Neuroscience*, 69(2), 567–583. [https://doi.org/10.1016/0306-4522\(95\)00272-K](https://doi.org/10.1016/0306-4522(95)00272-K)
- Pavlov, I. P., 1849-1936, Pavlov, I. P., 1849-1936, & Gantt, W. H. (William H., 1892-1980, ed. and tr. (1928). *Lectures on conditioned reflexes*,. Liveright.
- Paxinos, G., & Watson, C. (2007). *The rat brain in stereotaxic coordinates* (14605705; 6th ed., Vol. 1–1). Academic Press/Elsevier. Publisher description <http://www.loc.gov/catdir/enhancements/fy0745/2006937142-d.html>
- Peyron, C, Petit, J.-M., Rampon, C., Jouvett, M., & Luppi, P.-H. (1997). Forebrain afferents to the rat dorsal raphe nucleus demonstrated by retrograde and anterograde tracing methods. *Neuroscience*, 82(2), 443–468. [https://doi.org/10.1016/S0306-4522\(97\)00268-6](https://doi.org/10.1016/S0306-4522(97)00268-6)
- Peyron, Christelle, Rampon, C., Petit, J.-M., & Luppi, P.-H. (2018). Sub-regions of the dorsal raphé nucleus receive different inputs from the brainstem. *Sleep Medicine*, 49, 53–63. <https://doi.org/10.1016/j.sleep.2018.07.002>
- Pryce, C. R., Lehmann, J., & Feldon, J. (1999). Effect of Sex on Fear Conditioning is Similar for Context and Discrete CS in Wistar, Lewis and Fischer Rat Strains. *Pharmacology Biochemistry and Behavior*, 64(4), 753–759. [https://doi.org/10.1016/S0091-3057\(99\)00147-1](https://doi.org/10.1016/S0091-3057(99)00147-1)
- Ray, M. H., Hanlon, E., & McDannald, M. A. (2018). Lateral orbitofrontal cortex partitions mechanisms for fear regulation and alcohol consumption. *PLoS One*, 13(6), e0198043. <https://doi.org/10.1371/journal.pone.0198043>
- Ren, J., Friedmann, D., Xiong, J., Liu, C. D., Ferguson, B. R., Weerakkody, T., DeLoach, K. E., Ran, C., Pun, A., Sun, Y., Weissbourd, B., Neve, R. L., Huguenard, J.,

- Horowitz, M. A., & Luo, L. (2018). Anatomically Defined and Functionally Distinct Dorsal Raphe Serotonin Sub-systems. *Cell*, 175(2), 472-487.e20. <https://doi.org/10.1016/j.cell.2018.07.043>
- Rescorla, R. A. (1970). Reduction in the effectiveness of reinforcement after prior excitatory conditioning. *Learning & Motivation*, 1, 372–381.
- Rescorla, R. A., & Wagner, A. R. (1972). A theory of Pavlovian conditioning: Variations in the effectiveness of reinforcement and nonreinforcement. In B. AH & P. WF (Eds.), *Classical Conditioning II: Current Research and Theory* (pp. 64–99). Appleton Century Crofts.
- Rizvi, T. A., Ennis, M., Behbehani, M. M., & Shipley, M. T. (1991). Connections between the Central Nucleus of the Amygdala and the Midbrain Periaqueductal Gray—Topography and Reciprocity. *Journal of Comparative Neurology*, 303(1), 121–131. <https://doi.org/10.1002/cne.903030111>
- Roesch, M. R., Calu, D. J., Esber, G. R., & Schoenbaum, G. (2010). Neural correlates of variations in event processing during learning in basolateral amygdala. *Journal of Neuroscience*, 30(7), 2464–2471.
- Roesch, M. R., Calu, D. J., & Schoenbaum, G. (2007). Dopamine neurons encode the better option in rats deciding between differently delayed or sized rewards. *Nature Neuroscience*, 10(12), 1615–1624.
- Romanski, L. M., & LeDoux, J. E. (1993). Information cascade from primary auditory cortex to the amygdala: Corticocortical and corticoamygdaloid projections of temporal cortex in the rat. *Cerebral Cortex (New York, N.Y.: 1991)*, 3(6), 515–532. <https://doi.org/10.1093/cercor/3.6.515>

- Roy, M., Shohamy, D., Daw, N., Jepma, M., Wimmer, G. E., & Wager, T. D. (2014). Representation of aversive prediction errors in the human periaqueductal gray. *Nat Neurosci*, 17(11), 1607–1612. <https://doi.org/10.1038/nn.3832>
- Rozeske, R. R., Jercog, D., Karalis, N., Chaudun, F., Khoder, S., Girard, D., Winke, N., & Herry, C. (2018). Prefrontal-Periaqueductal Gray-Projecting Neurons Mediate Context Fear Discrimination. *Neuron*, 97(4), 898-910 e6. <https://doi.org/10.1016/j.neuron.2017.12.044>
- Salinas-Hernandez, X. I., Vogel, P., Betz, S., Kalisch, R., Sigurdsson, T., & Duvarci, S. (2018). Dopamine neurons drive fear extinction learning by signaling the omission of expected aversive outcomes. *Elife*, 7. <https://doi.org/10.7554/eLife.38818>
- Samineni, V. K., Grajales-Reyes, J. G., Copits, B. A., O'Brien, D. E., Trigg, S. L., Gomez, A. M., Bruchas, M. R., & Gereau, R. W. (2017). Divergent Modulation of Nociception by Glutamatergic and GABAergic Neuronal Subpopulations in the Periaqueductal Gray. *ENeuro*, 4(2). <https://doi.org/10.1523/ENEURO.0129-16.2017>
- Samson, R. D., & Pare, D. (2005). Activity-dependent synaptic plasticity in the central nucleus of the amygdala. *Journal of Neuroscience*, 25(7), 1847–1855. <https://doi.org/10.1523/Jneurosci.3713-04-2005>
- Sarlitto, M. C., Foilb, A. R., & Christianson, J. P. (2018). Inactivation of the Ventrolateral Orbitofrontal Cortex Impairs Flexible Use of Safety Signals. *Neuroscience*, 379, 350–358. <https://doi.org/10.1016/j.neuroscience.2018.03.037>
- Schultz, W. (1997). Dopamine neurons and their role in reward mechanisms. *Curr Opin Neurobiol*, 7(2), 191–197.

- Schweimer, J. V., & Ungless, M. A. (2010). Phasic Responses in Dorsal Raphe Serotonin Neurons to Noxious Stimuli. *Neuroscience*, *171*(4), 1209–1215. <https://doi.org/10.1016/j.neuroscience.2010.09.058>
- Semenenko, F. M., & Lumb, B. M. (1992). Projections of anterior hypothalamic neurones to the dorsal and ventral periaqueductal grey in the rat. *Brain Research*, *582*(2), 237–245. [https://doi.org/10.1016/0006-8993\(92\)90139-Z](https://doi.org/10.1016/0006-8993(92)90139-Z)
- Sengupta, A., & McNally, G. P. (2014). A role for midline and intralaminar thalamus in the associative blocking of Pavlovian fear conditioning. *Front Behav Neurosci*, *8*, 148. <https://doi.org/10.3389/fnbeh.2014.00148>
- Sengupta, Ayesha, & Holmes, A. (2019). A Discrete Dorsal Raphe to Basal Amygdala 5-HT Circuit Calibrates Aversive Memory. *Neuron*, *103*(3), 489-505.e7. <https://doi.org/10.1016/j.neuron.2019.05.029>
- Shi, C., & Davis, M. (1999). Pain pathways involved in fear conditioning measured with fear-potentiated startle: Lesion studies. *J Neurosci*, *19*(1), 420–430.
- Smith, Y., & Pare, D. (1994). Intra-Amygdaloid Projections of the Lateral Nucleus in the Cat—Pha-L Anterograde Labeling Combined with Postembedding Gaba and Glutamate Immunocytochemistry. *Journal of Comparative Neurology*, *342*(2), 232–248.
- Steinbusch, H. W. M. (1981). Distribution of serotonin-immunoreactivity in the central nervous system of the rat—Cell bodies and terminals. *Neuroscience*, *6*(4), 557–618. [https://doi.org/10.1016/0306-4522\(81\)90146-9](https://doi.org/10.1016/0306-4522(81)90146-9)
- Suckow, S. K., Deichsel, E. L., Ingram, S. L., Morgan, M. M., & Aicher, S. A. (2013). Columnar Distribution of Catecholaminergic Neurons in the Ventrolateral

- Periaqueductal Gray (vIPAG) and Their Relationship to Efferent Pathways. *Synapse (New York, N.Y.)*, 67(2), 94–108. <https://doi.org/10.1002/syn.21624>
- Sun, N., & Cassell, M. D. (1993). Intrinsic GABAergic neurons in the rat central extended amygdala. *The Journal of Comparative Neurology*, 330(3), 381–404. <https://doi.org/10.1002/cne.903300308>
- Sun, Ning, Yi, H., & Cassell, M. D. (1994). Evidence for a GABAergic interface between cortical afferents and brainstem projection neurons in the rat central extended amygdala. *Journal of Comparative Neurology*, 340(1), 43–64. <https://doi.org/10.1002/cne.903400105>
- Takahashi, Y. K., Roesch, M. R., Wilson, R. C., Toreson, K., O'Donnell, P., Niv, Y., & Schoenbaum, G. (2011). Expectancy-related changes in firing of dopamine neurons depend on orbitofrontal cortex. *Nat Neurosci*, 14(12), 1590–1597. <https://doi.org/10.1038/nn.2957>
- Taylor, N. E., Pei, J., Zhang, J., Vlasov, K. Y., Davis, T., Taylor, E., Weng, F.-J., Van Dort, C. J., Solt, K., & Brown, E. N. (2019). The Role of Glutamatergic and Dopaminergic Neurons in the Periaqueductal Gray/Dorsal Raphe: Separating Analgesia and Anxiety. *ENeuro*, 6(1). <https://doi.org/10.1523/ENEURO.0018-18.2019>
- Terao, K., Matsumoto, Y., & Mizunami, M. (2015). Critical evidence for the prediction error theory in associative learning. *Scientific Reports (Nature Publisher Group); London*, 5, 8929. <http://dx.doi.org/10.1038/srep08929>
- Tobler, P. N., O'Doherty, J. P., Dolan, R. J., & Schultz, W. (2006). Human Neural Learning Depends on Reward Prediction Errors in the Blocking Paradigm. *Journal of Neurophysiology*, 95(1), 301–310. <https://doi.org/10.1152/jn.00762.2005>

- Todd, A. J. (2010). Neuronal circuitry for pain processing in the dorsal horn. *Nat Rev Neurosci*, 11(12), 823–836. <https://doi.org/10.1038/nrn2947>
- Tolin, D. F., & Foa, E. B. (2006). Sex differences in trauma and posttraumatic stress disorder: A quantitative review of 25 years of research. *Psychological Bulletin*, 132(6), 959–992. <https://doi.org/10.1037/0033-2909.132.6.959>
- Tovote, P., Esposito, M. S., Botta, P., Chaudun, F., Fadok, J. P., Markovic, M., Wolff, S. B. E., Ramakrishnan, C., Fenno, L., Deisseroth, K., Herry, C., Arber, S., & Lüthi, A. (2016). Midbrain circuits for defensive behaviour. *Nature*, 534(7606), 206–212. <https://doi.org/10.1038/nature17996>
- Tronson, N. C. (2018). Focus on females: A less biased approach for studying strategies and mechanisms of memory. *Current Opinion in Behavioral Sciences*, 23, 92–97. <https://doi.org/10.1016/j.cobeha.2018.04.005>
- Van der Werf, Y. D., Witter, M. P., & Groenewegen, H. J. (2002). The intralaminar and midline nuclei of the thalamus. Anatomical and functional evidence for participation in processes of arousal and awareness. *Brain Res Brain Res Rev*, 39(2–3), 107–140.
- Veening, J. G., Swanson, L. W., & Sawchenko, P. E. (1984). The organization of projections from the central nucleus of the amygdala to brainstem sites involved in central autonomic regulation: A combined retrograde transport-immunohistochemical study. *Brain Research*, 303(2), 337–357. [https://doi.org/10.1016/0006-8993\(84\)91220-4](https://doi.org/10.1016/0006-8993(84)91220-4)

- Vertes, R. P. (1991). A PHA-L analysis of ascending projections of the dorsal raphe nucleus in the rat. *J Comp Neurol*, 313(4), 643–668. <https://doi.org/10.1002/cne.903130409>
- Vianna, D. M. L., & Brandão, M. L. (2003). Anatomical connections of the periaqueductal gray: Specific neural substrates for different kinds of fear. *Brazilian Journal of Medical and Biological Research*, 36(5), 557–566. <https://doi.org/10.1590/S0100-879X2003000500002>
- Vidal-Gonzalez, I., Vidal-Gonzalez, B., Rauch, S. L., & Quirk, G. J. (2006). Microstimulation reveals opposing influences of prelimbic and infralimbic cortex on the expression of conditioned fear. *Learn Mem*, 13(6), 728–733. <https://doi.org/10.1101/lm.306106>
- Voulo, M. E., & Parsons, R. G. (2017). Response-specific sex difference in the retention of fear extinction. *Learning & Memory*, 24(6), 245–251. <https://doi.org/10.1101/lm.045641.117>
- Walker, R. A., Andreansky, C., Ray, M. H., & McDannald, M. A. (2018). Early adolescent adversity inflates threat estimation in females and promotes alcohol use initiation in both sexes. *Behav Neurosci*, 132(3), 171–182. <https://doi.org/10.1037/bne0000239>
- Walker, R. A., Wright, K. M., Jhou, T. C., & McDannald, M. A. (2019). The ventrolateral periaqueductal gray updates fear via positive prediction error. *Eur J Neurosci*. <https://doi.org/10.1111/ejn.14536>

- Watabe-Uchida, M., Zhu, L., Ogawa, S. K., Vamanrao, A., & Uchida, N. (2012). Whole-brain mapping of direct inputs to midbrain dopamine neurons. *Neuron*, 74(5), 858–873. <https://doi.org/10.1016/j.neuron.2012.03.017>
- Wright, K. M., DiLeo, A., & McDannald, M. A. (2015). Early adversity disrupts the adult use of aversive prediction errors to reduce fear in uncertainty. *Front Behav Neurosci*, 9, 227. <https://doi.org/10.3389/fnbeh.2015.00227>
- Yau, J. O., & McNally, G. P. (2015). Pharmacogenetic excitation of dorsomedial prefrontal cortex restores fear prediction error. *J Neurosci*, 35(1), 74–83. <https://doi.org/10.1523/JNEUROSCI.3777-14.2015>
- Yin, J.-B., Liang, S.-H., Li, F., Zhao, W.-J., Bai, Y., Sun, Y., Wu, Z.-Y., Ding, T., Sun, Y., Liu, H.-X., Lu, Y.-C., Zhang, T., Huang, J., Chen, T., Li, H., Chen, Z.-F., Cao, J., Ren, R., Peng, Y.-N., ... Li, Y.-Q. (2020). DmPFC-vIPAG projection neurons contribute to pain threshold maintenance and antianxiety behaviors. *The Journal of Clinical Investigation*, 130(12), 6555–6570. <https://doi.org/10.1172/JCI127607>